UNIVERSITÀ DEGLI STUDI
DI MILANO

Corso di Dottorato di Ricerca in Ematologia Sperimentale

Ciclo XXVIII

*Clinical relevance of **WNT10B** / **WNT10B^{IVS1}** allele variant expression and its potential in Acute Myeloid Leukemia risk assessment*

Dott. Mauro TURRINI

matr. R10256

Relatore: Prof. Alessandro BEGHINI

Correlatore: Dott.ssa Francesca LAZZARONI

Anno Accademico 2014-2015

a Elisabetta e Vittorio

alla mia famiglia

CLINICAL RELEVANCE OF WNT10B / WNT10B^{IVS1} ALLELE VARIANT EXPRESSION

AND ITS POTENTIAL IN ACUTE MYELOID LEUKEMIA RISK ASSESSMENT

Abstract

Acute myeloid leukemia (AML) develops as the consequence of a series of genetic changes in a hematopoietic precursor cell, that alter normal hematopoietic growth and differentiation, resulting in an accumulation of large numbers of abnormal, immature myeloid cells in the bone marrow and peripheral blood. The deceivingly homogeneous, undifferentiated morphology of the leukemic blasts is now known to mask a heterogeneous collection of cells that recapitulate the hierarchy of precursor cells that characterize the normal process of blood-cell differentiation. Leukemia-initiating cell (LIC) properties occur in a self-renewing non-hematopoietic stem cell progenitor cell population, preceded by the expansion of a pre-leukemic long-term hematopoietic stem cell (LT-HSC). The WNT/β-catenin pathway has been show to play a critical role in the regulation of cell proliferation, differentiation, and apoptosis of different malignant entities. Previous results obtained by our research team provided direct evidence that the WNT/β-catenin signaling is diffusely activated in the $AC133^{+}$ AML population, with a specific transcriptional signature involving over-expression of the WNT pathway agonists and down-modulation of the major antagonists. Appling the new *in situ* technique on AML bone marrow sections, we confirmed a dramatic increase of WNT10B expression and protein release within the microenvironment in the large majority of sample. Conversely, the activation of WNT signaling, marked by expression of the dephosphorylated β-catenin, was restricted only to a smaller subpopulation of $AC133^{bright}$ cells.

Focusing our attention on the major locus associated to the regenerative function, in the actual study we performed a 5'-RACE analysis on WNT10B mRNA, evidencing the presence of a non-physiological transcript variant named $WNT10B^{IVS1}$, retaining 77 nucleotide of IVS1 and lacking exon1. In order to provide accurate quantification of mRNA levels of WNT10B and the related $WNT10B^{IVS1}$ transcript variant and to analyze the clinical relevance of their expression, we carried out the gene expression analysis by Droplet Digital^{TM} PCR on mononucleated cells derived from 125 AML patients. Analyzing patients according to specific genetic or risk profiles, we demonstrated that canonical WNT10B mRNA was highly expressed in all *de novo* AML patients here examined, representing the gene with the highest expression in leukemic patients among all the genes actually known. Furthermore, non-physiological $WNT10B^{IVS1}$ variant was highly expressed in all non-favorable risk *de novo* AML, whereas it has non-detectable levels in core-binding factor AML, acute promyelocytic leukemia, and therapy-related disease.

The results presented here provided a compelling evidence that regeneration-associated WNT signaling exceeds the homeostatic range in the majority of human AML cases. These newly discovered genetic abnormalities WNT10B / $WNT10B^{IVS1}$ seem to be associated with clinical, morphologic, and phenotypic features that allow identification of specific leukemic entity. Finally, we presented distinct molecular signatures capable of distinguish with extremely high accuracy *de novo* AML patients from both favorable-risk and therapy-related patients, using a non-time consuming and inexpensive test. These findings, if confirmed in a larger population of patients, may help in refine diagnostic or prognostic criteria for previously described neoplasms, and to introduce newly recognized disease entities possibly characterized by distinct causative pathogenic mechanisms.

List of Abbreviations

AML	Acute myeloid leukemia
APC	Axin/adenomatous polyposis coli
APL	Acute promyelocytic leukemia
BM	Bone marrow
CBF	Core-binding factor
CEBPA	CCAAT/enhancer binding protein
CK1	Casein kinase 1
CR	Complete remission
CRD	Cycteine-rich domains
ddPCR	Droplet Digital PCR
DFS	Disease-free survival
DKK	Dickkopfs
Dvl	Dishevelled protein
ELN	European LeukemiaNet
FAB	French-American-British
FLT3	FMS-like tyrosine kinase 3
FZD	Frizzled
GSK3	Glycogen synthase kinase 3
HIC1	Hypermethylated in cancer 1
HSC	Hematopoietic stem cells
ITD	Internal tandem duplications
LIC	Leukemia-Initiating Cells
LSC	Leucekia stem cells
MDS	Myelodysplasia
MDS/MPN	Myelodysplastic/myeloproliferative
MRC	Medical Research Council
NCCN	National Comprehensive Cancer
NES	Nuclear export signal
NLS	Nuclear localization signal
NPM1	Nucleophosmin-1
OLA	Oligonucleotide ligation assay
OS	Overall survival
Porc	Porcupine protein
RCP	Rolling circle product
RFS	Relapse free survival
RI	Relapse incidence
ROC	Receiver operating characteristic
SFRP	Secreted Frizzled-related proteins
TCF/LEF	T-cell / lymphoid enhancer factor
TKD	Tyrosine kinase domain
Wg	Wingless
WHO	World Health Organizzation
WIF1	Wnt inhibitory factor 1
WREs	Wnt response elements

List of Figures

List of Tables

List of Papers

- Cairoli R, Beghini A, Turrini M, Bertani G, Nadali G, et al. *Old and new prognostic factors in core-binding factor beta acute myeloid leukemia*. American Journal of Hematology 2013; 88:594.
  2013 Impact factor: 4.671
  Times Cited: 3

- Trojani A, Greco A, Tedeschi A, Lodola A, Di Camillo B, Ricci F, Turrini M, et al. *Microarray demonstrates different gene expression profiling signatures between Waldenstrom Macroglobulinemia and IgM Monoclonal Gammopathy of Undetermined Significance*. Clinical Lymphoma, Myeloma and Leukemia 2013; 13:208.
  2013 Impact factor: 1.929
  Times Cited: 2

- Beghini A, Corlazzoli F, Del Giacco L, Re M, Lazzaroni F, et al. *Regeneration-associated Wnt signaling is activated in long-term reconstituting AC133^{bright} acute myeloid leukemia cells*. Neoplasia 2012; 14:1236.
  2012 Impact factor: 5.946
  Times Cited: 5

- Cairoli R, Beghini A, Turrini M, Bertani G, Morra E. *Prognostic markers in AML: focus on CBFL*. Leukemia Supplements 2012; 1:S12.
  2012 Impact factor: 10.164

- Brioschi M, Fischer J, Cairoli R, Rossetti S, Pezzetti L, Nichelatti M, Turrini M, Beghini A, et al. *Down-regulation of microRNAs 222/221 in acute myelogenous leukemia with deranged core-binding factor subunits*. Neoplasia 2010; 12:866.
  2010 Impact factor: 5.025
  Times Cited: 19

- Marbello L, Ricci F, Nosari AM, Turrini M, Nador G, Nichelatti M, et al. *Outcome of hyperleukocytic adult acute myeloid leukaemia: A single-center retrospective study and review of literature*. Leukemia Research 2008; 32:1221.
  2008 Impact factor: 2.390
  Times Cited: 36

- Cereda E, Turrini M, Ciapanna D, Marbello L, Pietrobelli A, Corradi E. *Assessing energy expenditure in cancer patients: A pilot validation of a new wearable device*. Journal of Parenteral and Enteral Nutrition 2007; 31:502.
  2007 Impact factor: 1.773
  Times Cited: 34

1. INTRODUCTION

1.1. LEUKEMIA INITIATING CELL

Acute myeloid leukemia (AML) consists of a group of relatively well-defined hematopoietic neoplasms involving precursor cells committed to the myeloid line of cellular development. AML develops as the consequence of a series of genetic changes in a hematopoietic precursor cell. These changes alter normal hematopoietic growth and differentiation, resulting in an accumulation of large numbers of abnormal, immature myeloid cells in the bone marrow and peripheral blood. These cells are capable of dividing and proliferating, but cannot differentiate into mature hematopoietic cells.

Cell of origin: normal counterpart

Leukemia is a heterogenous group of diseases characterized by clonal cells that exhibit maturation defects that correspond to stages in hematopoietic differentiation. Hematopoietic stem cells are multipotent and have the capacity to differentiate into the cells of all 10 blood lineages (ie, erythrocytes, platelets, neutrophils, eosinophils, basophils, monocytes, T and B lymphocytes, natural killer cells, and dendritic cells). In order to sustain hematopoiesis, stem cells are part of a developmental hierarchy capable of three basic functions:

1. maintenance in a non-cycling state
2. self-renewal, allowing production of additional stem cells
3. production of committed progenitor cells

These progenitor cells commit to subsets of myeloid and lymphoid lineages, and ultimately to single developmental pathways, resulting in the expression of the terminally differentiated stage of each cell type (see **Figure 1**) [1,2].

Normal hematopoiesis is a dynamic, highly regulated process controlled by the combined effects of growth factors that permit cellular proliferation, and nuclear transcription factors that activate specific genetic programs, resulting in commitment to a specific lineage and in terminal differentiation (see **Figure 2**) . Many of the regulatory growth factors and a number of specific transcription factors have been identified that play critical roles in lineage commitment, and in the subsequent development of the mature lymphoid and myeloid (erythroid,granulocytic/monocytic, and megakaryocytic) lineages [3,4].

A number of genes encoding these transcription factors are involved in recurring chromosomal translocations seen in AML, suggesting that the AML variants arise because the translocations result in significant alterations in regulatory processes controlling growth and differentiation programs [5].

<u>Figure 1</u> - Regulation of hematopoiesis via growth factors and cytokines

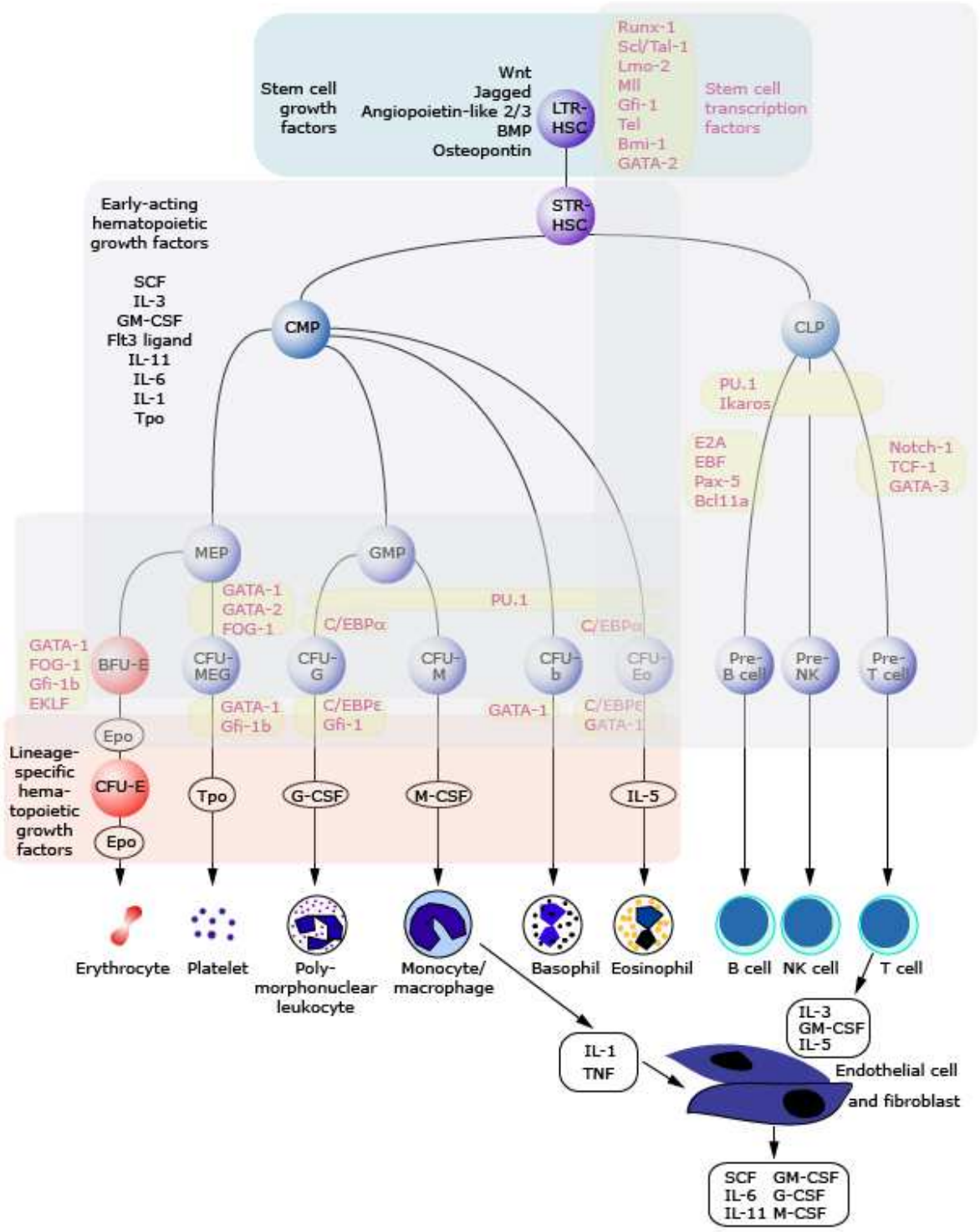

Hierarchical relationships of multipotent hematopoietic stem cells, progenitors, and mature cells of the myelopoietic, erythrocyte, and platelet lineages together with major growth factors, cytokines, and their actions.

LTR-HSC: long-term repopulating hematopoietic stem cell; STR-HSC: short-term repopulating hematopoietic stem cell; SCF: stem cell factor: IL: interleukin; CMP: common myeloid progenitor; CLP: common lymphoid progenitor; MEP: megakaryocyte-erythroid progenitor; GMP: granulocyte-myeloid progenitor; CFU: colony-forming unit; BFU: blast-forming unit; Epo: erythropoietin; Tpo: thrombopoietin; G-CSF: granulocyte colony-stimulating factor; M-CSF: monocyte/macrophage colongy-stimulating factor; GM-CSF: granulocyte-macrophage colony-stimulating factor; TNF: tumor necrosis factor.

Reproduced from: Sieff CA, Zon LI. Anatomy and Physiology of Hematopoiesis. Elsevier, Philadelphia 2009.

Figure 2 - Transcription factors essential for normal hematopoietic development

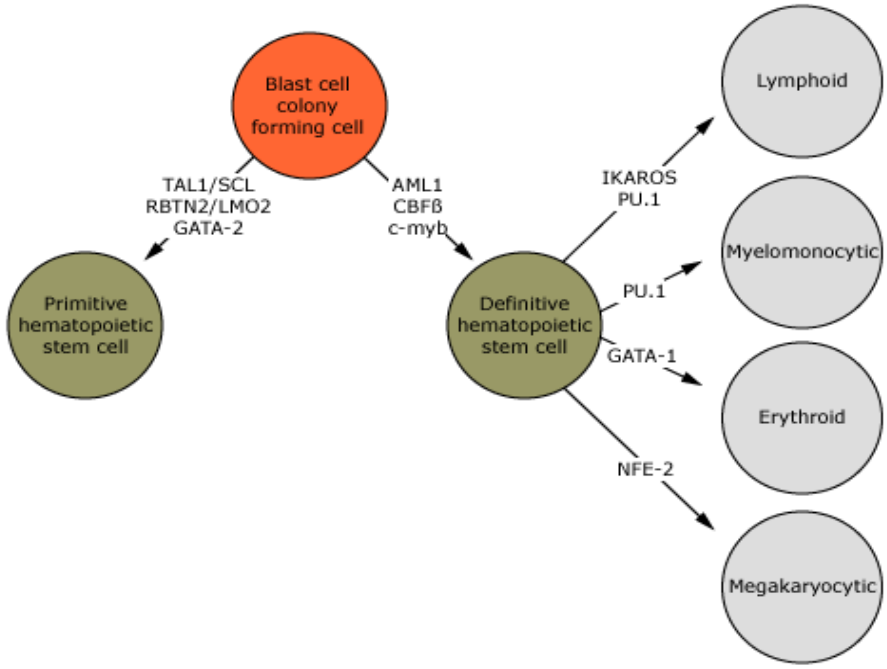

The primitive hematopoietic stem cell gives rise to nucleated erythroid cells at the yolk sac stage of development. Subsequently, multilineage hematopoiesis is thought to be derived from the the definitive hematopoietic stem cell.

Reproduced from: Kennedy M, Firpo M, Choi K, et al. A common precursor for primitive erythropoiesis and definitive haematopoiesis. Nature 1997; 386:488.

Clonality

AML is a clonal process that develops from a single transformed hematopoietic progenitor cell. It is believed that virtually all cases of AML are preceded by a premalignant proliferative disorder characterized by clonal hematopoiesis. Three large sequencing studies identified clonal hematopoiesis in approximately 4 percent of the general population and the incidence increased with age: 6 percent of persons 60 to 69 years; 10 percent of persons 70 to 79 years; 12 percent of persons 80 to 89 years; and 18 percent of persons 90 years or older [6-8]. Clonal hematopoiesis most commonly involved a mutation in DNMT3A, TET2, or ASXL1, mutations that are associated with myeloid malignancies. While clonal hematopoiesis was associated with an increased risk of hematologic cancer, the absolute risk of progression was very small.

Studies of isoenzyme restriction in leukemic myeloblasts of females heterozygous for the A and B isoforms of glucose 6-phosphate dehydrogenase (G6PD) have demonstrated the clonal origin of AML. The G6PD locus is on a portion of the X chromosome that undergoes inactivation in XX somatic cells (Lyonization). Approximately one-half of the cells in normal somatic tissue will have randomly inactivated one or the other of the X chromosomes, allowing expression of the A and B isoforms in approximately equal amounts. Cells of clonal origin, however, express only one type of G6PD. In each of the G6PD heterozygous females with AML, both types of enzyme were found in normal tissues, but only a single type was observed in the leukemic myeloblasts [9-11]. Similar conclusions were reached using X-linked recombinant DNA probes, standard cytogenetics, and fluorescence in situ hybridization (FISH) [12-14].

Leukemic stem cells

AML is a heterogenous disease with leukemic cells of different subtypes resembling normal cells at various stages of maturation. However, there is growing information to support that all leukemias, including AML, appear to be maintained by a pool of self-renewing malignant cells. Based on their ability to serially transfer the disease upon xenotransplantation into immunodeficient mice, it has been hypothesized that limited numbers of cells within the bulk population of leukemic cells have the capacity to function as stem cells that maintain the potential for unlimited self-renewal [15]. These leukemic stem cells (**LSC**, also **leukemia-initiating cells**) may be more immature than the majority of circulating leukemic cells, and are thought to have originated from cells with existing self-renewal capacity or from progenitors that have re-acquired this stem cell-like property. According to this hypothesis, the majority of leukemia cells do not have unlimited self-renewal and exhibit some features of partial differentiation depending on the genetic aberration present.

1.2. ACUTE MYELOID LEUKEMIA: STATE OF THE ART

Two models have been proposed to explain the heterogeneity of AML observed at the molecular, cytogenetic, phenotypic, and clinical level: transformation to leukemia occurring at one of several developmental stages, or transformation to leukemia occurring within primitive multipotent cells.

1. Transformation at one of several developmental stages

This model proposes that any cell type within the stem cell/progenitor cell hierarchy, from primitive multipotent stem cell to lineage-committed progenitor cell, is susceptible to leukemic transformation, resulting in the expansion of abnormal cells that exhibit different stages of differentiation. For AML, this model predicts that the phenotype of the leukemic stem cells restricted to the granulocytic-monocytic series differs from that of cells with involvement of erythroid, megakaryocytic, and granulocytic-monocytic lineages (see **Figure 1**).

The correlation between specific cytogenetic and molecular genetic aberrations and the morphologic appearance of leukemic cells might suggest that the transforming event occurs at different stages of myeloid differentiation. This hypothesis is underscored by the French-American-British (FAB) classification for AML, which distinguishes different subtypes of AML based upon the stage of apparent differentiation (see **Table 1**). Support for this model includes flow cytometric/molecular analyses of the leukemic cell in acute promyelocytic leukemia (APL) that suggest that the leukemic cell arises in a committed lineage-restricted, CD34+/CD38+ progenitor cell [16].

2. Transformation within primitive multipotent cells

A second model proposes that mutations responsible for leukemic transformation and progression occur only in primitive multipotent stem cells, with disease heterogeneity resulting from a variable ability of these primitive stem cells to differentiate and acquire specific phenotypic lineage markers [17,18].

Hematopoietic stem cells express a characteristic cell surface antigen (CD34), and can be further subdivided by the expression of additional cell surface antigens, including CD38 and HLA-DR (see **Figure 3**) [19-22]:

- CD34+/CD38-/HLA-DR- cells are multipotential hematopoietic stem cells, give rise to mixed-lineage granulocytic-erythroid-megakaryocytic colonies in culture, can repopulate immune deficient mice with normal hematopoietic cells in vivo, and demonstrate self-renewal capacity, as assessed by their ability to be serially transplanted into secondary recipient mice. There are data to suggest that, in some cases of AML, the leukemic stem cell may be quite similar to normal hematopoietic stem cells.
- CD34+/CD38+/HLA-DR+ cells define a committed population of myeloid progenitor cells.

Table 1 - French-American-British (FAB) classification of acute myeloid leukemia

FAB type	% Blasts (all cells)	% Blasts (NEC)	Erythroid progenitors	Morphology	Cytochemistry
M0	>30	>90	<50	Blasts resemble L2 variant of ALL Cytoplasmic granules and Auer rods are not seen	MPO+ <3% SBB+
M1	>30	>90	<50	>30% type 1 and type 2 blasts <10% differentiated myeloid cells Auer rods seen in about 50 percent of cases	MPO+ >3% SBB+
M2	>30	>30-89	<50	>30% type 1 and type 2 blasts >10% differentiated myeloid cells Auer rods seen in about 70 percent of cases	MPO+ SBB+ NSE+ <20% PAS–
M3	>30*	>30-89	<50	>20% abnormal hypergranular progranulocytes Blast count may be <30% Auer rods and faggot cells seen in virtually all cases	MPO+ SBB+ PAS– NSE±
M3V	>30*	>30-89	<50	>20% abnormal hypogranular progranulocytes Blast count may be <30% Auer rods and faggot cells seen in virtually all cases	MPO+ SBB+ PAS– NSE±
M4	>30	>30-79	<50	>20% promonocytes and monocytes >20% granulocytic cells Peripheral monocytosis (>5 x 10^9) Auer rods seen in about 65% of cases	MPO+ >20% NSE+
M4eo	>30	>30-79	<50	>5% eosinophils and cells with mixed basophilic and eosinophilic granules, plus M4 features	MPO+ >20% NSE+
M5a		>80	<50	>80% of nonerythroid cells are monoblasts Auer rods usually not seen	NSE+
M5b		>80	<50	>80% of nonerythroid cells are monocytes, promonocytes, and monoblasts Auer rods can be seen in a minor population of myeloblasts (30% of cases)	NSE+
M6		>30	>50	Erythroid predominance and dysplasia >30% blasts among non-erythroid cells Auer rods present in blasts in 60% of cases	PAS+ (erythroid cells); blasts are MPO+
M7	>30		<50	Blasts with cytoplasmic blebbing ± platelet shedding Marrow fibrosis Auer rods are not seen	Platelet MPO+ on EM

NEC: nonerythroid cells; MPO: myeloperoxidase; SBB: Sudan black; NSA: nonspecific esterase; PAS: periodic acid-Schiff.
** Abnormal progranulocytes and blasts.*

Figure 3 - Stem cell properties

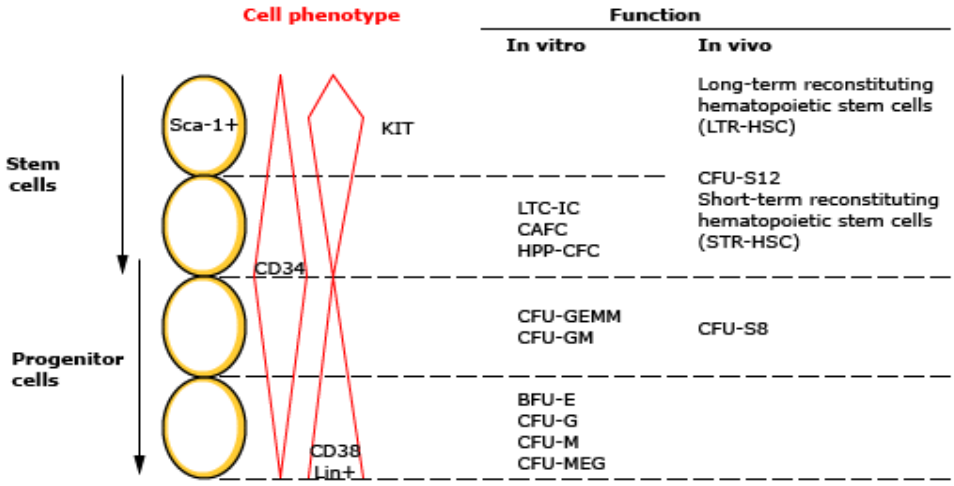

Schematic view of some general properties and assays for the heterogeneous cells that compromise the stem cell and progenitor cell compartments. Reproduce from: UpToDate Topic 4493 Version 30.0 Graphic 77910 Version 4.0.

Cytogenetic and FISH studies of sorted stem cell compartments from patients with AML evolving from a prior myelodysplastic syndrome and patients with de novo AML have shown that the characteristic cytogenetic abnormality from both groups was present in the CD34+/CD38- multipotential stem cell compartment [23-25]. Similar findings were noted in patients with the 5q- syndrome [26] and monosomy 7 [27], myelodysplastic disorders with differing risks of leukemic transformation.

More compelling evidence comes from studies in which purified stem cell subpopulations from normal subjects and those with AML were transplanted into mice with severe combined immunodeficiency disease (SCID). These experiments have detected approximately one SCID mouse leukemia-initiating cell (SL-IC) in 10^5 AML cells, which can repopulate immune deficient mice with leukemic cells phenotypically identical to those of the AML patient from which they were derived [25,28,29].

Using a non-obese diabetic (NOD)/SCID mouse [30], SL-ICs were found to reside only in the CD34+/CD38- fraction [15]. This was consistent regardless of the AML subtype, lineage markers, or percentage of leukemic blast cells expressing the CD34 antigen. The SL-ICs also demonstrated self-renewal capacity, a requirement for maintenance of the leukemic clone. The uniformity of the leukemic stem cell phenotype strongly suggests that the leukemia initiating transformation and progression-associated genetic events occur in primitive cells and not in committed progenitors.

Two-hit hypothesis of leukemogenesis

Progression to acute leukemia may require a series of genetic events beginning with clonal expansion of a transformed leukemic stem cell [31-33]. The specific mutational event(s) required for this progression are not currently well defined.

The "two-hit hypothesis" of leukemogenesis implies that AML is the consequence of at least two mutations, one conferring a proliferative advantage (class I mutations) and another impairing hematopoietic differentiation (class II mutations) [34]. Type I mutations include those of FLT3-ITD, K-RAS mutations, and KIT mutations, while mutations in CEBPA are type II abnormalities [35].

Important insights have been obtained from human leukemias:

- A variety of clonality studies have shown that patients with AML in clinical remission may still have clonal, rather than polyclonal, hematopoiesis [12,36-38]. Such clonal remission may represent the presence of a "preleukemic stem cell" that has undergone an initial transforming event but has not acquired the additional mutation(s) essential to progression to overt leukemia. In these cases, it is presumed that the transformed, overtly leukemic cell probably represented a subclone of the original "preleukemic stem cell" which secondarily acquired the additional genetic mutations required for the definitive block in differentiation and manifestation of the leukemic phenotype.
- On average, AML clones have 8 to 13 mutations found within the coding regions of the genome. The accumulation of these lesions in a step-wise process within a hematopoietic stem cell was demonstrated in a study that compared gene mutations found in de novo AML with patient-matched residual non-leukemic hematopoietic stem cells in long-term survivors [39], and it suggests that several hits are required for the development of AML.
- Whole genome or whole exome sequencing of 200 cases of de novo AML reported an average of 13 gene mutations per tumor [40]. Of these, each tumor had an average of five genes known to be one of a group of 23 genes recurrently mutated in AML that can be broadly grouped into nine categories of genes thought to be involved in leukemogenesis. Mutations were found in genes associated with transcription-factor fusions (18%), nucleophosmin (27%), tumor suppression (16%), DNA-methylation (44%), signaling (59%), chromatin-modification (30%), myeloid transcription factor (22%), the cohesin-complex (13%), and the spliceosome complex (14%). Some mutation pairs occurred more commonly than expected (eg, NPM1 and FLT3), suggesting synergy, while others were mutually exclusive, suggesting duplicative pathways.
- In one study of seven patients with AML that had evolved from MDS, approximately 85 percent of bone marrow cells were clonal at the time of MDS diagnosis [41]. Whole genome sequencing of paired skin and bone marrow samples identified 11 recurrently mutated genes. Genotyping of bone marrow samples from the same patients collected at the time of AML diagnosis identified those mutations that were present at the time of MDS diagnosis (ie, NPM1, RUNX1, SMC3, STAG2, TP53, U2AF1, UMODL1, and ZSWIM4) and those that developed subsequently (ie, CDH23, PTPN11, WT1).

Consistent with the two-hit theory, expression of a chimeric protein represents only one of the genetic modifications necessary for the development of cancer and leukemia, and that the affected cell requires **additional mutational events** in order to express the transformed phenotype.

As an example, the presence of cells with the RUNX1/RUNX1T1 fusion transcript may not be sufficient, in itself, to result in AML, and may require a "second hit" for the development of AML:

- Remission bone marrow samples from patients with de novo AML (FAB -M2) with t(8;21)(q22;q22) and the RUNX1/RUNX1T1 fusion transcript have been found to harbor the aberrant fusion transcript for as many as 8 years following cessation of all chemotherapy [42].
- The RUNX1/RUNX1T1 fusion transcript has been detected in bone marrow samples from patients in remission following allogeneic bone marrow transplantation for AML [43].

Mechanisms of genetic damage

Genetic changes associated with leukemogenesis can occur following chemotherapy, ionizing radiation, chemical exposure, and infection with retroviruses. In addition, certain familial disorders are associated with an increased incidence of acute myeloid leukemia (AML). However, it must be emphasized that the vast majority of patients with de novo AML show no evidence of any of these risk factors, and the etiologic factors contributing to the development of AML remain unknown. Interestingly, in a series of 127 patients with a previous primary malignancy and secondary AML, 30 percent did not receive any chemotherapy or radiation treatment prior to the development of AML [44].

Chemotherapy-induced AML. The development of myelodysplastic syndromes (MDS) and AML following chemotherapy for a variety of malignancies (eg, breast cancer, etc) is an unfortunate complication of curative treatment strategies [45]. This identification of an increasing incidence of therapy-related AML (t-AML) in an attempt to improve cure rates emphasizes the critical importance of understanding the underlying pathogenetic mechanisms for development of t-AML [46,47].

t-AML typically develops following alkylating agent-induced damage, at a median of three to five years following therapy for the primary malignancy and is usually associated with an antecedent myelodysplastic disorder [48]. This latency period suggests that multiple mutational events are involved in the development of the malignant phenotype [31].

- Clonal chromosomal abnormalities have been reported in the majority of cases of t-AML, the most frequently reported abnormalities involving complete loss or interstitial deletions of the long arm of chromosomes 7 and/or 5.
- Other therapy-related leukemias are associated with rearrangements of the MLL gene in chromosome band 11q23. AML associated with 11q23 often develops after treatment with drugs that target DNA-topoisomerase II (eg, epipodophyllotoxins, anthracyclines) with a very short latency of 12 to 18 months following treatment, and are not typically associated with an antecedent myelodysplastic syndrome [49-52].

Ionizing radiation. Ionizing radiation shares with alkylating agents the ability to damage DNA, usually by inducing double strand breaks that may cause the mutations, deletions, or translocations required for hematopoietic stem cell transformation [45,53]. As examples, an increased incidence of AML, which may have been directly proportional to the radiation exposure [54], has been noted in atomic bomb survivors [55] as well as in radiologists and radiologic technologists chronically exposed to high levels of radiation in the period before 1950 [56]. Ionizing radiation used in the treatment of malignancies (eg, Hodgkin lymphoma, breast cancer, uterine cancer, lung cancer) has also been linked to the development of AML [57].

Chemical exposure. Exposure to high levels of benzene has been associated with a higher risk of developing AML [58,59]. Relatively low-level exposure to benzene by petroleum distribution workers has been associated with an increased risk of developing myelodysplastic syndrome, but not AML [60,61]. The risk of developing a myeloid malignancy after benzene exposure appears to be dose-related and it is unknown whether there is any safe threshold for benzene exposure [62]. Polymorphisms resulting in inactivation of NAD(P)H:quinone oxidoreductase 1 (NQO1), an enzyme which detoxifies quinones and reduces oxidative stress, have been associated with an increased risk of de novo [63] and therapy-related acute leukemia [64], as well as a greater risk of benzene-induced hematotoxicity and leukemia [65]. For de novo AML, the most significant effect of low or null NQO1 activity was observed among patients with chromosomal translocations and inversions (odds ratio: 2.4), and was especially high for those with inv(16) (odds ratio: 8.1) [63].

Infections. In a number of animal models, retroviruses have been demonstrated to play an important role in leukemogenesis, and the human T-lymphotropic virus type I (HTLV-I) is associated with adult T cell leukemia-lymphoma [66]. In AML, however, despite extensive investigation, there has been no clear association of a retrovirus with leukemogenesis [67].

1.2.1. Molecular genetics of acute myeloid leukemia

Acute myeloid leukemia develops as the consequence of a series of genetic changes in a hematopoietic precursor cell. These changes alter normal hematopoietic growth and differentiation, resulting in an accumulation of large numbers of abnormal, immature myeloid cells in the bone marrow and peripheral blood. These cells are capable of dividing and proliferating, but cannot differentiate into mature hematopoietic cells. Similar to other malignancies, the genetic alterations in AML include mutation of oncogenes as well as the loss of tumor suppressor genes. In contrast to most solid tumors, many hematologic malignancies are associated with a single characteristic cytogenetic abnormality and specific cytogenetic abnormalities identified by karyotype analysis have considerable prognostic significance for patients with AML and affect treatment planning.

1.2.1.1. Cytogenetics in acute myeloid leukemia

Cytogenetic analysis of metaphase cells is a key component to the evaluation of all patients with newly diagnosed or suspected AML. The malignant cells in most patients with AML have non-random, acquired clonal chromosomal abnormalities. The principal classes of cytogenetic alterations are:

- chromosomal translocation (**t**): process by which a break in at least two different chromosomes occurs, with exchange of genetic material. Reciprocal translocation refers to an exchange between two or more chromosomes in which there is no obvious overall loss of chromosomal material.
- chromosomal inversion (**inv**): two breaks in the same chromosome with rotation of the intervening material.
- chromosomal deletion (**del**): loss of chromosomal material. An interstitial deletion results from two breaks in a single chromosome with the loss of intervening material.
- monosomy: a form of genetic loss in which an entire chromosome is lost.

Using standard banding techniques, 50 to 60% of patients with AML de novo have abnormal karyotypes [68]. The most common karyotype results are:

- normal (41%)
- t(15;17)(q24.1;q21.1) and variants (13%)
- trisomy 8 (10%)
- t(8;21)(q22;q22) and variants (7%)
- 11q rearrangements (6%)
- inv(16)(p13.1q22)/t(16;16)(p13.1;q22) (5%)

In some cases, specific cytogenetic abnormalities are closely, and sometimes uniquely, associated with morphologically and clinically distinct subsets of the disease. As such, the 2008 WHO classification of tumors of the hematopoietic and lymphoid tissues uses genetic findings in addition to morphologic, immunophenotypic, and clinical features to define distinct subtypes of AML. In addition to establishing the type of AML, specific cytogenetic abnormalities have diagnostic, prognostic, and therapeutic importance (see below, **"Classification of acute myeloid leukemia"**).

1.2.1.2. Gene mutations

Gene sequencing studies have shown that, on average, de novo AML cases contain more than 10 significant gene mutations, many of which can be broadly grouped into 9 categories of genes thought to effect leukemogenesis [69]:

1. DNA-methylation
2. tumor suppression
3. transcription-factor fusions
4. nucleophosmin
5. signaling
6. chromatin-modification
7. myeloid transcription factor
8. cohesin complex
9. spliceosome complex

The most common genes mutated and the prognostic significance in adult patients with AML are reported in **Table 2** [70-72]. Abnormalities in FLT3, NPM1, KIT, and CEBPA have been the most widely studied. Other gene mutations, such as those involving WT1 (Wilms tumor 1), meningioma 1 (MN1), RUNX1, TET2, IDH1, IDH2, ASXL1, DNMT3A, or RAS, may also have prognostic significance, but need further confirmation in prospective studies.

Table 2 - Molecular markers in acute myeloid leukemia

Gene	Frequency in de-novo AML	Frequency in CN AML	Associations	Esclusions	Prognostic significance
***FLT3*-ITD**	20 - 25%	30 - 35%	APL, t(6;9),*NPM1*	---	Adverse in CN AML
***FLT3*-TKD**	5%	14%	*NPM1*	---	Controversial
NPM1	35%	50%	*FLT3*-ITD, *FLT3*-TKD, *DNMT3A*, *IDH1*,*IDH2*	Biallelic *CEBPA*	Favorable in CN AML
CEBPA	7%	8 - 19%	*FLT3*-ITD	*NPM1*	Biallelic favorable in CN AML
KIT	6%	25%	CBF AML	Other karyotypes	Adverse in CBF AML
DNMT3A	14 - 22%	20 - 33%	*NPM1*, *FLT3*	*CEBPA*, *MLL* r	Possibly adverse in CN AML
TET2	8 - 12%	23%	---	*IDH1*, *IDH2*	Controversial
IDH1*, *IDH2	8 - 16%	30%	*NPM1*, *FLT3*	*TET2*, *WT1*	Controversial
ASXL1	5 - 30%	10%	---	Possibly *CEBPA*	Adverse in CN AML

CBF: core-binding factor; CN: cytogenetically normal; APL: acute promyelocytic leukemia

FLT3. FLT3 (FMS-like tyrosine kinase 3) is a transmembrane tyrosine kinase receptor that stimulates cell proliferation upon activation.

There are two main types of FLT3 mutations. The most common are internal tandem duplications (ITD) of different length, that result in ligand-independent activation of the FLT3 receptor and a proliferative signal [73-76]. Alternatively, point mutations in the activating loop of the kinase domain (TKD) of FLT3 may result in tyrosine kinase activation of FLT3 [77]. Internal transmembrane duplications of the FLT3 gene (FLT3-ITD) are quite common in AML, particularly in patients with normal karyotypes. It has been proposed that FLT3-ITD mutational status is the primary predictor of poorer survival among patients with intermediate-risk AML by karyotype analysis [78-83], with an estimated 2-year progression-free survival rates of 20% and 4-year overall survival of approximately 20% [84]. In contrast, the FLT3-TKD mutations do not appear to be associated with the same poor outcome as FLT3-ITD [85].

NPM1. Nucleophosmin (NPM1) is a ubiquitously expressed phosphoprotein that normally shuttles between the nucleus and cytoplasm. It is involved in ribosomal protein assembly and transport and the regulation the tumor suppressor ARF (cyclin-dependent kinase inhibitor 2A). Abnormalities in the nucleophosmin (NPM1) gene are found in approximately 25 and 50 percent of patients with de novo AML or de novo normal karyotype AML, respectively. Mutation of NPM1 in AML impairs its transport to the nucleus such that it is retained in the cytoplasm [86]. Younger and older patients with NPM1 mutation without FLT3-ITD demonstrated improved outcomes, although the mechanism for increased chemosensitivity is not known [68,82,87-91].

CEBPA. The CCAAT/enhancer binding protein alpha (CEBPA) gene encodes a transcription factor essential for myeloid differentiation [92-93]. CEBPA mutations can be found in approximately 7 percent of patients with newly diagnosed AML [83,94] and in 8 to 19 percent of patients with cytogenetically normal AML [70]. Patients with cytogenetically normal AML, double mutations of CEBPA (either two different mutations or one homozygous mutation) and negative for FLT3-ITD mutations have a significantly longer median overall survival that is independent of other high-risk molecular features [82,94-100].

KIT. Mutations of the KIT gene can be detected in approximately 6% of newly diagnosed AML and in 20 to 30 percent of patients with AML and either t(8;21) or inv(16). While some studies suggest that KIT gene mutations confer a higher risk of relapse and adversely affect overall survival in core-binding factor AML [101-102], others suggest that this negative prognostic effect is only seen among AML with t(8;21) [83,103-104].

Gene expression profiling. Several studies have analyzed leukemia cells from patients with AML and have identified gene signatures that may be used to distinguish subsets with different outcomes [105-107]. Subgroups with different gene expression profiles have been found in patients with normal cytogenetics, as well as those with well defined cytogenetic changes, such as t(8;21) and inv(16), while other groups, such as

t(15;17), appeared to be more homogeneous in their signature [108-109]. There was still a wide range of outcomes in the prognostic groupings defined by GEP and gene profiling in AML cannot as yet be used as a predictor in individual patients. However, these initial GEP data confirm the importance of cytogenetic subgroups of AML as relatively homogeneous diseases, since leukemias with distinct translocations tend to have very similar gene expression patterns [110], and may contribute to subdivide the large group of patients with normal karyotypes into different biological subsets with different outcomes [111]. Furthermore, GEP data suggest the role of a leukemic stem cell in the pathogenesis of AML [112].

1.2.2. Classification of acute myeloid leukemia

Classification of the acute leukemias has traditionally relied upon the French-American-British (FAB) morphologic classification system, reflecting the predominant cell type and relating that cell to its presumed normal counterpart (see **Table 1**) [113,114]. Actually, AML is classified using the World Health Organization (WHO) classification system based upon a combination of morphology, immunophenotype, genetics, and clinical features [115,116].

There are four main groups of AML recognized in the 2008 WHO classification system (see **Table 3**):

- AML with recurrent genetic abnormalities
- AML with myelodysplasia-related features
- Therapy-related AML
- AML, not otherwise specified

Table 3 - WHO classification of acute myeloid leukemia

AML with recurrent genetic abnormalities	**% of AML**
AML with t(8;21)(q22;q22); *RUNX1-RUNX1T1*	7
AML with inv(16)(p13q22) or t(16;16)(p13;q22); *CEFB-MYH11*	5
Acute promyelocytic leukemia with t(15;17)(q22;q12); *PML-RARA*	13
AML with t(9;11)(p22;q23); *MLLT3-MLL*	6
AML with t(6;9)(p23;q34); *DEK-NUP214*	1
AML with inv(3)(q21q26.2) or t(3;3)(q21;q26.2); *RPN1-EVI1*	1
AML (megakaryoblastic) with t(1;22)(p13;q13); *RBM15-MKL1*	<0.5
AML with mutated NPM1 (provisional entity)	30
AML with mutated CEBPA (provisional entity)	6-15
AML with myelodysplasia-related features	
Therapy related AML	
AML, not otherwise specified	**% of AML** (% of AML, NOS)
AML with minimal differentiation (M0)	<5 (6)
AML without maturation (M1)	5-10 (25)
AML with maturation (M2)	10-14 (28)
Acute myelomonocytic leukemia (M4)	5-10 (21)
Acute monoblastic/acute monocytic leukemia (M5)	5-10 (15)
Acute erythroid leukemia (M6)	<5 (4)
Acute megakaryoblastic leukemia (M7)	<1 (1)
Acute basophilic leukemia	<1
Acute panmyelosis with myelofibrosis	<1

1.2.2.1. AML with recurrent genetic abnormalities

This group includes seven specific AML subtypes with defined structural abnormalities (see **Figure 4**) and two provisional entities identified at the molecular level (mutated NPM1 and mutated CEBPA).

- AML with the **t(8;21)(q22;q22);RUNX1-RUNX1T1** is seen in approximately 7 percent of adults with newly diagnosed AML. This translocation juxtaposes the RUNX1 (previously AML1 or core binding factor alpha-2) gene on chromosome 21 with the RUNX1T1 (previously ETO or MTG8) gene on chromosome 8 to form a RUNX1/RUNX1T1 chimeric product. RUNX1 heterodimerizes with another protein, core binding factor beta (CBFB), to form a transcription factor. The RUNX1/CBFB transcription factor binds directly to an enhancer core motif that is present in the transcriptional regulatory regions of a number of genes that are critical to hematopoietic stem and progenitor cell growth, differentiation, and function. Leukemogenesis by RUNX1-RUNX1T1 probably results from both altered transcriptional regulation of normal RUNX1 target genes and activation of new target genes that prevent programmed cell death and/or cellular differentiation pathways. Cases of AML with the t(8;21) have a morphologically distinct phenotype, characterized by myeloblasts with basophilic cytoplasm, indented nuclei, and prominent Auer rods. It portends a favorable prognosis in adults.

- AML with the **inv(16)(p13.1q22)** or **t(16;16)(p13.1;q22);CBFB-MYH11** represents approximately 5 percent of newly diagnosed AML and typically demonstrates monocytic and granulocytic differentiation with abnormal eosinophils in the bone marrow. The inversion breakpoint at 16q22 occurs near the end of the coding region of the core binding factor beta (CBFB) gene, which encodes one subunit of the heterodimeric RUNX1/CBFB transcription factor. This transcription factor binds directly to an enhancer core motif that is present in the transcriptional regulatory regions of a number of genes that are critical to myeloid cell growth, differentiation, and function. A smooth muscle myosin heavy chain gene (MYH11) is interrupted by the breakpoint on 16p. A fusion protein is produced containing the 5' region of CBFB (165 of 182 amino acids), including the domain that heterodimerizes with RUNX1, fused to the 3' portion of MYH11. The resultant CBFB/MYH11 fusion protein appears to act by disrupting the function of the RUNX1/CBFB transcription factor, resulting in the repression of transcription. Patients with inv(16) or t(16;16) generally have a good response to intensive chemotherapy.

- the balanced translocation **t(15;17)(q24.1;q21.1)** is seen in 13 percent of newly diagnosed AML and it is highly specific for acute promyelocytic leukemia (APL). The breakpoint on chromosome 17 occurs within the first intron of the alpha retinoic acid receptor gene (RARA) in most patients, whereas the break on chromosome 15 occurs within the PML gene. The translocation results in a PML/RARA fusion gene that contains most of the PML coding sequences, and the DNA binding and ligand binding domains of the RARA gene. The PML/RARA fusion protein shows reduced sensitivity to retinoic acid in terms of dissociation of N-CoR, a ubiquitous nuclear protein that mediates transcriptional repression. This could lead to persistent transcriptional repression, thereby preventing differentiation of promyelocytes. APL is a unique clinicopathological entity characterized

by the infiltration of the bone marrow by promyelocytes, often with a folded, reniform or bilobed nucleus, in association with clinical or laboratory evidence of disseminated intravascular coagulation and fibrinolysis. APL represents a medical emergency with a high rate of early mortality, often due to hemorrhage from disseminated intravascular coagulation. It is critical to start treatment as the diagnosis is suspected based upon cytologic criteria, and before definitive cytogenetic confirmation of the diagnosis. Patients with APL have an excellent prognosis when appropriate treatment is begun promptly. Several variant chromosome translocation involving RARA, but not PML have been identified in APL, such as the t(5;17), and t(11;17).

- **Rearrangements of 11q** are seen in approximately 6 percent of young adults with newly diagnosed AML. There are over 100 different recurring rearrangements that involve 11q23, with many different translocation partners in AML, especially the monoblastic and myelomonocytic types. Translocations of 11q23 involve the KMT2A gene (lysine (K)-specific methyltransferase 2A, previously called mixed-lineage, leukemia [MLL]). All known breakpoints fall within an 8.3 kb breakpoint cluster region of the gene encompassing exons 5 to 11. KMT2A is a DNA-binding protein that methylates histone H3 lysine 4 (H3K4), and positively regulates gene expression by binding to open chromatin structures at the active promoter regions of various genes, including multiple Hox genes, that are important in hematopoietic and lymphoid cell development, including myelomonocytic differentiation. Translocations of KMT2A result in the formation of a chimeric gene on the derivative 11 chromosome, consisting of the 5' region of KMT2A and the 3' region of the partner gene from the other chromosome, with subsequent expression of fusion mRNAs. The most common translocation involves KMT2A and the MLLT3 (AF9) gene at 9p22 in the t(9;11)(p22;q23). The t(9;11) translocation can present with a high white count, disseminated intravascular coagulation, and gingival or skin infiltration. Morphologically, monoblasts and promonocytes usually predominate. In general, patients with t(9;11)(p22;q23); KMT2A-MLLT3 tend to have an intermediate response to standard therapy, while leukemia patients with other 11q23/KMT2A rearrangements have a very dismal prognosis.

- AML with **t(6;9)(p23;q34); DEK-NUP214** is seen in approximately 1 percent of patients with newly diagnosed AML. The translocation results in the juxtaposition of DEK on chromosome 6 with NUP214 (also known as CAN) on chromosome 9. This results in the creation of a nucleoporin fusion protein that acts as a transcription factor and also alters nuclear transport. This subtype of AML typically presents with basophilia, pancytopenia, single or multilineage dysplasia with circulating monoblasts and promonocytes. Patients with the t(6;9)(p23;q34) typically have a poor outcome with standard therapy, which may be a result of the lesion itself or may reflect the higher than normal prevalence of FLT3 internal tandem duplications mutations (70%), which are known to convey a poor prognosis.

- AML with **inv(3)(q21q26.2)** or **t(3;3)(q21;q26.2);RPN1-EVI1** account for approximately 1 percent of AML cases. Cytogenetic abnormalities of 3q are associated with thrombocytosis in the peripheral blood and increased atypical megakaryocytes in the bone marrow of patients with AML. These

abnormalities are seen in de novo AML and in therapy-related MDS/AML and are associated with a poor response to therapy. The specific cytogenetic abnormalities involve bands 3q21 and 3q26.2 simultaneously, and they include the inv(3)(q21q26.2), t(3;3)(q21;q26.2), and the ins(5;3)(q14;q21q26.2) (insertion of chromosomal material from 3q into 5q). These abnormalities result in the activation of the MECOM (EVI1) gene, located at 3q26.2. MECOM encodes a zinc-finger transcription factor that interacts with a number of transcriptional and epigenetic regulators (CREBBP, CTBP, HDAC, KAT2B [P/CAF], SMAD3, GATA1, GATA2, DNMT3A, and DNMT3B), and mediates chromatin modifications and DNA hypermethylation. Depending on its binding partners, MECOM can act as a transcriptional activator to promote the proliferation of hematopoietic stem cells (eg, when bound to GATA2) or as a transcriptional repressor inhibiting erythroid differentiation (eg, when bound to GATA1). Abnormal expression of MECOM has also been detected in patients with myeloid leukemia and a normal karyotype, suggesting that inappropriate activation of this gene occurs through various mechanisms.

- AML with the **t(1;22)(p13;q13);RBM15-MKL1** is a rare entity accounting for <0.5 percent of cases of newly diagnosed AML. It is typically a megakaryoblastic process occurring in infants, who present with marked hepatosplenomegaly, anemia, thrombocytopenia, and a moderately elevated white cell count, and sometimes it can present as a mass and mimic sarcoma. This translocation involves the RNA-binding motif protein-15 (RBM15, also known as OTT) and a DNA binding motif protein known as megakaryocyte leukemia-1 (MKL1, also known as MAL). MKL1 is involved in the normal production of platelets. The role of the resultant chimeric protein in leukemogenesis is poorly understood, but may include the modulation of chromatin organization, HOX-induced differentiation, or extracellular signalling pathways. The prognostic significance of the t(1;22)(p13;q13) with modern therapy is unclear.

Figure 4 - Recurring chromosomal abnormalities in acute myeloid leukemia

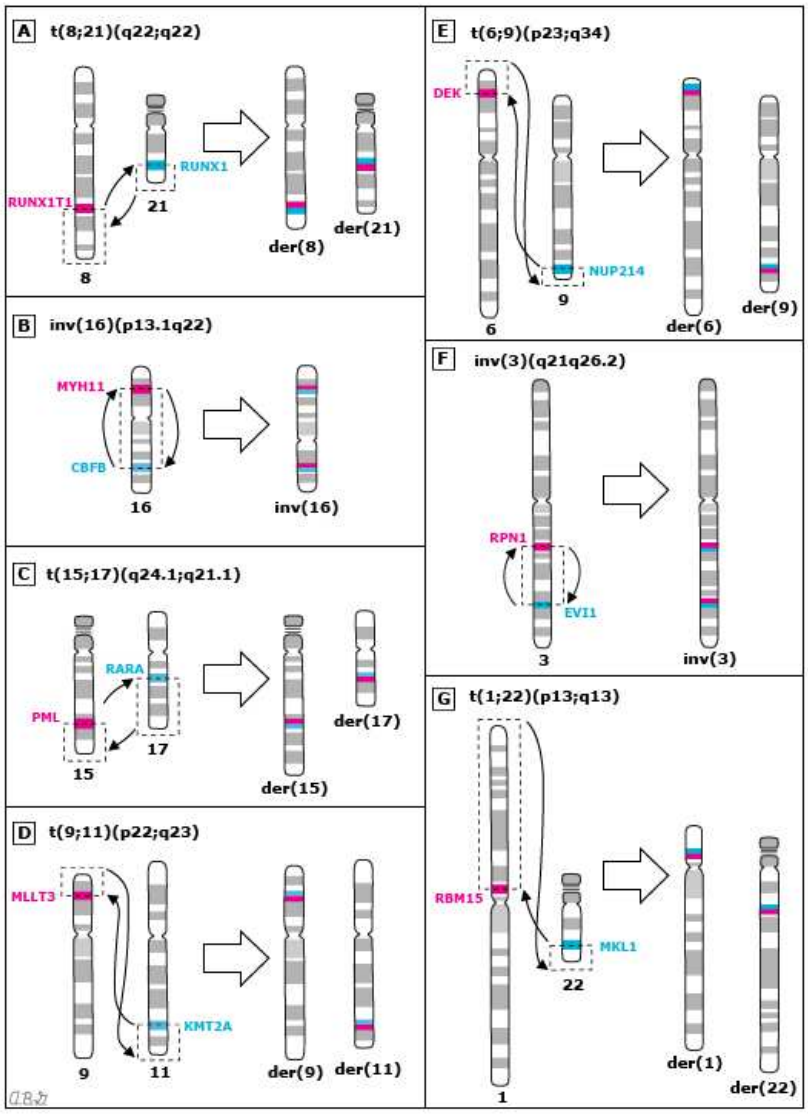

Reproduce from: UpToDate Topic 4544 Version 19.0 Graphic 53821 Version 8.0.

1.2.2.2. AML with myelodysplasia-related features

AML with myelodysplasia (MDS)-related features (previously called AML with multilineage dysplasia) is defined by cases that fit the criteria for a diagnosis of AML (≥20 percent blasts), without a history of prior cytotoxic therapy for an unrelated disease, with one or more of the following three characteristics associated with myelodysplasia;

- AML that evolves from previously documented myelodysplastic syndrome
- AML that demonstrates MDS-related cytogenetic abnormalities, such as monosomy 5 or del(5q), monosomy 7 or del(7q), isochromosome 17p
- AML with morphologically identified multilineage dysplasia, defined as dysplasia present in ≥50 percent of cells in two or more hematopoietic lineages

Patients with AML who have a prior history of MDS or have MDS-related cytogenetic abnormalities have a poor outcome with conventional therapy. Such patients frequently demonstrate multilineage dysplasia. In contrast, the identification of multilineage dysplasia in the absence of these two features may not predict a poor outcome.

1.2.2.3. Therapy-related myeloid neoplasm

Persons who are exposed to cytotoxic agents are at risk of developing acute myeloid leukemia (t-AML), myelodysplastic syndrome (t-MDS), and myelodysplastic syndrome/myeloproliferative neoplasms (t-MDS/MPN). These conditions lie along a continuum of disease and are categorized by the 2008 WHO classification system as therapy-related myeloid neoplasms (t-MN) [116]. This is a heterogeneous and poorly defined group of patients who have a shorter median survival than patients with de novo AML, MDS, or MDS/MPN.

The diagnosis of therapy-related myeloid neoplasm (t-MN) is made when evaluation of the peripheral blood and bone marrow demonstrates morphologic, immunophenotypic, and cytogenetic changes consistent with the diagnosis of AML, MDS, or MDS/MPN in a patient with prior exposure to cytotoxic agents. Therapy-related myeloid neoplasms account for approximately 10 to 20 percent of all cases of AML, MDS, and MDS/MPN [117]. The incidence among patients treated with cytotoxic agents varies according to the underlying disease, specific agents, timing of exposure, and dose [118,119]. Patients can present at any age, but the median age at diagnosis is 61 years [120,121]. The proportion of patients with a prior hematologic malignancy or a prior solid tumor is approximately equal and accounts for the large majority of cases. Five to 20 percent of patients will have a history of exposure to cytotoxic therapy for benign disorders while a similar proportion will have undergone an autologous hematopoietic cell transplantation (HCT).

Several cytotoxic agents have been implicated (see **Table 4**). The latency period between first exposure to a cytotoxic agent and the development of t-MN ranges from one to 10 years and varies by cytotoxic agent:

- t-MN after exposure to alkylating agents or radiation therapy typically presents after a latency period of approximately 5 to 7 years. Two-thirds of these patients are first recognized by evidence of myelodysplasia (usually trilineage dysplasia), marrow failure, and pancytopenia. The chromosomal abnormalities seen in these t-MNs often involve complex abnormalities and monosomies such as -5 or -7 that have been associated with unfavorable risk
- t-MN that develops after the use of topoisomerase II inhibitors has a considerably shorter latency period of one to three years and most often presents with overt leukemia and rarely with MDS or MDS/MPN. The cytogenetic alterations typically apparent in these t-MNs often involve 11q23 abnormalities, such as t(9;11), or 21q22 abnormalities, such as t(8;21) or t(3;21)

The latency periods with other agents are not as clear. In addition, patients often have a history of exposure to multiple agents making the responsible factor difficult to determine.

Clonal chromosomal abnormalities are usually present in t-MDS prior to the evolution to leukemia, and these changes are often multiple and complex. Multiple clinical and biological subsets of t-MN have been recognized, and these are correlated with the specific therapy administered for the primary disease.

Table 4 - Cytotoxic agents implicated in therapy-related myeloid neoplasm

Class	Agent
Alkylating agents	melphalan, cyclophosphamide, nitrogen mustard, chlorambucil, busulfan, carboplatin, cisplatin, dacarbazine, procarbazine, carmustine, mitomycin C, thioTEPA, lomustine, bendamustine, and others
Topoisomerase II inhibitors	etoposide, teniposide, doxorubicin, daunorubicin, mitoxantrone, epirubicin, amsacrine, and actinomycin
Antimetabolites	thiopurines, mycophenolate, and fludarabine
Antitubulin agents *(usually in combination with other agents)*	vincristine, vinblastine, vindesine, paclitaxel, and docetaxel
Ionizing radiation therapy	given as large fields that include the bone marrow

Alkylating agents and/or radiation therapy. Following alkylating agents and/or radiation therapy the most common type of t-MN is due to damage from alkylating agents. The alkylating agents react directly with DNA, inducing t-MN with unbalanced aberrations, primarily loss of chromosome material. Involvement of chromosomes 5 and/or 7 are characteristic of this subtype of therapy-related disease [122-128], and may be related to polymorphisms in enzymes responsible for modifying host responses to damage caused by leukemogens such as benzene and alkylating agents [129-131].

In a series of 306 patients with t-MN, 92 percent had clonal cytogenetic abnormalities and an abnormal karyotype with loss of all or part of chromosomes 5 and/or 7 was observed in 93 percent [127]:

- Normal karyotype 8%
- Abnormalities of chromosomes 5 and/or 7 70%
    - -7 or del(7q) 50%
    - del(5q)/t(5q) 43%

Some specific translocations also occur in t-MN following multiagent chemotherapy, as chromosomal rearrangements at 11p15 (NUP98 gene, which encodes a component of the nucleoporin complex) [132,133] or mutations and loss of heterozygosity of the TP53 tumor suppressor gene located on chromosome band 17p13 [134]. Mutations of TP53 are associated with abnormalities of chromosome 5 and a complex karyotype.

DNA topoisomerase II inhibitors. The second subtype of t-MN occurs in patients who have been treated with chemotherapeutic drugs that inhibit DNA topoisomerase II (eg, etoposide, teniposide, doxorubicin, mitoxantrone, epirubicin, dexrazoxane).

Balanced translocations occur in this type of t-MN, and most often involve the KMT2A gene at 11q23 or the RUNX1 gene at 21q22 [122,125,128,135,136]. Another recurring translocation that also involves the KMT2A gene, t(11;16)(q23;p13.3), has been described only in t-MN following exposure to a topoisomerase II inhibitor [137,138]. Patients with this translocation may present with a MDS, which is rarely seen with other 11q23 translocations [138]. The fusion gene with t(11;16)(q23;p13.3) consists of KMT2A fused to the gene that encodes CREB-binding protein (CREBBP or CBP) [137]. The fusion product retains the histone acetyltransferase domain of CREB binding protein; this may promote leukemogenesis by inducing histone acetylation of genomic regions targeted by KMT2A [139]. Topoisomerase II inhibitor therapy has also been associated with t(15;17)(q24.1;q21.1) and acute promyelocytic leukemia [140-143], as well as t(4;11) and acute lymphoblastic leukemia [144].

Mechanisms of dysplasia and leukemogenesis

The high frequency of loss of 5q and/or 7q in t-MN due to alkylating agents and/or radiation therapy suggests that critical genes located at these sites are related to myelodysplasia and myeloid leukemogenesis [145,146].

del(5q). Cytogenetic and molecular analysis of MDS, AML and t-AML with a del(5q) has resulted in the identification of a region of approximately 1 Mb that is deleted in all patients (referred to as the commonly deleted segment) proposed to contain critically important genes [146-149]. A second, distal commonly deleted segment has been identified in 5q32-q33.1 in patients with MDS with an isolated del(5q) (5q- syndrome) [150]. A number of genes located on 5q including RPS14, miR-145/46a, EGR1, NPM1, APC, and CTNNA1 have been implicated in the development of myeloid disorders due to a gene dosage effect [151].

The gene encoding RPS14 located in 5q32, which is required for the processing of 18S pre-rRNA, was identified as a candidate disease gene in the 5q- syndrome [152]. Downregulation of RPS14 in CD34+ bone marrow cells blocks the differentiation of erythroid cells, and increases apoptosis in differentiating erythroid cells in vitro. Other studies have shown haploinsufficiency of two micro-RNAs (miRNAs), miR-145 and miR-146a, that are abundant in hematopoietic stem/progenitor cells (HSPCs), are encoded by sequences near the RPS14 gene, and cooperate with loss of RPS14. The Toll-interleukin-1 receptor domain-containing adaptor protein (TIRAP) and tumor necrosis factor receptor-associated factor-6 (TRAF6) are respective targets of these miRNAs, implicating inappropriate activation of innate immune signals in the pathogenesis of the 5q- syndrome [153,154].

Other genes located on 5q that are deleted in MDS, AML, or therapy-related MDS/AML with a del(5q) include EGR1, NPM1, CTNNA1, and APC. Loss of function of Apc (adenomatosis polyposis coli gene, Apc tumor suppressor gene) in animal models produces a condition simulating MDS [155]. Similarly, loss of

function of Egr1 cooperates with mutations induced by alkylating agents to induce myeloid neoplasms in mouse models [156]. Loss of expression of the alpha-catenin (CTNNA1) gene in hematopoietic stem and progenitor cells, as a result of chromosomal deletion or epigenetic silencing, may also contribute to transformation of myeloid cells in AML patients with a del(5q) [157]. Although Npm1 heterozygous mice (Npm1+/-) develop erythroid dysplasia and dysplastic megakaryocytes, the role of NPM1 in the pathogenesis of MDS/AML is unclear, since NPM1 is neither deleted in many patients with a del(5q), nor have mutations been identified in the remaining allele [158]. These results provided support to the current model that the cooperative loss of multiple genes on 5q is required for the pathogenesis of myeloid disorders with a del(5q).

del(7q) — To determine the location of genes on 7q that may be involved in myelodysplasia and myeloid leukemogenesis, the breakpoints and the extent of the del(7q) were evaluated in 55 patients with primary MDS or de novo AML and in 26 patients with t-MN [159]. This analysis suggested that there may be two distinct deleted segments of chromosome 7. The majority of patients had proximal breakpoints in q11.2-22 and distal breakpoints in q22-36. The smallest overlapping deleted segment was within q22. A minority of patients had involvement of q31-36, with a commonly deleted segment consisting of q32-33.

FISH was used to define the deleted segment at 7q22 [159]. The commonly deleted segment was 2 to 3 Mb; a slightly more distal, but an overlapping, commonly deleted segment was identified in 7q in another report [160]. An overlapping, but slightly proximal, commonly deleted segment was identified, which contains the gene encoding the transcription factor CUX1, hypothesized to act as a tumor suppressor by regulating genes that promote hematopoiesis [161]. Patients with de novo or therapy-related malignant myeloid disorders with del(7q) demonstrate haploinsufficiency for CUX1. Further study is needed to determine whether haploinsufficiency of CUX1 is sufficient for the development of myeloid malignancies, or whether haploinsufficiency of additional genes on 7q are necessary. Patients with the less frequent loss of band 7q32 have a very poor prognosis, suggesting that critical genes may be present at this site [162].

Microarray-based studies of MDS and myeloproliferative neoplasma (MPN) have implicated another region on 7q, band 7q36, in the pathogenesis of these diseases. These studies revealed the presence of acquired uniparental disomy (aUPD, or acquired copy-neutral loss of homozygosity) in some cases. Further analysis led to the identification of rare patients with microdeletions and the subsequent identification of mutations in the EZH2 gene within the deleted segment. Homozygous EZH2 mutations are found in approximately 75 percent of patients with aUPD, and in 12 percent of patients with MDS/MPN (both monoallelic and biallelic mutations were detected) [163,164]. Notably, these patients typically do not have cytogenetically visible abnormalities of chromosome 7. EZH2 encodes the catalytic subunit of the polycomb repressive complex 2 (PRC2), a highly conserved histone H3 lysine 27 (H3K27) methyltransferase that influences stem cell renewal by epigenetic repression of genes involved in cell fate decisions. EZH2 was previously reported to be an oncogene in epithelial tumors, such as breast cancer; however, the mutations identified in MDS/MPN result in loss of function of the histone methyltransferase activity, suggesting that EZH2 acts as a tumor suppressor for myeloid malignancies.

1.2.2.4. AML, not otherwise specified

In addition to AML with recurring balanced translocations, and chromosomal gains and losses described above, about 40 to 50 percent of de novo AML and up to 10 percent of t-AML will have a normal karyotype by conventional cytogenetic analysis. This is a very heterogeneous group of patients with variable age, morphological features, and clinical course [68,111]. In a study of 5876 young adults with newly diagnosed de novo or secondary AML, 41 percent of patients had a normal karyotype [68]. These patients had rates of complete remission and 10-year survival of 90 percent and 38 percent, respectively.

These cases of AML that do not meet the criteria for the categories described above are classified as AML, not otherwise specified (NOS). These cases are further subclassified by morphology that is similar to that used in the previous FAB classification system (see **Table 1**). This subclassification of patients with AML, NOS does not provide additional prognostic information.

Using genomic microarray analysis, and other molecular techniques, many novel gene mutations have been identified in normal karyotype AML. These include FLT3-ITD/TKD and KMT2A-PTD, as well as mutations of NPM1, NRAS CEBPA, BAALC, and WT1. Identification of these mutations provides new insights into the pathogenesis of this group of AML with a normal karyotype, and it also is important in further clarifying prognosis.

1.2.3. Prognosis in Acute Myeloid Leukemia

Karyotype analysis with metaphase cytogenetics is a key component of the initial evaluation of a patient with AML and specific cytogenetic abnormalities in AML have considerable prognostic significance and affect treatment planning (see **Table 5**). The value of risk stratification by karyotype has been illustrated in several analyses of patients enrolled in prospective clinical trials. The largest studies were cooperative group efforts from the Medical Research Council (MRC), the Southwest Oncology Group/Eastern Cooperative Oncology Group (SWOG/ECOG), and the Cancer and Leukemia Group B (CALGB). All studies confirmed earlier results from other groups attesting to the importance of pre-treatment karyotype (see **Figure 5**) [68,165-171].

Figure 5 - Overall survival in AML patients according to cytogenetic risk categories (CALGB 8641)

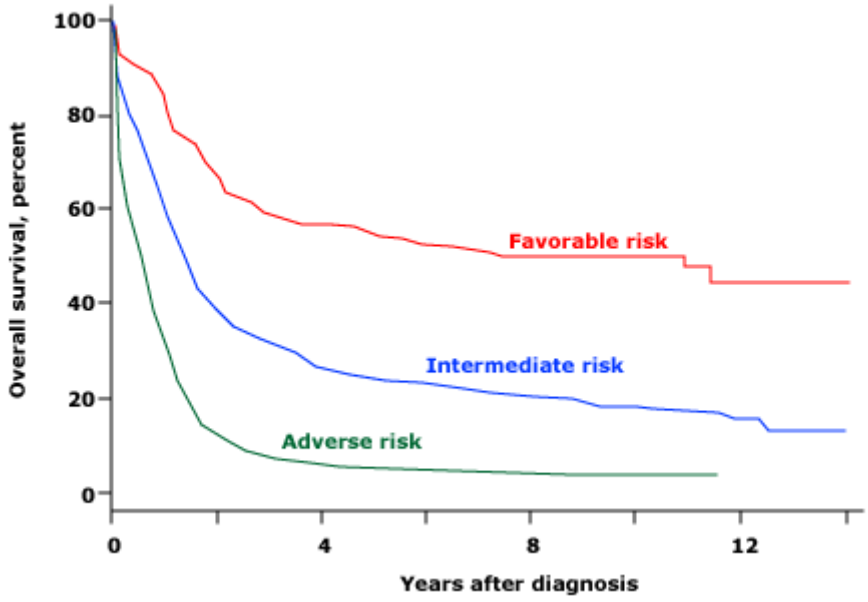

See Reference 169 (Byrd JC, Blood 2002). Favorable risk (median survival 7.6 years): t(8;21); inv(16) or t(16;16); del(9q). Intermediate risk (median survival 1.3 years): normal karyotype; -Y; del(5q); loss of 7q; t(9;11); +11; del(11q); abn(12p); +13; del(20q); +21. Adverse risk (median survival 0.5 years): complex karyotype (≥3 abnormalities); inv(3) or t(3;3); t(6;9); t(6;11); -7; +8 (sole abnormality); +8 with one other abnormality other than t(8;21), t(9;11), inv(16), or t(16;16); t(11;19)(q23;p13.1).

The specifics regarding what constitutes favorable, intermediate, and unfavorable risk have varied among the cooperative groups. While there has been general agreement that t(8;21), inv(16), and t(15;17) predict a good outcome, there has been disagreement regarding what abnormalities determine an unfavorable risk and how additional chromosomal abnormalities impact the prognostic value of known markers.

Table 5 - Recurring karyotypic abnormalities in acute myeloid leukemia

Cytogenetic	Affected genes	Clinical features	Prognosis	Incidence
t(8;21)	*RUNX1/RUNX1T1*	Younger adults (average age 30 years) AML with maturation (FAB M2) Auer rods usually present	Favorable	5 to 7%
t(15;17)	*PML/RARA*	Younger adults (average age 40 years) Atypical promyelocytes with bilobed nucleus and granules (APL, FAB M3) Disseminated intravascular coagulation	Favorable	5 to 8%
t(11;17)	*ZBTB16/RARA*	Similar to APL but with sparser granules, lack of faggot cells, and absence of the typical bilobed nucleus	Poor response to ATRA	<1%
abn(16q22)	*CBFB/MYH11*	Younger adults (average age 40 years) Acute myelomonocytic leukemia (M4) with eosinophilia	Favorable	5%
abn(11q23)	*MLL* and many partners	Older adults (average age >50 years) Acute monoblastic/monocytic leukemia (M5) Hyperleukocytosis and extramedullary disease common	Poor, except t(9;11)	3%
+8	---	Older adults (average age >60 years) Varied morphology Often associated with other chromosomal additions and deletions	Poor	3 to 10%
del 5, del 7, 5q-, 7q-, or combinations	---	Older adults (average age >60 years) Varied morphology, common in acute erythroid leukemia (M6) Common in secondary AML and MDS	Poor	15 to 20%
Inv 3	*RPN1/MECOM*	Abnormal megakaryocytes and increased platelet count Other abnormalities common (del 5,7)	Poor	<1%
abn(p17)	*TP53*	Younger adults (average age <60 years) Varied morphology Other abnormalities common (del 5,7, complex karyotype)	Poor	5%
+13	---	Older adults (average age >60 years) Varied morphology and hybrid features	Poor	1 to 2%
t(6;9)(p2;q34)	*DEK/NUP214*	AML with maturation (M2) and acute myelomonocytic leukemia (M4) with prominent basophilia	Poor	1 to 2%
t(9;22)	*BCR/ABL1*	Older adults (average age >50 years) Usually AML with minimal differentiation (M1), prominent splenomegaly, possible transformation of unrecognized CML	Poor	1%
t(1;22)	*RBM15/MKL1*	Infants (aged 0 to 3 years) Often acute megakaryoblastic leukemia (M7), prominent organomegaly	Poor	<1%
t(8;16)	*KAT6A/CREBBP*	Acute myelomonocytic leukemia (M4) and acute monoblastic and monocytic leukemia (M5), erythrophagocytosis	Poor	<1%

1.2.3.1. Medical Research Council classification

In the hierarchical Medical Research Council (MRC) cytogenetic classification system, which was developed more than a decade ago by the analysis of a cohort of 1612 children and younger adults (< 55 years), 3 cytogenetic risk groups were distinguished [172,173]. Patients with t(15;17), t(8;21), and inv(16), irrespective of the presence of additional cytogenetic changes, were assigned to the "favorable risk" group; patients lacking any of these aberrations and found to have abn(3q), del(5q), -5/-7, or complex karyotype (ie, 5 or more unrelated cytogenetic abnormalities) were defined as "adverse risk." The remaining patients, that is, those with normal karyotype and other structural or numerical abnormalities, comprised the "intermediate-risk" group. More recently, information from 5876 adults with newly diagnosed de novo (93%) or secondary AML enrolled on prospective MRC trials [68] was used to modify the MRC's prior stratification system (see **Table 6**). Using these definitions, rates of OS at 10 years were 69, 38, 33, and 12 percent for patients with favorable risk, normal karyotype, intermediate risk, and adverse risk, respectively.

Table 6 - Prognostic value of Medical Research Council classification

Risk group	Subsets	Incidence (%)	10yOS (%)
Favorable	t(15;17)(q22;q21); *PML-RARA*	16	69
	t(8;21)(q22;q22); *RUNX1-RUNX1T1*		
	inv(16)(p13.1q22) / t(16;16)(p13.1;q22);*CBFB-MYH11*		
Intermediate	Abnormalities not described in favorable or unfavorable	59	35
Adverse	abn(3q) *[excluding t(3;5)(q21-25;q31-35)]*	25	12
	inv(3)(q21q26.2) or t(3;3)(q21;q26.2); *RPN1-EVI1*		
	add(5q), del(5q), -5,		
	-7, add(7q)/del(7q),		
	t(6;11)(q27;q23)		
	t(10;11)(p11_13;q23)		
	t(11q23) *[excluding t(9;11)(p21-22;q23) and t(11;19)(q23;p13)]*		
	t(9;22)(q34;q11)		
	-17/abn(17p),		
	Complex (≥4 unrelated abnormalities)		

**: Irrespective of additional cytogenetic abnormalities*

1.2.3.2. European LeukemiaNet classification

The European LeukemiaNet (ELN) classification system integrates cytogenetic and molecular features (ie, FLT3-ITD, CEBPA, and NPM1) in AML to divide cases into four prognostic risk groups. In an analysis of 818 younger adults (<60 years) and 732 older adults with primary AML treated within cooperative group trials, the ELN classification prognostic groups had significantly different rates of complete remission (CR), disease-free survival (DFS), and overall survival (OS) at three years (see **Table 7**) [174].

Table 7 - Prognostic value of European LeukemiaNet classification

Risk group	Subsets	CR (%)	3yDFS (%)	3yOS (%)
Favorable	t(8;21)(q22;q22); *RUNX1-RUNX1T1*	Y: 96 O: 83	Y: 55 O: 24	Y: 66 O: 33
	inv(16)(p13.1q22) / t(16;16)(p13.1;q22);*CBFB-MYH11*			
	Mutated *NPM1* without *FLT3*-ITD (normal karyotype)			
	Mutated *CEBPA* (normal karyotype)			
Intermediate-I*	Mutated *NPM1* and *FLT3*-ITD (normal karyotype)	Y: 76 O: 61	Y: 23 O: 10	Y: 28 O: 11
	Wild-type *NPM1* and *FLT3*-ITD (normal karyotype)			
	Wild-type *NPM1* without *FLT3*-ITD (normal karyotype)			
Intermediate-II	t(9;11)(p22;q23); *MLLT3-MLL*	Y: 79 O: 63	Y: 34 O: 11	Y: 45 O: 16
	Cytogenetic abnormalities not classified as favorable or adverse			
Adverse	inv(3)(q21q26.2) or t(3;3)(q21;q26.2); *RPN1-EVI1*	Y: 50 O: 39	Y: 10 O: 6	Y: 12 O: 3
	t(6;9)(p23;q34); *DEK-NUP214*			
	t(v;11)(v;q23); *MLL* rearranged			
	–5 or del(5q); –7; abnl(17p); complex karyotype$^{\Delta}$			

CR: complete remission; DFS: disease-free survival; OS: overall survival; Y: younger patients; O: older patients.

** Includes all AMLs with normal karyotype except for those included in the favorable subgroup*

$^{\Delta}$ Three or more chromosome abnormalities in the absence of one of the WHO designated recurring translocations or inversions, that is, t(15;17), t(8;21), inv(16) or t(16;16), t(9;11), t(v;11)(v;q23), t(6;9), inv(3) or t(3;3)

1.2.3.3. National Comprehensive Cancer Network classification

The National Comprehensive Cancer Network (NCCN) risk classifications vary slightly from those of the MRC or ELN group. The main differences between NCCN and ELN classification are that NCCN has continued to place normal karyotype AML with FLT3-ITD mutation in the unfavorable risk group rather than in the intermediate risk group, and that patients with the favorable-risk CBF-AML [eg, t(8;21) or inv(16)/t(16;16)] with the presence of c-KIT mutation are considered in the intermediate risk group because of an higher risk of relapse (see **Table 8**) [175].

Table 8 - Prognostic value of National Comprehensive Cancer Network classification

Risk group	Subsets
Favorable	t(15;17)(q22;q21); *PML-RARA*
	t(8;21)(q22;q22); *RUNX1-RUNX1T1* without c-KIT mutation
	inv(16)(p13.1q22) / t(16;16)(p13.1;q22);*CBFB-MYH11* without c-KIT mutation
	Normal kariotype with NPM1 mutation in the absence of FLT3-ITD mutation
	Normal kariotype with biallelic CEBPA mutation in the absence of FLT3-ITD mutation
Intermediate	Normal karyotype
	+8 alone
	t(9;11)(p22;q23); *MLLT3-MLL*
	t(8;21) or inv(16) / t(16;16) with c-KIT mutation
	Other non defined
Adverse	-5, del(5q), - 7, del(7q)
	inv(3)(q21q26.2) or t(3;3)(q21;q26.2); *RPN1-EVI1*
	t(11q23) *[excluding t(9;11)(p21-22;q23)]*
	t(9;22)(q34;q11)
	t(6;9)(p23;q34); *DEK-NUP214*
	Monosomal karyotype *
	Complex (≥3 clonal chromosomal abnormalities)
	Normal karyotype with FLT3-ITD mutation

**: monosomal karyotype is defined as at least two autosomal monosomies or a single autosomal monosomy in the presence of one or more structural cytogenetic abnormalities*

1.3. WNT SIGNALING PATHWAY AND ACUTE MYELOID LEUKEMIA

Wnt/β-catenin signaling directs cell proliferation and cell fate during embryonic development and adult homeostasis. Wnt proteins were originally identified in Drosophila [176] and mice [177], which were called Wingless(Wg) and Int1, hence the name **Wnt**. In humans there are 19 secreted Wnt ligands acting both on the secreting cell and neighbouring cells and 10 frizzled receptors that can activate the canonical (Wnt/β-catenin), or non-canonical (Wnt/PCP or Wnt/Ca+) Wnt pathways. In the absence of Wnt ligand or presence of Wnt antagonists, the axin/adenomatous polyposis coli (APC)/casein kinase 1 (CK1)/glycogen synthase kinase 3 (GSK3) protein complex binds and phosphorylates β-catenin resulting in ubiquitination and proteosomal degradation of β-catenin. The pathway is activated when a Wnt ligand binds to the transmembrane domain receptor of the Frizzled family (FZD) and its co-receptor low-density lipoprotein receptor-related protein 5 or 6 (LRP5/6). FZD receptors are seven-pass transmembrane receptors which have cycteine-rich domains (CRD) in their N-terminus. Through the CRD, FZD receptor binds Wnt ligands. After an activating Wnt signal the protein Dishevelled (Dvl) is recruited to the receptor complex and the cytoplasmic tail of LRP5/6 is phosphorylated by CK1 and GSK3β. This provides a docking site for Axin1, which is then recruited to the receptor complex. Nonphosphorylated active β-catenin is then accumulated and transported to the nucleus. β-catenin forms complexes with the TCF/LEF transcription factors. In the absence of β-catenin TCF forms a transcriptional repressor complex with Groucho. Groucho is physically displaced by β- catenin and Pygopus and Legless are recruited to assemble a transcriptional activator complex. β-catenin is rapidly turned over by ubiquitination and degradation by the proteasome pathway under unstimulated conditions. This requires phosphorylation of β-catenin by a “degradation complex” consisting of APC, Axin, GSK3, and CK1, followed by binding of β -Trcp. Several Wnt inhibitors have been identified such as the extracellular Dickkopfs (DKK), secreted Frizzled-related proteins (SFRP1-5) and Wnt inhibitory factor 1 (WIF1) that prevent ligand-receptor interactions [178]. Intracellular inhibitors are DACT that interacts with Dvl [179], Wilms tumour protein 1 (WT1) that promote β-catenin ubiquitination and degradation, the nuclear proteins SRY-box containing genes (SOX) and the transcriptional repressor Hypermethylated in cancer 1 (HIC1) that interacts with the β-catenin/TCF/LEF complex, inhibiting transcription of Wnt target genes [180]. Furthermore, menin encoded by the MEN1 (Multiple endocrine neoplasia type 1) gene, inhibits the transcriptional activity of β-catenin by transporting β-catenin out of the nucleus [181].

1.3.1. Wnt/ β-catenin signaling pathway

Wnt proteins are characterized by a high number of conserved cysteine residues and are glycosylated and lipid modified at two conserved residues, which makes Wnt proteins highly hydrophobic. The palmitate is added in the endoplasmatic reticulum by the protein Porcupine (Porc) and is essential for signaling. Wnt proteins bind to the extracellular N-terminal cysteine-rich domain of the Frizzled (Fz) receptor, which is in a complex with the low density lipoprotein receptor-related protein 5 or 6 (LRP5/6). After an activating Wnt

signal the protein Dvl is recruited to the receptor complex and the cytoplasmic tail of LRP5/6 is phosphorylated by CK1 and GSK3β. This provides a docking site for Axin1, which is then recruited to the receptor complex. Axin1 is sequestered and assembly of the destruction complex is disrupted. β-catenin will accumulate in the cytoplasm and translocate to the nucleus, where it initiates transcription by activating T cell factor/lymphoid enhancer factor (TCF/LEF) transcription factors. In the absence of β -catenin TCF forms a transcriptional repressor complex with Groucho. Groucho is physically displaced by β- catenin and Pygopus and Legless are recruited to assemble a transcriptional activator complex [182-185]. β-catenin is rapidly turned over by ubiquitination and degradation by the proteasome pathway under unstimulated conditions. This requires phosphorylation of β-catenin by a “degradation complex” consisting of APC, Axin, GSK3, and CK1, followed by binding of β -Trcp [186,187]. Wnt ligands interact with the cell surface receptor, Frizzled (FZD). The initial connection between seven-transmembrane-span proteins of the Fz family and Wnt proteins came from studies in Drosophila cell culture. FZD receptors are seven-pass transmembrane receptors which have cycteine-rich domains in their N-terminus. Through the CRD, FZD receptor binds Wnt ligands. In general, it is thought that a monomeric FZD receptor transmit signals downstream upon binding with Wnt ligand, however, the crystallographic resolution of the structure of the mouse FZD8 and sFRP3 CRD domains suggested that CRDs might be able to homodimerise or heterodimerise. Furthermore, there are reports showing that dimerisation of FZD receptor activates the Wnt/β-catenin pathway and that FZD form specific homo-and hetero-oligomers. These reports suggest the wide possibility of the signal transmission mechanism downstream of FZD receptor. Upon the binding of Wnt to FZD receptor, the intracellular amino sequences, K-T-X-X-X-W directly binds to Dishevelled proteins. There are 10 reported human frizzled receptors. Phylogenetically, the Frizzled receptors fall into four groups [188].

In the late 1980s, β-catenin was independently discovered twice, on the basis of its different functions: structural and signalling. The group of Rolf Kemler isolated β- catenin, together with two other molecules (α-catenin and γ-catenin/plakoglobin), as proteins associated with E-cadherin, the key molecule of Ca2-dependent cell adhesion. These proteins were named catenins to reflect their linking of E-cadherin to cytoskeletal structures [189]. The signalling potential of β-catenin was exposed through its Drosophila orthologue Armadillo: the armadillo gene was discovered in the seminal screens for mutations affecting segmentation of the Drosophila embryo [190]. This finding was a key step in the subsequent characterization of the Wnt/β-catenin (or Wingless/ Armadillo, respectively) signalling cascade, and of the functions and mutual interactions of its individual components. Finally in the mid- 1990’s several groups independently found that the signalling function of β- catenin/Armadillo in the nucleus is mediated via TCF/LEF transcription factors, which in association with β-catenin trigger Wnt-mediated transcription [191-195]. The β-catenin protein (781 aa residues in humans) consists of a central region (residues 141–664) made up of 12 imperfect Armadillo repeats (R1–12) that are flanked by distinct N- and C-terminal domains, NTD and CTD, respectively. A specific conserved helix (Helix-C) is located proximally to the CTD, adjacent to the last ARM repeat (residues 667–683) [196]. The NTD and the CTD may be structurally flexible, whereas the central region forms a relatively rigid scaffold. This scaffold serves as an interaction platform for many β-catenin binding partners, at the membrane, in cytosol, and in the nucleus [197]. Free β-catenin is recognized by the key scaffold molecules Axin and APC, both of which can directly interact with β-catenin and also inter se. The scaffold establishes a platform for 68 associated kinases to phosphorylate β-catenin [198,199]. CK1a

phosphorylates β-catenin and therefore the scaffolding proteins Axin and APC are essential for the GSK3-mediated phosphorylation of β-catenin: although GSK3 can modify a plethora of different proteins within a cell as a free molecule, it modifies β-catenin only if it is associated with Axin and APC [200,201]. APC contributes to the establishment of the destruction complex, and stabilizes β-catenin's phosphorylation status. If N-terminally phosphorylated β-catenin is not associated with APC, after leaving the destruction complex, then it is immediately dephosphorylated by PP2A [202]. Activation of Wnt signalling leads to the disassembly of the β-catenin destruction complex and GSK3 activity is blocked. β-Catenin can dynamically shuttle between the cytoplasm and nucleus. Surprisingly, it does not contain any classical nuclear localization signal (NLS) or nuclear export signal (NES) within its polypeptide sequence. Indeed nuclear import of β-catenin was shown to occur importin-karyopterin independently [203]. Recently, β-catenin was shown to directly interact with different nuclear pore complex components (NPCs) [204,205]. By transiently and sequentially binding to different NPCs, β-catenin could pass through the nuclear pores. nucleus Once in the nucleus β-catenin can activate transcription of Wnt/β-catenin target genes. Hence, β-catenin initiates transcription onlyas a member of bipartite or multimeric complexes wherein one partner provides association with specific responseelements on target genes (e.g., Wnt response elements, WREs) and β-catenin acts as the central transcriptional activator. TCF/Lef transcription factors serve as the main nuclear partners of β catenin guiding it to specific DNA loci. Within the coactivator complex, β-catenin functions as a scaffold to link the LEF-1/TCF proteins to specific chromatin remodeling complexes, as well as to the Wnt coactivators, Bcl-9/Lgs and Pygopus. Bcl-9/Lgs and Pygopus are implicated in nuclear localization of β-catenin [206] as well as transcription [207,208].

1.3.2. Induction of WNT signaling pathway in AML

Aberrant activation of Wnt/β-catenin signaling has been linked to several cancers, including the progression of AML and other haematological malignancies [209,210]. Several studies pointed out the important role of the Wnt signaling in regulating mitotic divisions of hematopoietic stem cells (HSCs) [211]. The requirement of WNT signalling activity in HSC self-renewal and bone marrow repopulation has been indicated by the positive effect of WNT activation on hematopoietic stem cells (HSC) recovery in transplantation studies [211,212] and that WNT activation through TCF / β -catenin signalling was necessary for optimal HSC formation [213] and HSC integrity [214]. The control of self-renewal is mediated by WNT proteins produced by stromal cells and the niche and, in some cases, from the same HSCs through a paracrine/autocrine mechanism. Wnt pathway dysregulation exists in myeloid leukemias [211]; indeed, a Wnt pathway requirement for leukemia-initiating cell development in AML has emerged in a mouse model [215].

1.3.3. WNT signaling in long-term reconstituting AC133^{bright} leukemia cells

Acute myeloid leukemia is a genetically heterogeneous clonal disorder characterized by two molecularly distinct self-renewing leukemic stem cell (LSC) populations most closely related to normal progenitors and organized as a hierarchy. Ample evidence exists in mouse models that AML develops through the stepwise

acquisition of collaborating genetic and epigenetic changes in self-renewing LICs, which exhibit a committed myeloid immunophenotype and give rise to nonleukemogenic progeny in a myeloid-restricted hierarchy [216-218]. Leukemia-initiating cells are restricted only to the $CD34^{+}CD38^{-}$ population. The AC133 antigen (a glycosylation-dependent epitope of CD133) defines a desirable population of stem and progenitor cells containing in turn all the $CD34^{bright}CD38^{-}$ progenitors, as well as the $CD34^{bright}CD38^{+}$ cells committed to the granulocytic/monocytic lineage [219]. According to literature's data, the AC133 antigen expression is restricted to a rare cell population with long-term reconstituting activity, ranging from 20% to 60% of all CD34+ cells, and resulting barely detectable in $CD34^{-}$ Lin^{-} cells. In a previous study [220], our research team demonstrated the clonogenic ability of $AC133^{+}$ selected cell in qualitative terms (as capacity to produce colony forming-units granulocyte/macrophage and/or burst-forming units-erythroid in presence of appropriate stimulation) as well as in quantitative term (comparing the results with those obtained from unsorted bone marrow mononuclear cells).

In order to highlight the de-regulated pathways involved in the maintenance of a self-renewing state in LICs, in a previous study our research team performed a genome-wide functional enrichment analysis on gene expression microarray data of $AC133^{+}$ cells isolated from 33 newly diagnosed unselected non-promyelocytic AML patients and 10 healthy donors [221]. The functional enrichment methods selected the term "WNT receptor signaling pathway" (GO:0016055) as the most specific self-renewal associated dysregulated pathway in $AC133^{+}$ AML cells. Among the 103 differentially expressed Wnt genes identified, genes shown to be highly AML-specific include the WNT ligands *WNT2B, WNT6, WNT10A*, and *WNT10B* [222], the WNT/β-catenin signaling agonists including *SMYD3* [223], *DKK2* [224], *SOX4* [225], *PROP-1* [226], and *PYGO2* [227,228], antagonists including *WIF-1* [229], *KLHL12* [230], *LRP6* [231], *KREMEN1* [232], *E2F1* [233], *DACT1* [234], and *HBP1* [235], and the deregulated WNT targets including *STAT3, MYCN, ABCC4, DLX3, MARK4, RUNX2, CD24*, and *CD44* [236]. Notably, *WNT2B, WNT6, WNT10A*, and *WNT10B*, known to promote hematopoietic tissue regeneration [222], are the WNT mediators specifically upregulated in the $AC133^{+}$ AML cells. Collectively, these data were consistent with ligand-dependent activation of the regeneration-associated WNT pathway [222,237].

1.3.4. Qualitative evaluation of WNT10B and detection of $AC133^{bright}$ subpopulation

According to these data, indicating transcriptional activation of canonical WNTs, we investigated how expression of WNT is related to AML phenotype through new *in situ* approaches. The attention was placed on WNT10B, a well-known hematopoietic stem cell regenerative-associated molecule, which was the only one to be expressed by all AML patients. *In situ* mRNA detection by target-primed Rolling Circle Amplification (RCA) analysis detected WNT10B-related transcript in bone marrow (BM) sections obtained from two randomly selected AML patients at diagnosis, with β-actin as reference transcript in consecutive sections.

Visualization by using high-performance fluorescence microscopy showed a diffuse localization pattern in the tissues (see **Figure 6**), and signal distribution and RCP quantification showed a *β-actin/WNT10B* ratio close to 1, suggesting a constitutive activation of *WNT10B* transcription in the BM. In addition, we analyzed transcriptional activation of canonical WNTs focusing on genes that have been shown to be potent regulators

of stem cell functions. N-terminally dephosphorylated β-catenin (ABC) was increasingly accumulated as determined by immunoblot analysis. Remarkably, we confirmed a dramatic increase in WNT10B expression in all patient samples, except for the only patient affected by therapy-related AML.

Figure 6 - WNT10B mRNA *in situ* detection

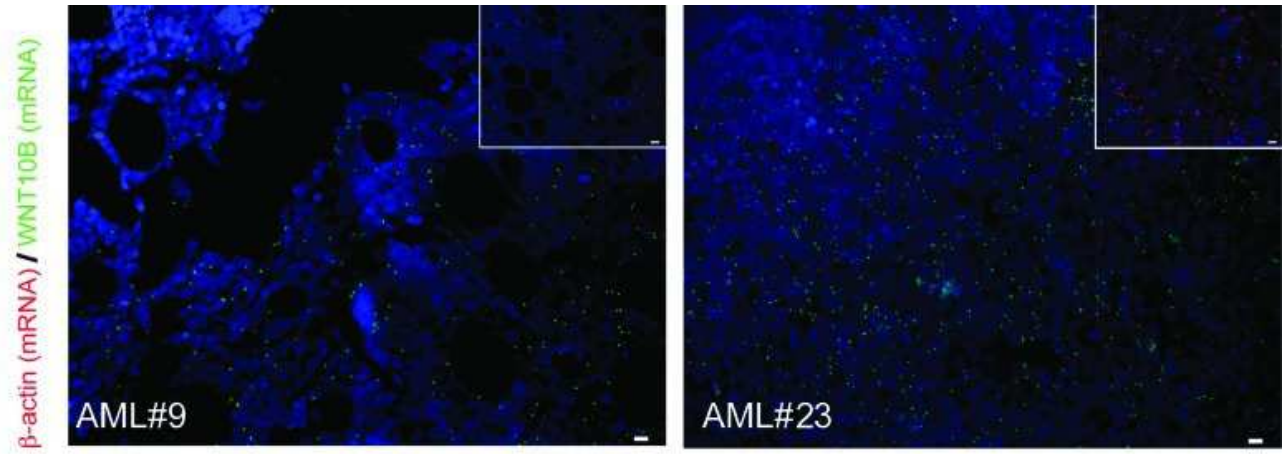

Detection with padlock probe and target-primed rolling circle amplification of individual WNT10B transcripts on BM slides from AML patients. WNT10B RCPs are shown in green (Cy5, while red RCPs represent β-actin transcripts in consecutive sections. Cell nuclei are shown in blue. Images were acquired with x20 magnification. Scale bar, 10 µm.

To better elucidate the impact of the broad WNT10B overexpression on the leukemic microenvironment, we examined its expression in histologic preparations of BM from five randomly selected AML patients at diagnosis. The AC133 immunostaining revealed islands of highly positive cells ($AC133^{bright}$) in an estimated proportion of 8% of cells, amid $AC133^{dim}$ or negative tumor blasts (**Figure 7**). These $AC133^{bright}$ showed a small diameter of the nuclei (8-10 µm) and a clonal appearance with an increased nuclear/cytoplasmatic ratio. The double immunostaining for WNT10B and ABC confirmed that WNT10B was expressed by a high proportion of leukemic cells, as well as in interstitial spaces, suggesting its secretion and release in the BM microenvironment (**Figure 8D**). In order to define the spatial relationship between AC133 and ABC positive cells in AML bone marrow cell population, we performed a double immunostaining AC133/ABC (**Figure 9**). We observed a stringent correlation between AC133 and ABC signal, suggesting that the WNT signal responsiveness function is strictly associated to $AC133^{bright}$ cells. Using ImageJ, we noted that there are two types of signal positivity: the AC133 signals were localized around the membrane perimeter, while the ABC signals defined the cytoplasmatic area. While WNT10B is diffusely expressed at mRNA and protein levels on both leukemic blasts and stromal-like cells (**Figure 8A/8D**), activation of WNT signaling marked by expression of the dephosphorylated β-catenin (ABC) was restricted to the smaller population of $AC133^{bright}$ leukemic cells (**Figure 8B/8C**), likely induced through an autocrine/paracrine mechanism (**Figure 8B/8D**).

Figure 7 - Detection of AC133^{bright} cells

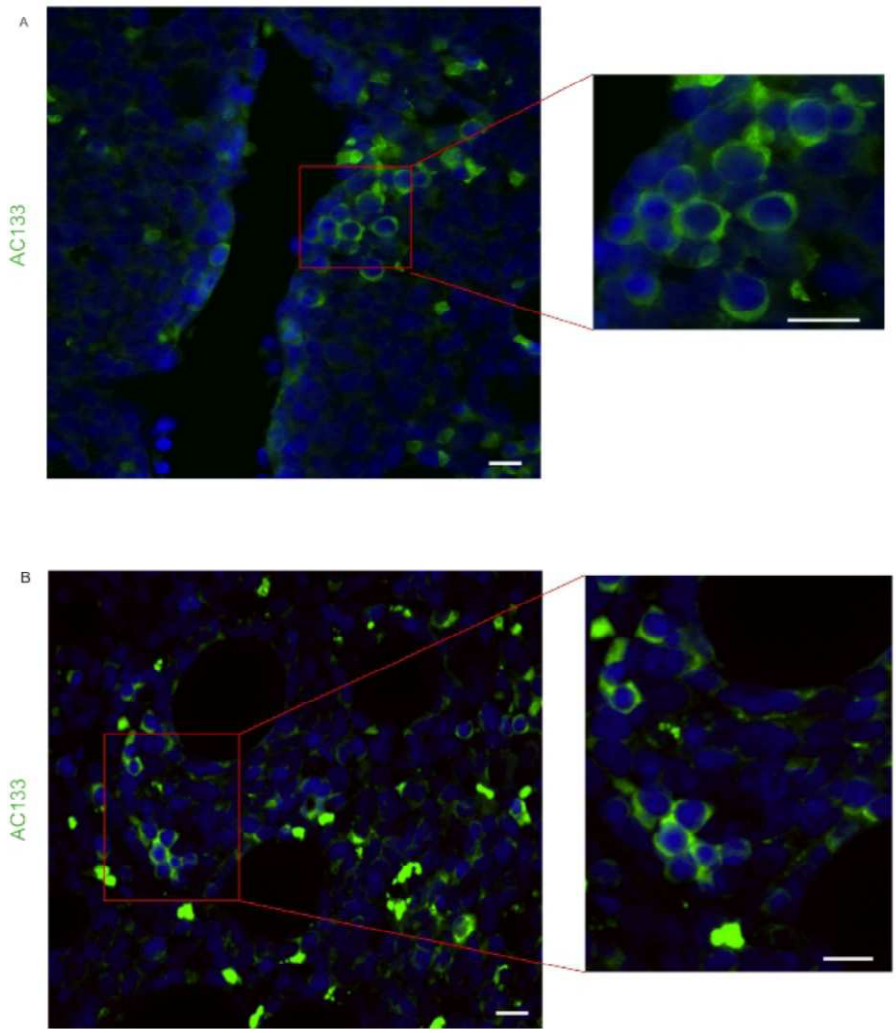

AC133 direct immunostaining on two bone marrow sections derived from AML patients, AML9 (A) and AML63 (B). The green signals, obtained with hybridization antibody labeled with dye 488 nm, define the AC133-positive cells. Two types of AC133-positive cells can be observed: a rare group of cells characterized by high bright positivity, and other cells showing a dim cytoplasmatic signal. Cell nuclei are shown in blue. Scale bar 10 µm. ***(Unpublished data, corollaries of [221])***

Figure 8 - β-Catenin activation in the subpopulation of AC133^{bright} AML cells expressing WNT10B

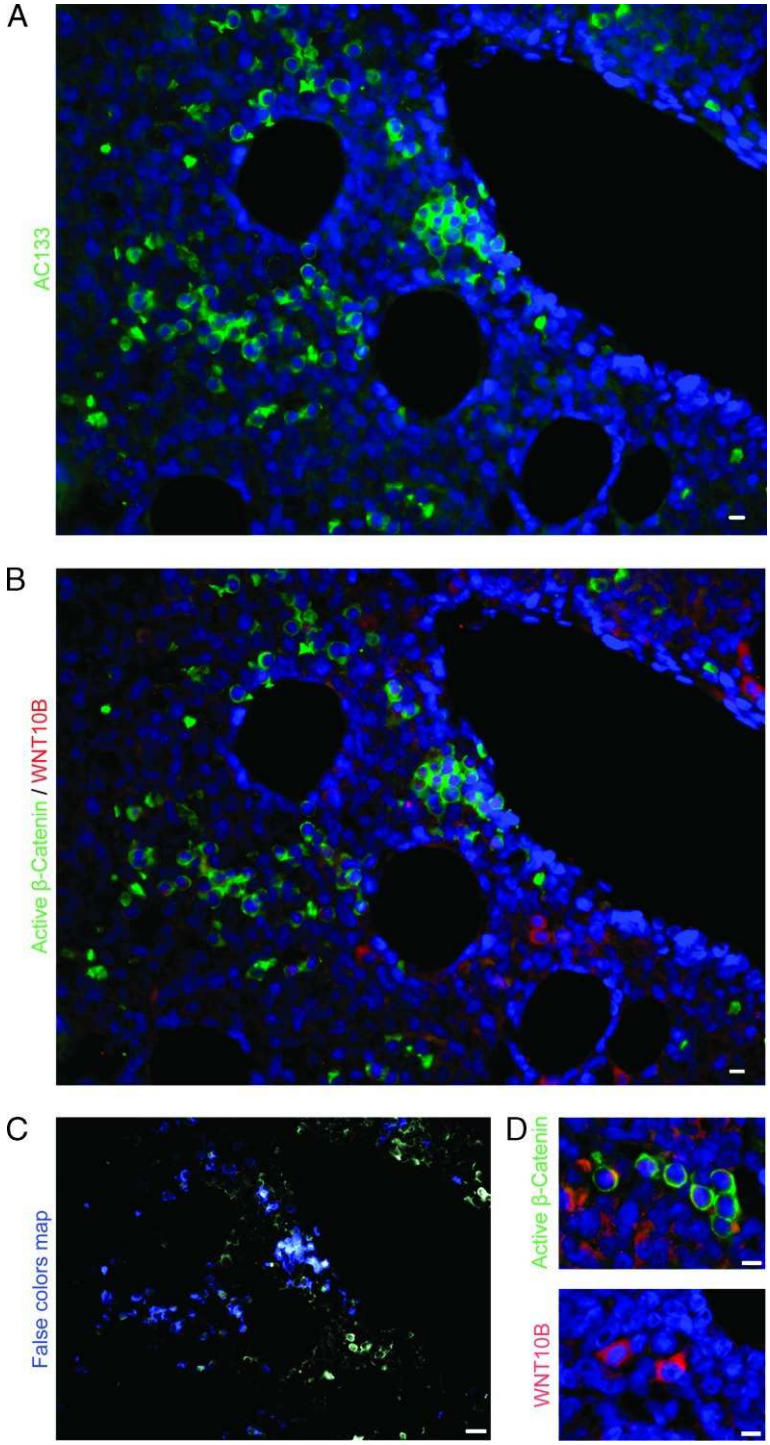

(A) Representative immunostaining micrographs show green fluorescence of cells expressing AC133 in a BM section. Cell nuclei are shown in blue. Scale bar represents 10 µm. (B) Co-staining of BM from adjacent serial section for expression of ABC (green) and WNT10B (red). Cell nuclei are shown in blue. (C) False color maps of ABC/WNT10B double positive cells (blue). (D) Morphologic detail of cells showing intense specific staining for ABC (top panels) and WNT10B (bottom panels).

Figure 9 - AC133^{bright} as marker of WNT signaling activation

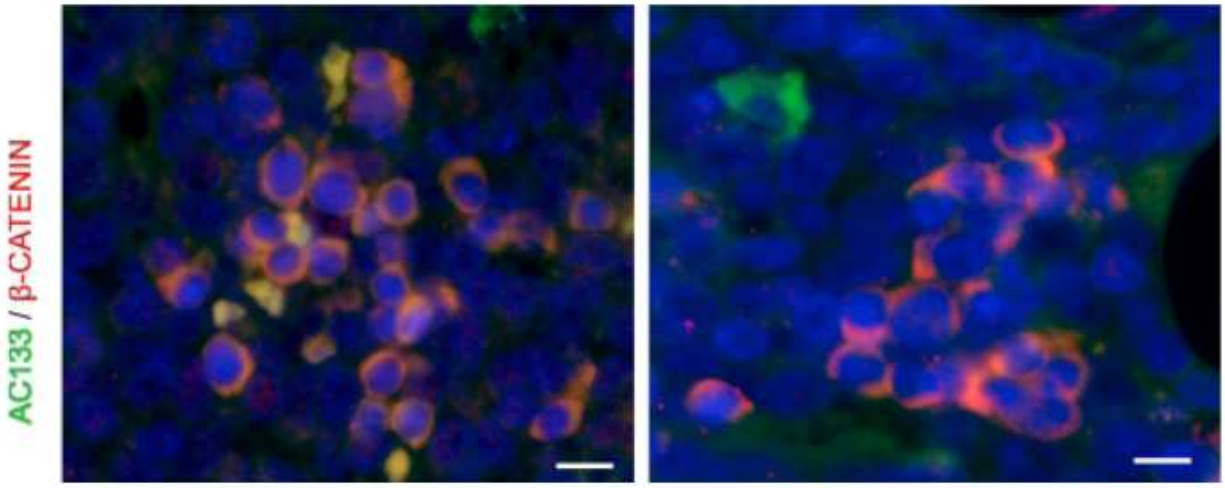

Double immunostaining for AC133 and ABC detection, on bone marrow section derived from AML9 patient. Cell nuclei are shown in blue. Scale bar 10 µm. ***(Unpublished data, corollaries of [221])***

We established a primary AC133^{+} cell culture (termed A46) selected from a 66-year-old male at diagnosis of AML-M2 with diploid karyotype and a dominant CD133.1^{+}CD34^{+}CD38^{-}CD45^{+}CD117^{+} blast population. Comparative immunostaining and conditioned medium analysis of AC133-selected A46 leukemic and normal cells revealed that AC133^{+} A46 cells synthesize and secrete WNT ligands, whereas normal BM-derived AC133^{+} cells resulted negative. Subsequently, we showed a dramatic increase of WNT10B expression and protein release within the microenvironment in the large majority of samples from AML patients recruited to this study, with the exception of a therapy-related AML patient. In accordance with previous reports [238], we have not detected *WNT10B* gene expression in normal AC133^{+} hematopoietic cells.

Leukemic stem cell functional activity in AC133+ cells was tested and significant levels of engraftment were found upon transplantation of A46 cells into sublethally irradiated Rag2-/-γc-/- mice. Then, we explored the physiological relevance of tumor-derived WNT signals by using the developing zebrafish as a biosensor. We hypothesized that WNT-secreting A46 cells transplanted into developing zebrafish embryos might act as ectopic sources of maternal WNT ligands. Consistent with our hypothesis, A46 cells retained a dorsal organizer-inducing activity with developement of ectopic axial structures, possibly correlated with their strong WNT signaling activation (see **Figure 10**). Conversely, control embryos grafted with normal AC133^{+} cells did not display alterations of the normal phenotype.

<u>Figure 10</u> – AC133+ A46 AML cells induce ectopic gene expression and secondary body axis formation upon transplantation in zebrafish embryos

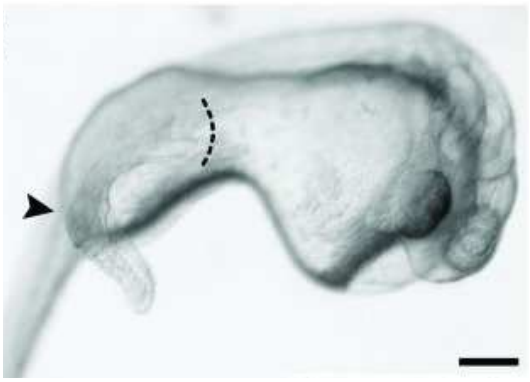

Bright-field microscopy of a 24-hpf zebrafish embryo injected with A46 AML cells (lateral view). The arrowhead and the dotted line indicate the secondary trunk/tail induced by A46 cells. Scale bars represent 150 μm.

These findings provided direct evidence that the WNT/β-catenin signaling is diffusely activated and exceeds the homeostatic range in the majority of human AML cases, with a specific transcriptional signature involving overexpression of the WNT pathway agonists and down-modulation of the major antagonists.

2. MATERIALS AND METHODS

2.1. Study population

2.1.1. Patients' characteristics and data collection

One hundred twenty-five patients with untreated AML were included in this study. Patients' characteristics are shown in **Table 9**. Each patient gave his/her informed consent for collection of clinical data, the cryopreservation of bone marrow samples and the performance of DNA-analysis for scientific purposes, in accordance with institutional guidelines. Bone marrow samples from each patient were collected and cryopreserved at diagnosis and then centrally analyzed at the University of Milan, Italy.

For each patient, data regarding history, haematologic parameters, bone marrow morphology, immunophenotype, cytogenetic, molecular analysis, and diagnosis of extra-medullary leukemia were recorded. Treatment schedule and outcome data were available for 116 out of 125 patients. Patients' data were periodically updated, centrally verified for consistency and completeness and subsequently submitted for statistical analysis. The study design adhered to the Declaration of Helsinki and approval for this study was obtained from the Niguarda Hospital Review Board.

2.1.2. Definitions and criteria for treatment response

Complete remission (CR) was defined as less than 5% of bone marrow blasts, regression of extramedullary disease, transfusion independency with peripheral neutrophil count greater than 1 000/μL and platelet count greater than 100 000/μL and disappearance of the cytogenetic and molecular markers [239,240]. Recurrent disease is defined as the reappearance of ≥ 5% blasts in the bone marrow or in the peripheral blood or as the appearance of a new extramedullary site of diseas in patients with a previously documented CR. Extramedullary disease was defined as any leukemic collection outside the bone marrow and its presence was documented either by histological, cytological or radiological criteria.

Overall survival (OS) was calculated from the date of diagnosis until death, where all living patients were censored at the time of last contact. The duration of CR was calculated from the date of the first CR until the date of the first relapse. Relapse-free survival (RFS) was calculated from the date of the first CR until the date of the first relapse, where patients were censored at the time of last contact or death not due to recurrent disease.

Table 9 - Clinical and genetic characteristics at presentation

Characteristics		
Patients, no.	125	
Median age, years (range)	51	(15 - 76)
No. men/no. women	67/58	
Median WBC, x 10^9/L (range)	16.3	(0.3 - 345)
Median Hb, g/dl (range)	8.8	(4.2 - 12.0)
Median PLT, x 10^9/L (range)	34.5	(7 - 296)
Median LDH, U/L (range)	792	(172 - 1500)
Median marrow blast, % (range)	75.0	(20 - 98)
Median peripheral blast, % (range)	58.0	(0 - 97)
Extramedullary disease, no. (%)	12	(9.6)
Cytogenetic features		
Without additional abnormalities, no. (%)	48	(38.4)
No. Abnormalities, no. (%)	13	(10.4)
Structure abnormalities, no. (%)	64	(51.2)
t(8;21)	18	
inv(16)/t(16;16)	24	
t(15;17) or variant	8	
Mutational status		
FLT3-ITD mutated cases, no. (%)	15/86	(17.4)
FLT3-TKD mutated cases, no. (%)	5/83	(6.0)
NPM1 mutated cases, no. (%)	20/46	(43.5)
Biallelic CEBPA mutated cases, no. (%)	2/11	(--)
Classification		
de novo AML, no.	112	
AML with myelodysplasia-related features, no.	6	
Therapy-related AML, no.	7	

2.1.3. Statistical analyses

All collected variables were submitted to usual descriptive methods. In particular, for continuous variables the distribution was firstly evaluated by the Shapiro-Wilk test, so that normally distributed variables were summarized with mean and standard deviation, while non-normal variables were summarized with median and range. The Pearson's chi-square test with Yates' correction for continuity and the Fisher's exact test (if applicable) were used to check the association between categorical data, after cross-tabulation. Comparisons of normally distributed continuous variables were carried out by Student's t-test or by Welch test (in the case of non-homogeneous variances between groups, previously verified by Levene's test). The Kruskal-Wallis test and the Mann-Whitney U-test were used for comparison of continuous non-normally distributed variables.

The survival analysis was carried out using the Kaplan-Meier product limit method, followed by the logrank test, to evaluate the possible differences in survival between groups. Cox univariate and multivariate regression models were also used to analyse the effects of continuous variables on survivorship. The optimal multivariate model was chosen using a backward stepwise elimination after inserting all variables showing $p < .20$ at univariate analysis.

The receiver operating characteristics curve (ROC) was traced to analyse the role of WNT transcript levels on survivorship and to search for an optimal cut-off value for WNT transcript itself. For all possible cut-off points, the total accuracy was considered together with sensitivity, specificity, positive predictive value and negative predictive value; however, the choice was made according to Youden.

Statistical analysis was done using MedCal 9.3.7.0. Statistical significance was assumed for all tests with $p < .05$.

2.2. Single cell analysis: mRNA in situ detection and Droplet Digital PCR

At present, cell and tissue analysis of cellular pathways altered in disease, including transcripts, and protein levels, localizations, modifications and dynamic interactions, offer insights into the molecular basis of disease, and it will also provide a basis for directed biomarker discovery efforts and for identifying promising drug targets. Therefore, the single cell analysis of tumor specimens may allow the identification of cancer sub-clones that is a prerequisite for a more advanced and personalized therapeutic approaches. Advanced methods for single cell analysis have been developed to obtain comprehensive biological information from a snapshot of individual cells, and to pinpoint any essential disease related alterations in cellular pathways. The study of cell-to-cell variation has now become an important focus of biological and clinical research. In fact, when addressing cell-to-cell variation, single-cell analyses are necessary in order to study and characterize the intrinsic heterogeneity of cell populations, which are masked in bulk measurements [241-243]. Single-cell analyses carried out *in situ* enable the identification and discrimination of cells within a microenvironment, thereby identifying subpopulations of cells with a particular expression profile or signaling activity status from the bulk of others in the original environment. Then, gene expression and protein analysis are pushed to include four foundamental parameters: analytical resolution, throughput, multiplexibility and spatial resolution.

mRNA in situ detection

Taking this issues into consideration, in situ analyses of mRNA and protein complexes can achieve precise and spatial localization within morphological preserved cells or tissues as they occur in their natural situation. Spatial resolution is an intrinsic property of *in situ* techniques because the molecular reactions are performed directly on the tissue section and the spatial information is readily visible. The concept with padlock probes was invented two decades ago and is an extension of the oligonucleotide ligation assay (OLA) [244], offering highly selective detection of DNA and RNA in solution and in situ. First, padlock probes are linear oligonucleotides of approximately 70 to 100 nucleotides in length with target- complementary 5´- and 3´-ends which constitute dual target recognition when both probe arms must hybridize correctly to the target.

This property allows for highly multiplex assays with limited cross-reactivity between probes [245-247]. Secondly, when the padlock probes hybridize to their correct target the ends of the padlock probe are brought together in a head to tail orientation, with only a nick in between. The nicks can be sealed by a DNA ligase creating circles that are locked onto the target strands as padlocks [248]. Only a perfect match in the junction enables ligation, which creates a circular DNA molecule that subsequently can be detected. RCA, also known as rolling circle replication (RCR), is an isothermal amplification technique of circular DNA molecules that creates long single stranded DNA molecules with tandem repeats of complements of the original circles [249]. Thus, RCA generates copies at a rate that is linear over time unlike PCR that proceed in an exponential fashion. Since the contiguous rolling circle products (RCPs) will by nature collapse into micrometer-sized DNA-bundles, RCA is highly suitable for localized detection. RCA consists of an isothermal amplification of a circular single-stranded DNA molecule. A 100 nt-long circle is replicated several hundred times per hour thanks to the high processivity of this polymerase ($1x10^3$ nt/min) [250]. Some of the characteristics of this mechanism make RCA an exquisite signal amplification system, especially for *in situ* applications The RCPs become detectable in a fluorescence microscope by the local enrichment of short fluorescent probes that hybridize to the detection sites of the coiled RCPs [251]. A great advantage with the appearance of single RCPs, being distinct bright signals representing individual molecules, is that it permits exact quantification of detected targets in a solution or in situ.

Droplet Digital PCR

The concept of digital PCR was first described in 1992 by Sykes et al., who recognized that the combination of limiting dilution, end-point PCR, and Poisson statistics could yield an absolute measure of nucleic acid concentration (252). Subsequently, Vogelstein and Kinzler at Johns Hopkins University developed a method whereby a sample is diluted and partitioned to the extent that single template molecules can be amplified individually, each in a separate partition, and the products detected using fluorescent probes (253). The term “digital PCR” was coined to describe this novel method. Digital PCR improves upon the sensitivity of real-time PCR and enables the detection of rare events such as single-nucleotide mutations in a population of wild-type sequences. In conventional real-time PCR, the signal from wild-type sequences can dominate and obscure the signal from the rare sequence. By minimizing the effects of competition between targets, digital PCR overcomes the difficulties inherent to amplifying rare sequences, and allows for sensitive and precise absolute quantification of nucleic acids.

A critical step in digital PCR is sample partitioning (ie, the division of each sample into discrete subunits) prior to amplification by PCR. The sample is prepared in a manner similar to that for real-time PCR but is then separated into thousands of partitions, each ideally containing either zero or at most a few template molecules. Each partition behaves as an individual PCR reaction and, as with real-time PCR, fluorescent probes are used to identify amplified target DNA. Each partition can then be readily analyzed after amplification to determine whether or not it contains the target sequence. Samples containing amplified product are considered positive (fluorescent), and those without product, and thus with little or no fluorescence, are negative. The ratio of positives to negatives in each sample is the basis of quantification. Unlike real-time PCR, digital PCR does not rely on the number of amplification cycles to determine the initial

amount of template nucleic acid in each sample; rather, it relies on Poisson statistics to determine the absolute template quantity.

The unique sample partitioning step of digital PCR, paired with Poisson statistical data analysis, allows higher precision than traditional PCR and real-time PCR methods. Accordingly, digital PCR is particularly well suited for applications that require the detection of small amounts of input nucleic acid or finer resolution of target amounts among samples, for example, rare sequence detection, copy number variation analysis, and gene expression analysis of the rare targets [254].

2.2.1. mRNA *in situ* detection

In situ detection of individual mRNA molecules was performed as described. Bone marrow biopsies of AML patients, previously embedded in paraffin blocks, were cut in 5 µm thick sections and mounted on slides. Slides were dewaxed as follows: twice in 100% xylene for 15 minutes and 10 minutes, twice in 100% EtOH for 2 minutes, twice in 95% EtOH for 2 minutes, twice in 70 % EtOH for 2 minutes, and washed in DEPC-H2O for 5 minutes and in DEPC-PBS for 2 minutes. Tissue fixation was performed in 3.7% (w/v) paraformaldehyde in PBS for 10 minutes at room temperature. After a wash in DEPC-PBS for 2 minutes, the tissue sections were then permeabilized with 2 mg/ml pepsin (Sigma Aldrich, St. Louis, US) in 0.1 M HCl at 37° C for 2 minutes. Slides were washed in DEPC-H2O for 5 minutes, in DEPC-PBS for 2 minutes and then fixed in 3.7% (w/v) paraformaldehyde in PBS for 10 minutes at room temperature. Tissue sections were then dehydrated through a series of 70%, 85% and 100% ethanol for 1 minutes each. Molecular reactions were carried out with a reaction volume of 100 µl in secure-seals (13 mm in diameter, 0.8 mm deep; Grace Bio-Labs) mounted over the tissue. One µM of locked nucleic acid (LNA)-modified cDNA primer (Exiqon, Vedbaek, Denmark; see **Table 10a**) was added to the slide with 10 U/µl of M-MULV reverse transcriptase (Fermentas), 500 nM dNTPs (Invitrogen), 0.2 µg/µl BSA (New England Biolabs, NEB) and 1 U/ µl RiboLock RNase Inhibitor (Fermentas) in the M-MULV reaction buffer. Slides were incubated for 3 hours at 37° C. After incubation, slides were washed in PBS-T (DEPC-PBS with 0.05% Tween20), followed by a post-fixation step in 3.7% (w/v) paraformaldehyde in DEPC-PBS for 30 min at room temperature. After post-fixation the sample were washed twice in DEPC PBS-T. To make the target cDNA strands available for padlock probe hybridization, the RNA portion of the created RNA-DNA hybrids was degradated with RNaseH (Fermentas). Ligation was then carried out with 0.1 µM of the β-actin padlock probe, WNT10B padlock probe and WNT10B^{IVS1} padlock probe (Sigma-Aldrich, St Louis, MO; see **Table 10b)** and in a mix of 0.5 U/µl Ampligase (Epicentre), 0.4 U/µl RNase H (Fermentas), 1 U/µl RiboLock RNase Inhibitor (Fermentas), Ampligase buffer, 50 mM KCl and 20% formamide. Incubation was performed first at 37° C for 30 minutes, followed by 45 minutes at 45° C. After ligation reaction, the slides were washed twice in DEPC-PBS with 0.05% Tween20. Rolling Circle Amplification (RCA) was performed with 1 U/µl DNA Polymerase (Fermentas) in the supplied reaction buffer, 1 U/µl RNase Inhibitor (Fermentas), 250 µM dNTPS (Invitrogen), 0.2 µg/µl BSA (NEB) and 5% glycerol. Incubation was carried out for 5 hours at 37° C, and it was followed by a twice wash in PBS-T. Rolling Circle Particles (RCPs) were visualized using 100 nM of detection probe (Sigma-Aldrich; see **Table 10c**) in 2X SSC and 20% formamide at 37° C for 20 minutes. Slides were then washed in DEPC-PBS. Nuclei were counterstained with 100 ng/ml Hoechst 33258 (Sigma-Aldrich). The Secure-seals were removed and

the slides were dehydrated using a series of 70%, 85% and 99.5% ethanol for 3 minutes each. The dry slides were mounted with Invitrogen Slowfade. Images of bone marrow tissue slides were acquired using an Axioplan II epifluorescence microscope (Zeiss) equipped with a 100 W mercury lamp, a CCD camera (HRM, Zeiss), and a computer-controlled filter wheel with excitation and emission filters for visualization of DAPI, Cy3, and Cy5.A x20 (Plan Apocromat, Zeiss) and x40 (Plan Neofluar, Zeiss) objective were used for capturing the images. Images were collected using the Axiovision software (release 4.3, Zeiss). Exposure times for slides images were 520–680 ms (at 20X magnification), 320–480 ms (X40) for DAPI; 300 ms (x20), 650 ms (Å~40) for Cy3; 250 ms (Å~20), 580 ms (Å~40) for Cy5. Images were collected as z-stacks to ensure that all RCPs were acquired, with a maximum intensity project created in Axiovision. For quantification, the numbers of 153 RCPs and cell nuclei in images were counted digitally using CellProfiler (www.cellprofiler.org) on three x20 microscope images. The total number of RCPs was divided by the number of nuclei for each image. The average for each sample was then calculated from the result of the five images and is reported as RCPs per cell. The threshold for different color channels was set with ImageJ 1.41 .

Table 10 – Primer, padlock probe and detection probe for mRNA *in situ* detection

A. LNA PRIMERS
β-actin
5′-C+TG+AC+CC+AT+GCCCACCATCACGCCC-3′
WNT10B
5′-C+A+G+G+C+CGGACAGCGTCAAGCACACG-3′

B. PADLOCK PROBES
β-actin
5′-[Phos] GCCGGCTTCGCGGGCGACGATTCCTCTATGATTACTGACCTATGCGTCTATTTAGTGGAGCCTCTTCTTTACGGCGC CGGCATGTGCAAG-3’
WNT10B
5′-[Phos] ACCGTGCCTGTCGGACCCTCCTCTATGATTACTGACCTAAGTCGGAAGTACTACTCTCTTCTTCTTTTAGTGAAGCCC AGGCAACCCA-3′
WNT10B^{IVS1}
5’-[Phos] AGTCTCCCGTCCCGCAGGTCTCCTCTATGATTACTGACCTATGCGTCTATTTAGTGTATCCTCTTCTTTCTATTCCTG AACCCGCATCA-3’

C. DETECTION PROBES
***β-actin*, CY3**
5′-[Cy3]-TGCGTCTATTTAGTGGAGCC-3’
***WNT10B*, CY5**
5′-[Cy5]-AGTCGGAAGTACTACTCTCT-3′

FLUOROPHORES	λ ABSORPTION	λ EMISSION
HOECHST 33258	346 nm	460 nm
CY3	550 nm	570 nm
CY5	622/36 nm	667/30 nm

2.2.2. RNA isolation

Total RNA for expression profiling analysis was extracted using RNAqueus 4PCR kit (Ambion, Austin TX) from mononucleated cells derived AML samples. 500 µL of Lysis/Binding Solution was added to a sample and vortexed vigorously; an equal volume of 64% Ethanol was added to the lysate and the tube was inverted several times. The samples were applied to columns, spun for 30 seconds at 10,000 RCF, and the flow through was discarded. 700 µL of Wash Solution #1 was added, centrifuged, the flow through was then discarded. Then 500 µL of Wash Solution #2/3, was added and centrifuged and the flow thought was subsequently discarded. This process was repeated with another 500 µL of Wash Solution #2/3. RNA was eluted with 50 µL of preheated Elution Solution, and centrifuged at 10,000 RCF for 30 seconds, and eluted again with 15 µL of Elution Solution. Solution was then treated with 7.5 µL of 10x DNase1 buffer and 1.0 µL of DNase1 enzyme to destroy residual DNA. The product was then incubated for 30 minutes at 37º C before 8.0 µL of DNase1 inactivation reagent was added and incubated for 2 minutes at room temperature. The tube was then spun down at 10,000 RCF for 1 minute to pellet the inactivation reagent.

2.2.3. RNA quality evaluation

Integrity of RNA samples extracted from dried blood spots was checked using Experion™ (Bio-Rad, USA). Experion system was included with automated electrophoresis station, priming station, vortex station for RNA analysis and RNA std sens analysis kit which included with chips and reagents for standard-sensitivity RNA. Following procedure performed for RNA analysis using the Experion system. In order to avoid any contamination during RNA integrity analysis, electrodes of the Experion system were cleaned using Experion electrode cleaner (800 µl) in the first step. After repeating this step for one more time, electrodes were rinsed with DEPC treated water (500 µl) for 5 minutes using electrode cleaning chip. At the end lid was kept open for 60 second to evaporate remaining water on electrodes. RNA stain, RNA loading buffer and RNA gel from the RNA std sens kit were removed from 4˚ C and equilibrated at room temperature for 20 minutes. RNA stain was wrapped in aluminum foil to avoid its light sensitive degradation. RNA gel was filtered from filter tube at 2000 RPM for 10 minutes. Filtered gel (65 µl) was taken into RNase-free microfuge tube and mixed with RNA stain (1 µl). RNA ladder was removed from -20˚ C and thawed it on ice for 10 minutes. RNA ladder (1 µl) and RNA samples (3 µl) was taken into RNase-free microfuge tube. RNA ladder and RNA samples were denatured at 70˚ C for 2 minutes. Ladder and samples were immediately placed on ice for 5 minutes, spun down for 2-5 seconds and stored on ice until needed. Gel-stain solution (9 µl) was taken in well labeled as GS on RNA std sens chip without forming any air bubble. Chip was primed by setting appropriate

pressure for sufficient time on priming station. Chip was inspected for any air bubbles in micro 133 channels and for incomplete priming. Gel-stain solution (9 µl) was taken other well labeled GS. Filtered gel (9 µl) was taken to well labeled as G. Loading buffer (5 µl) was taken to each sample well 1-12 including ladder well. RNA ladder (1 µl) was taken to the well labeled as L. RNA samples were taken to all wells numbered as 1-12. Chip was placed tightly and vortexed for 60 seconds on vortex station. Primed chip loaded with RNA samples and ladder was then kept on electrophoresis station for 5 minutes and electrophoresis run was started. The use of a RNA ladder as a mass and size standard during electrophoresis allows the estimation of the RNA band sizes. After completion of the run, electrodes were cleaned using DEPC water (800 µl) filled in a cleaning chip. Electropherograms generated were analyzed by Experion software version 3.2. Integrity of the RNA may be assessed by visualization of the 18S and 28S ribosomal RNA bands. The intact RNA preparation shows high 18S and 28S rRNA peaks as well as a small amount of 5S RNA.

2.2.4. Droplet Digital PCR

In our study, Droplet Digital PCR (ddPCR) experiments were performed using primers and probes listed in **Table 11**. We performed the experiment on Bio-Rad's QX100 ddPCR system and the reaction mixtures in a final 20 µl volume consisted of 10 µl of 2x One-Step RT-ddPCR Supermix (Bio-Rad, CA, USA), 1 mM Manganese Acetate solution (Bio-Rad, CA, USA), 0.5 µM of forward and reverse primers, 0.25 µM probes. The 0.1 mM RNA, extracted using the RNAqueous-4PCR kit following the manufacturer's instructions (Ambion, Austin, TX-Thermo Fisher Scientific), was denatured at 95° C for 5 minutes and kept on ice prior addition to the reaction. The 20 µL ddPCR reaction mixture was then loaded into the Bio-Rad DG8 droplet generator cartridge (Bio-Rad, CA, USA). Then, each oil well was filled with 70 µl of droplet generation oil (Bio-Rad, CA, USA) and the prepared cartridge was then loaded into the QX100 droplet generator (Bio-Rad, CA, USA). The generated droplets were transferred to a 96-well PCR plate, that was sealed with a BioRad pierceable foil heat seal, and then samples were amplified on the T100 BioRad thermal cycler. The thermal cycling conditions consisted of 30 minutes reverse transcription at 60° C, 5 minutes initial denaturation at 95° C, followed by 40 cycles of a two-step thermal profile of 30 seconds denaturation at 94° C and 60 seconds annealing-elongation at 60° C and a final 10 minutes denaturation step at 98° C. Then plates were transferred to the QX 100 droplet reader (Bio-Rad, CA, USA) and ddPCR data were analyzed with QuantaSoft analysis software (version 1.7.4).

The TaqMan® probe specific for WNT10B ties transcript exon 1 and it is marked by FAM fluorophore (λ_{abs} = 495 nm and λ_{em} = 520 - 495 nm), while the TaqMan® probe specific for WNT10B^{IVS1} ties transcript at intron 1 and is marked by the fluorophore HEX (λ_{abs} = 530 nm and λ_{em} = 560). The fraction of drops at high fluorescence intensity, distinct from the weak background signal due to imperfect quenching of the TaqMan® probes, was used to calculate by Poisson statistics the concentration of target in the original sample:

$$M = -\ln\left(1 - \left(\frac{P}{R}\right)\right)$$

M = average number of target molecules per droplet

P = number of positive droplet

R = number of analyzed droplet

Therefore, it is possible to derive the concentration of copies of target per microliter by multiplying M for $1000/V_d$, where V^d is the volume of each drop, and further calculate the concentration of the target in the initial solution by multiplying the concentration for the dilution factor (D) used.

Table 11 – Primer and TaqMan® probes in Droplet Digital PCR

PRIMER	*PRIMER SEQUENCE*
Forward WNT10B	5'-GCAGCACTAGTGAAGCCCAG-3'
Forward WNT10B^{IVS1}	5'-CCTGAACCCGCATCAAGTCTC-3'
Reverse	5'-ATCTCATTGCTTAGAGCCCGAC-3'

TARGET	*TAQMAN® SEQUENCE*
Forward WNT10B	5'-[6FAM]CACCCAAACCACTGGAGTCCTGATCG[BHQ1]-3'
Forward WNT10B^{IVS1}	5'-[HEX]TCTCCCGTCCCGCAGGTCCTGATCG[BHQ1]-3'

3. RESULTS

3.1. Identification of WNT10B^{IVS1} transcript variant

3.1.1. Characterization of 5' region of WNT10B

In order to understand the cause of the highly WNT10B regenerative molecule expression in the leukemia environment, we performed a deeply characterization of the WNT10B mRNA using 5' Rapid Amplification of cDNA Ends (5'-RACE). As the first step, we set up the 5'-RACE that was carried out on RNA extracted from AML46 patient. A gene-specific oligonucleotide that hybridizes to a known sequence within a characterized coding region is used to prime reverse transcription. Using a GSP2 primer, designed on WNT10B exon2, we obtained a product that was approximately 120bp long. To characterize the RACE product generated, the product was cloned into the pCR®IITOPO® vector (Invitrogen), and inserts were analysed by EcoRI restriction digest. Inserts that correlated in size with the PCR products generated by 5'-RACE were sequenced. We obtained three different results:

- clones 8-11: the correct canonical WNT10B sequence
- clones 1-4 and 31: characterized by the presence of 21bp at the beginning of WNT10B transcript
- clones 18-27: characterized by an Intron Retention IVS1 region of 77nt and by a stop of cDNA after the IVS1 sequence with the absence of exon 1 *(clones 18 and 27 were sequenced using universal primer M13 Fw and M13 Rw, and analyzed using BLAST and ASAPII (http://blast.ncbi.nlm.nih.gov; http://www.bioinformatics.ucla.edu/ASAP2)*

The molecular evaluation by 5'-RACE PCR of WNT10B transcript evidenced the presence of a non-physiological transcript variant, termed WNT10B^{IVS1}, characterized by the absence of exon 1 and partial retention of 77 nucleotides of intervening sequence 1 (see **Figure 11**). In order to characterize the WNT10B^{IVS1} region, we performed in silico analysis using free software as ASPIC (http://www.caspur.it/ASPIC/) and ESEFInder (http://exon.cshl.edu/ESE/). The in silico analysis, using our region as a "query", demonstrate that the Exon2-IVS1 splicing junction is correct, and that the end of the WNT10BIVS1 region corresponds with the end of the transcript. It's interesting to note that the ATG site, is localized in the WNT10B exon 2, suggesting that this alteration doesn't involve the protein expression. Then, the nature of the WNT10B^{IVS1} transcript remain unclear, but it will be the object for the future perspectives.

Figure 11 - Scheme of WNT10B and WNT10B^{IVS1} variant transcript

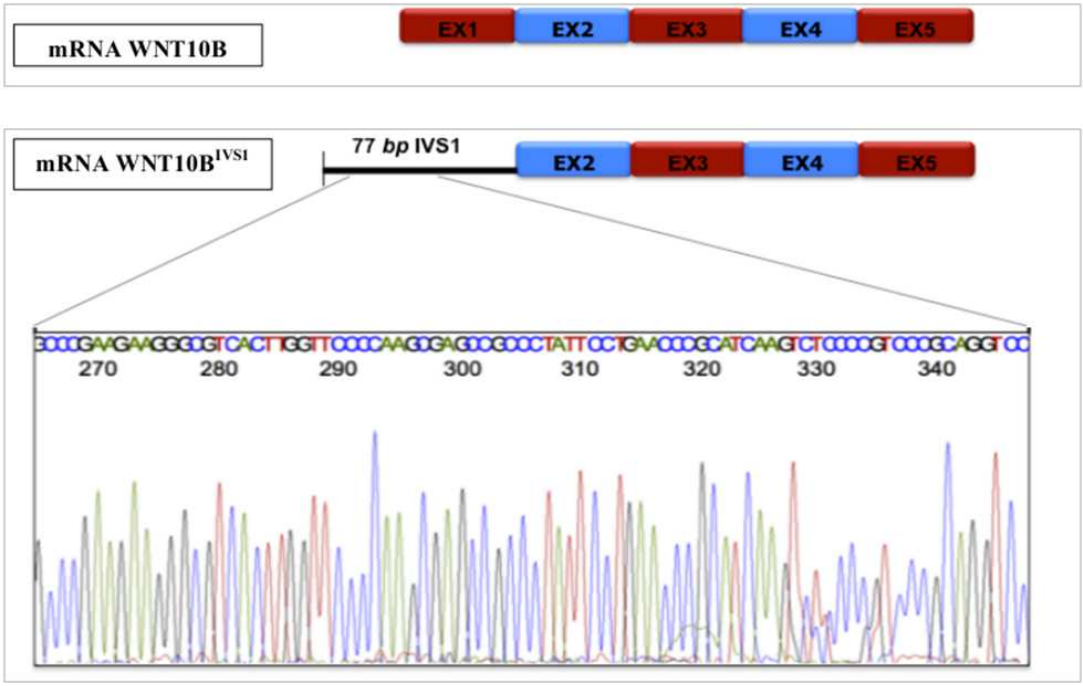

3.1.2. WNT10B and WNT10B^{IVS1} expression in AML cell line and patients samples

In order to define the distribution and localization of WNT10B^{IVS1}, we performed the mRNA *in situ* detection on AML46 spotted and fixed cells s, and on bone marrow biopsies. In our previous work [221], we demonstrated through establishment of a primary AC133+ AML cell culture (A46) that leukemia cells synthesize and secrete WNT ligands, increasing the levels of dephosphorylated β-catenin *in vivo*. Besides, the results of our experiments indicate that AC133 is expressed on AML-LSC in the A46 primary cells, suggesting that regeneration-associated Wnt expression signature is enriched in primary human AML LSC-containing fraction. Considering this background data, we performed the mRNA in situ detection on A46 cells, derived from AML46 patient (see **Figure 12**).

Figure 12 – β-actin mRNA *in situ* detection on AML46 cells

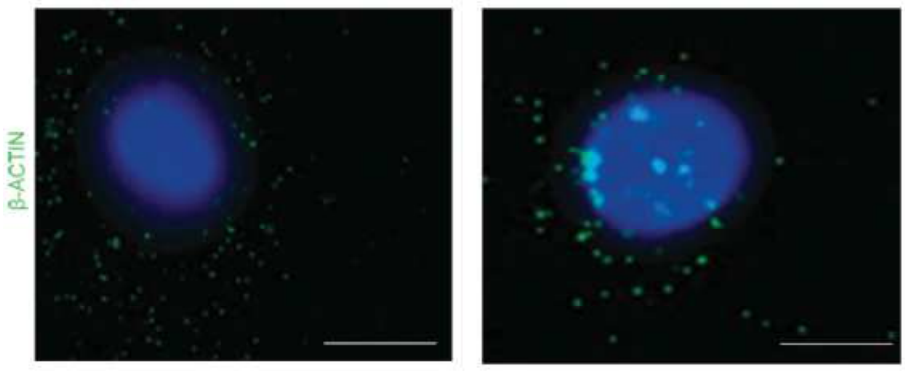

β-actin RCPs are shown in green. Nuclei are shown in blue. Scale bar 10 µm.

In order to define the ratio between WNT10B and WNT10B^{IVS1}, we set up the double detection *in situ* for both molecules. Using one common LNA primer for retrotranscription, we detected WNT10B and WNT10B^{IVS1} through two specific padlock probe (see **Figure 13**).

Figure 13 - WNT10B and WNT10B^{IVS1} detection *in situ* on AML46 cells

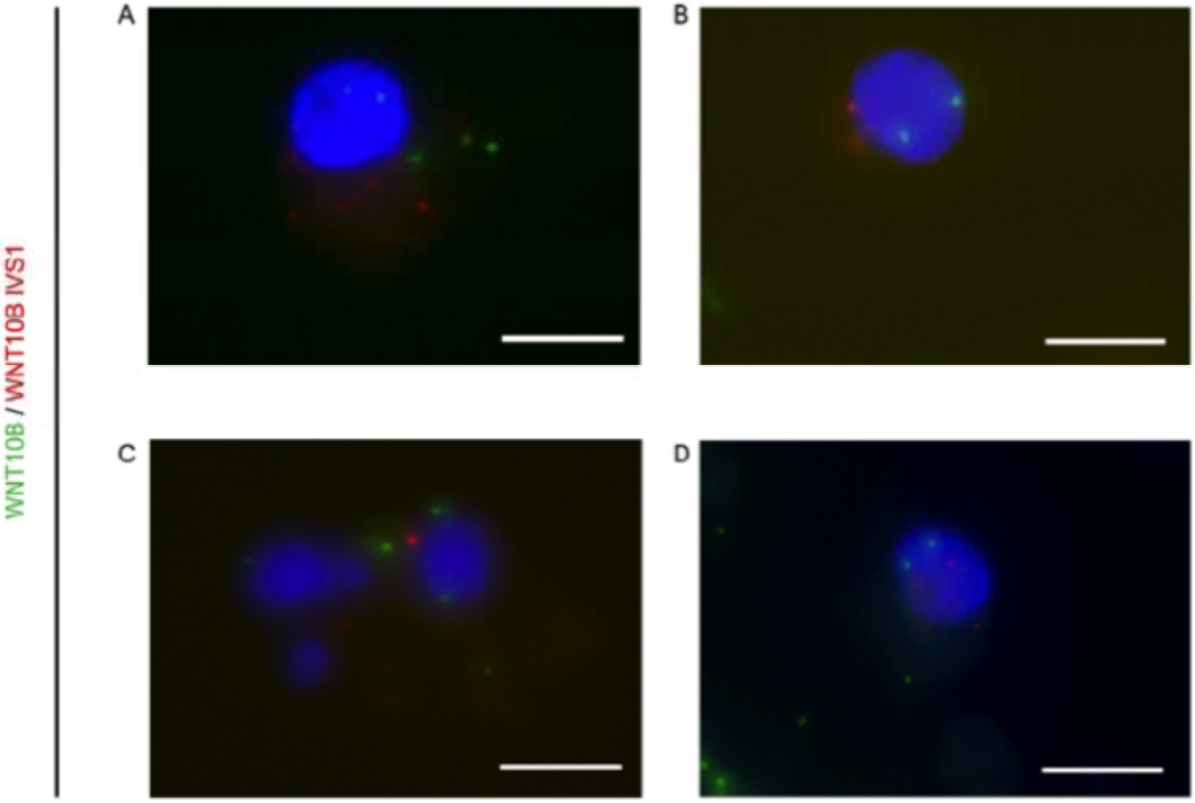

mRNA in situ detection of WNT10B and WNT10B^{IVS1} molecules on A46 cells. There are represented four fields (A,B,C,D). Cell nuclei are shown in blue. WNT10B RCPs are shown in green and WNT10B^{IVS1} are shown in red. Scale bare 10 µm.

It is of notice that RCPs counting of WNT10B and WNT10B^{IVS1} showed a ratio close to 1, suggesting a balance expression of this two expressed isoforms of transcript (see **Figure 14**).

Figure 14 - RCPs counting of WNT10B and WNT10B^{IVS1} on A46 cell line

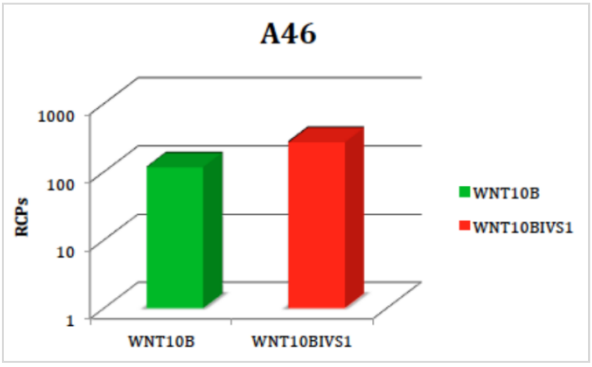

In order to observe and evaluate the localization and distribution of WNT10B^{IVS1} in the AML bone marrow context, we performed the mRNA *in situ* detection of WNT10B and WNT10B^{IVS1} mRNA molecules. We planned the experiments using only one LNA primer, mapped to WNT10B exon3 and two Padlock Probes: the WNT10B mRNA was detected by a Padlock probe designed on the exon 1, while WNT10B^{IVS1} was detected with a Padlock probe designed on IVS1-exon2 junction (see Figure 15).

Figure 15 - WNT10B and WNT10B^{IVS1} detection *in situ* on bone marrow biopsy

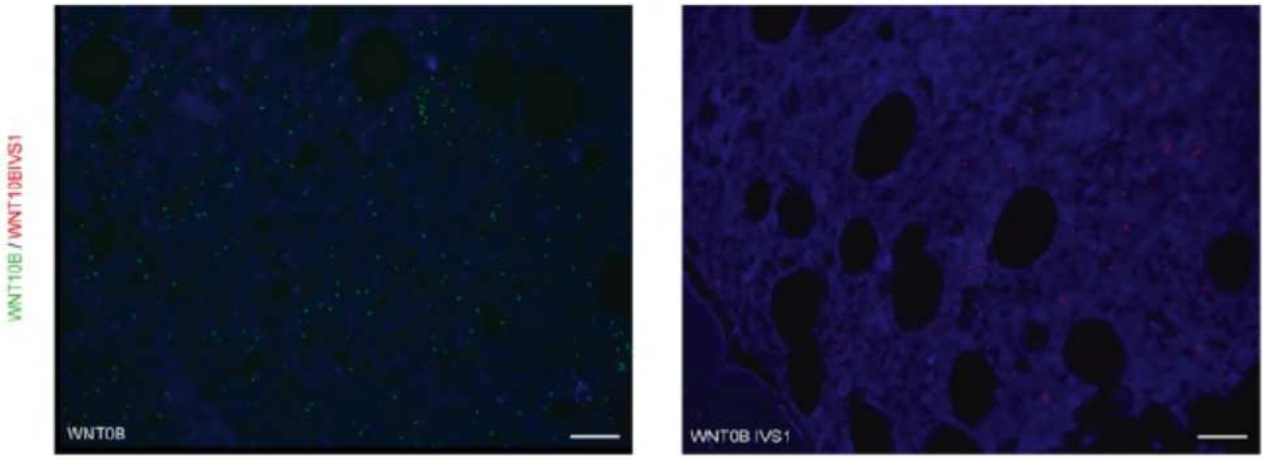

mRNA in situ detection of WNT10B and WNT10BIVS1 molecules on AML9 bone marrow biopsy. WNT10B RCPs are shown in green, WNT10BIVS1 RCPs are shown in red. Cell nuclei are shown in blue. Scale bare 20 µm.

Comparing the WNT10BIVS1 with the WNT10B mRNA distribution, we can note that the ratio results equal to 0.8 (see **Figure 16)**, suggesting that there is a bslance between WNT10B and WNT10B^{IVS1} expression.

Figure 16 - RCPs counting of WNT10B and WNT10B^{IVS1} on AML9 bone marrow biopsy

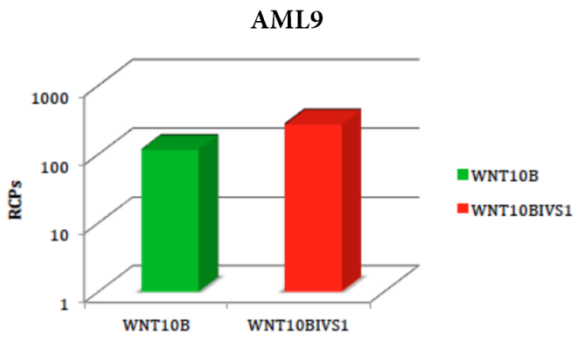

3.2. Droplet Digital™ PCR analysis

Absolute quantification of mRNA levels of WNT10B and related WNT10B^{IVS1} transcript variant were obtained as described by Droplet Digital™ PCR on mononucleated cells derived from the study cohort of 125 AML patients. Results are reported in **Table 12.**

Table 12 - mRNA levels of WNT10B and WNT10B^{IVS1} transcript variant by Droplet Digital ™ PCR

Code	WNT10B	WNT10B^{IVS1}	Code	WNT10B	WNT10B^{IVS1}	Code	WNT10B	WNT10B^{IVS1}	Code	WNT10B	WNT10B^{IVS1}
1	100000	96450	**41**	100000	98700	**209**	8940	28	**250**	6530	9610
2	7343	6234	**42**	9567	6532	**210**	6650	14	**256**	100000	50
3	6174	5678	**43**	9878	6123	**211**	8350	61	**257**	18300	9871
4	3043	1204	**44**	9981	60	**212**	8680	64	**258**	6220	9815
5	5822	4768	**46**	100000	100000	**213**	5170	72	**260**	10400	9126
6	5253	3349	**48**	9998	9538	**214**	7880	39	**262**	10300	10100
9	100000	100000	**49**	100000	99878	**215**	8920	33	**264**	8765	5349
10	7368	6523	**50**	9912	8139	**216**	100000	73	**265**	5790	10329
11	6642	6123	**51**	100000	100000	**217**	10500	32	**269**	8630	11231
12	7833	7655	**52**	9569	9324	**218**	10400	0	**270**	100000	11197
13	4639	2234	**53**	9876	9123	**219**	10500	0	**272**	8100	22
14	9733	9756	**54**	9878	3767	**220**	100000	45	**273**	6040	34
16	7696	7645	**55**	3192	3120	**221**	100000	36	**276**	100000	69
17	8733	8567	**57**	8213	5987	**222**	5860	32	**279**	13127	33
18	8343	8276	**59**	100000	98567	**223**	6990	65	**TR1**	123	32
19	5342	5304	**60**	100000	86549	**224**	7900	19	**TR2**	35	3
20	9838	9815	**61**	9992	4590	**225**	9740	7324	**TR3**	49	8
21	100000	100000	**62**	9438	8976	**226**	100000	100000	**TR4**	10	4
22	9547	9519	**63**	100000	97899	**228**	5250	4591	**TR5**	33	12
23	8345	8234	**64**	100000	30	**229**	6110	4456	**TR6**	28	21
24	100000	100000	**65**	56789	44356	**230**	5880	5789	**TR7**	14	9
25	9745	9679	**67**	100000	100000	**232**	9180	5182	**APL1**	100000	23
27	8345	8128	**68**	100000	98000	**233**	9090	8871	**APL2**	7720	33
28	100000	100000	**200**	14120	43	**235**	6000	16	**APL3**	8650	56
30	9378	9246	**201**	9378	10	**237**	5910	5643	**APL4**	6230	67
32	9415	9158	**202**	11560	65	**239**	5450	10	**APL5**	6980	31
33	7645	6529	**203**	11890	28	**240**	9820	73	**APL6**	**9520**	**29**
34	6989	6192	**204**	12416	57	**241**	17650	123	**APL7**	**9430**	**25**
35	9878	89	**205**	12789	36	**242**	5820	221	**APL8**	**9123**	**18**
37	9987	93	**206**	12983	18	**243**	10800	27			
38	9993	5399	**207**	10500	40	**245**	7620	7768			
39	9345	5911	**208**	776740	35	**248**	100000	7491			

3.3. Statistical analysis on study population

3.3.1. Treatment course and outcome

Treatment schedule and outcome data were available for 116 out of 125 patients. Those patients were assessed for response. CR was obtained from 97 out of 116 (83.6%) patients. Primary refractory diseases and 5 infectious complication during post-chemotherapy aplasia accounted for the 19 patients who did not achieve CR.

The median follow-up time was 65.5 months based on the reverse Kaplan-Meier method. The estimated 5-year OS and RI resulted 45.8% and 58.1% respectively, with 37 patients alive in CR1 and 16 patients alive in second or subsequent CR (see **Figure 17**).

Figure 17 - Kaplan-Meier plots showing OS and RI of AML patients

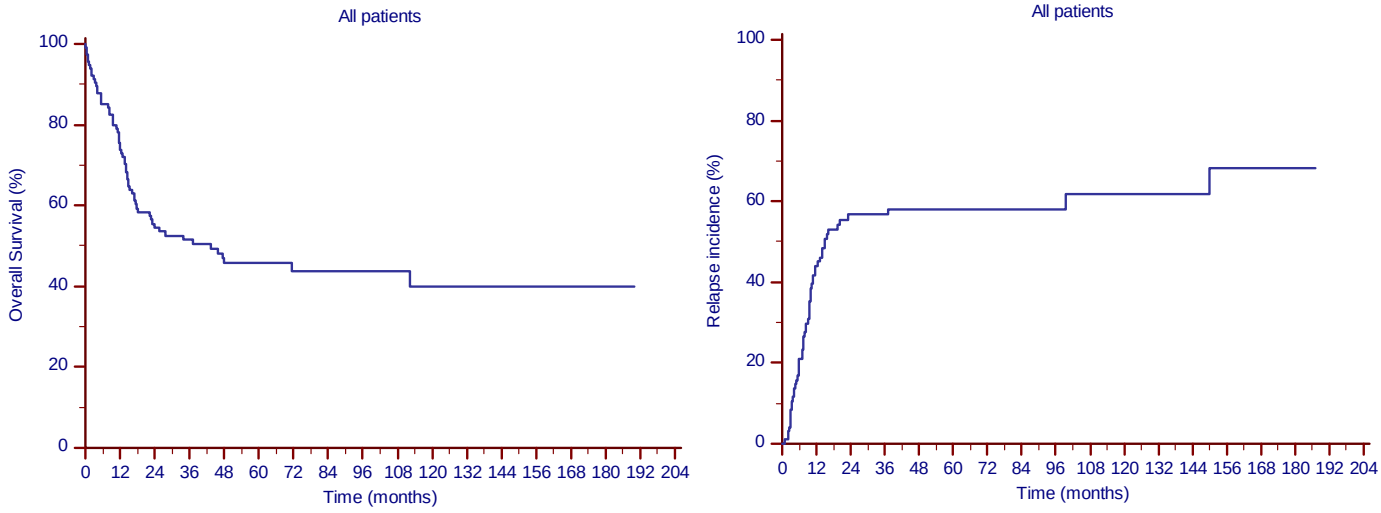

3.3.2. Outcome per risk classification

Patients were then divided on the basis of the three main classification system, formerly according to Medical Research Council (MRC), European LeukemiaNet (ELN), and National Comprehensive Cancer Network (NCCN) scoring system, respectively (see **Tables 6-8**). Numerical distribution of patients in the distinct risk groups belonging to the different classifications is showed in **Table 13**.

Table 13 – Distribution of patients belonging to different risk classifications

***Patients**, no.*	**MRC**	**ELN**	**NCCN**
Favorable	44	56	58
Intermediate	59	*INT-1:* 34 *INT-2:* 14	33
Adverse	13	12	25

Our study population demonstrated to be a representative sample of leukemic patients described in literature, and all three classification system adopted have proved to be able to distinguish patients at different outcomes with a statistically significative wise (see **Table 14** and **Figure 18**).

Table 14 – Outcome data per distinct risk classifications and risk groups

***Median survival** (months)*	**MRC**	**ELN**	**NCCN**
Favorable	NR	NR	NR
Intermediate	17.97	*INT-1:* 16.23 *INT-2:* 47.87	22.97
Adverse	14.97	14.57	11.80
***5-years OS** (%)*			
Favorable	54.9	54.7	53.6
Intermediate	43.7	*INT-1:* 39.3 *INT-2:* 49.0	45.9
Adverse	20.0	11.4	25.0
Significance (p)	***0.0314***	***0.0133***	***0.0010***

Figure 18 - Kaplan-Meier plots showing OS per risk classification

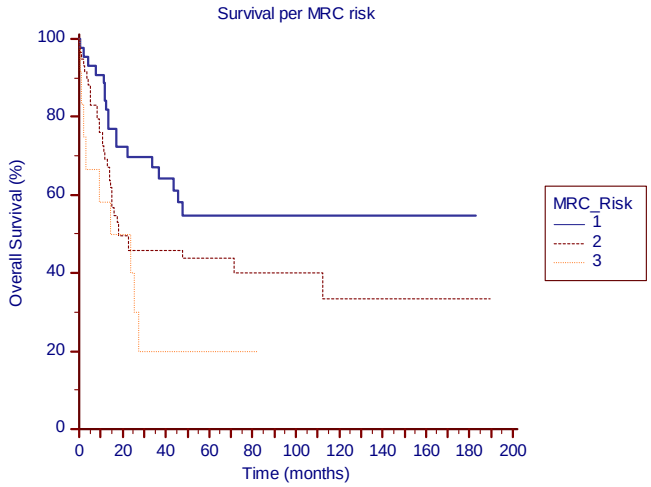

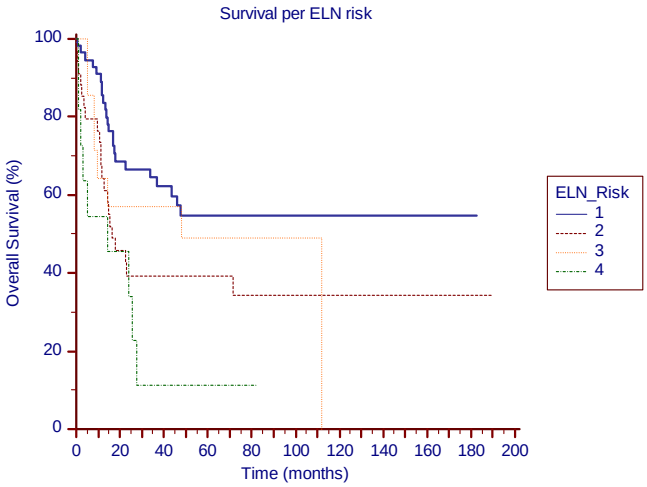

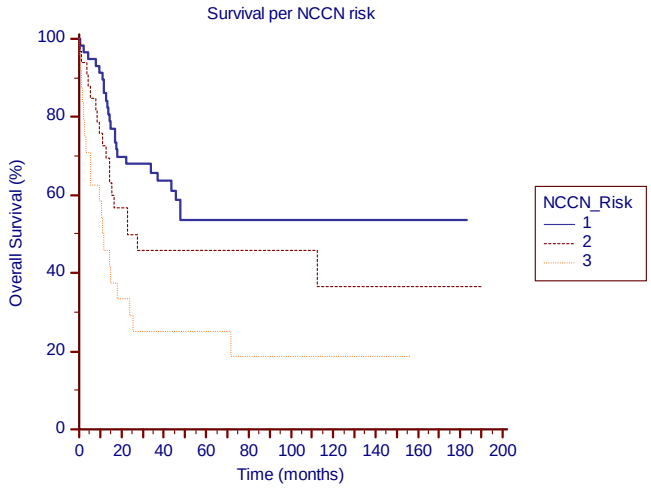

3.3.3. Differences in distribution of WNT10B and WNT10BIVS1 per risk classification

WNT10B transcript levels

WNT10B was highly expressed in every risk group according to the three different classification systems, and statistical analysis did not show significative difference in distribution of its transcript levels (*p* 0.6395, *p* 0.4295, and *p* 0.1786, respectively; Kruskal-Wallis test) (see **Figure 19**). These results were confirmed by comparative Mann-Whitney U-test.

Figure 19 - Box-plot distribution of WNT10B transcript per risk classification

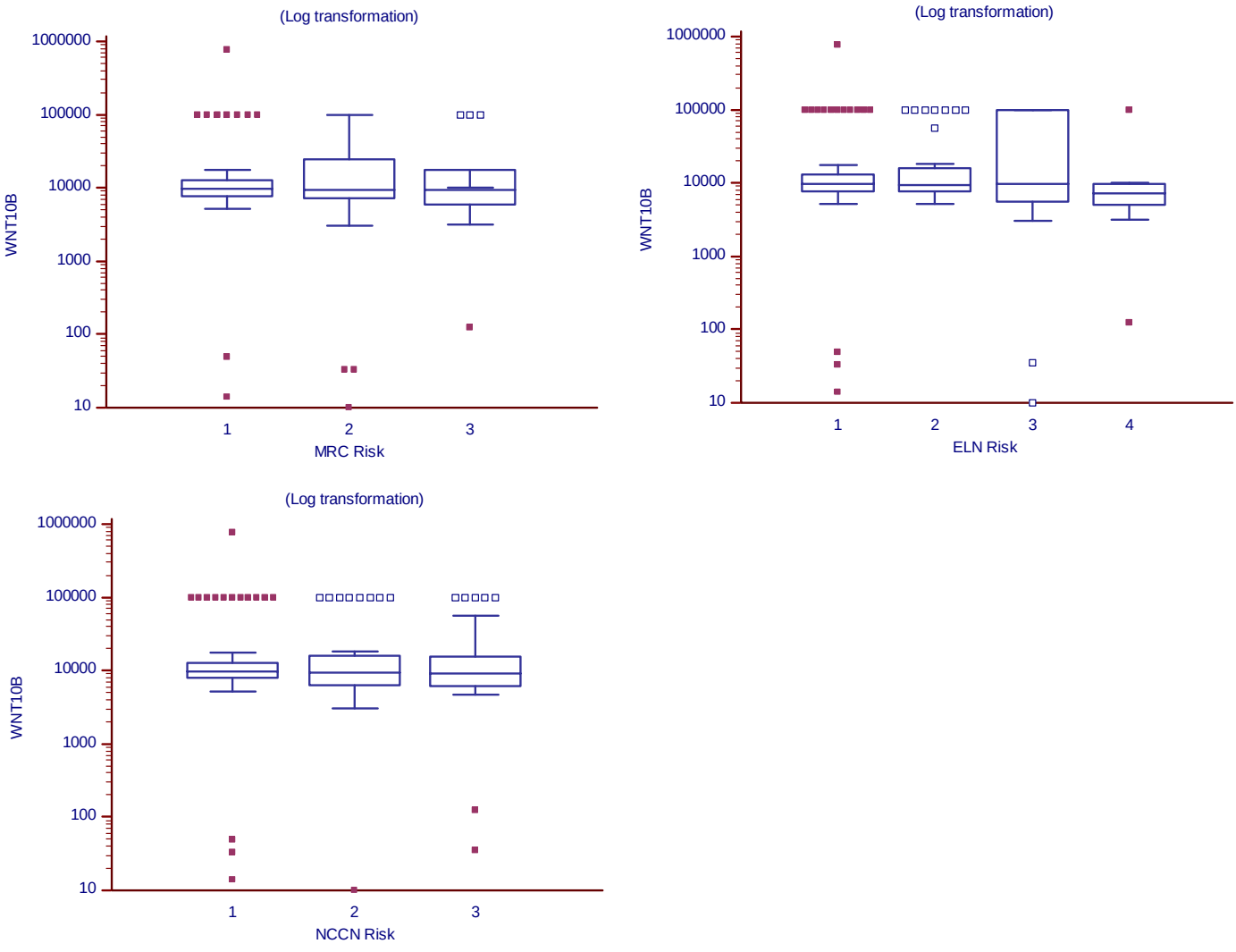

WNT10B^{IVS1} transcript levels

WNT10B^{IVS1} transcript levels showed a statistical significative difference between the specific risk classes (p <0.0001; Kruskal-Wallis test). Comparative Mann-Whitney U-test showed high expressed transcript levels in intermediate or adverse-risk patients, while WNT10B^{IVS1} showed a significant lacking of mRNA expression in patients classified as with favorable-risk prognosis (p <0.001 for all three classification system). No statistical significance in WNT10B^{IVS1} mRNA levels was found between intermediate and adverse-risk groups (MRC Int vs Adv: p 0.4864; ELN: Int-1 vs Int-2 p 0.1500; ELN Int-1/2 vs Adv: p 0.6963; NCCN Int vs Adv: p 0.9940) (see **Figure 20**).

Figure 20 - Box-plot distribution of WNT10B^{IVS1} transcript per risk classification

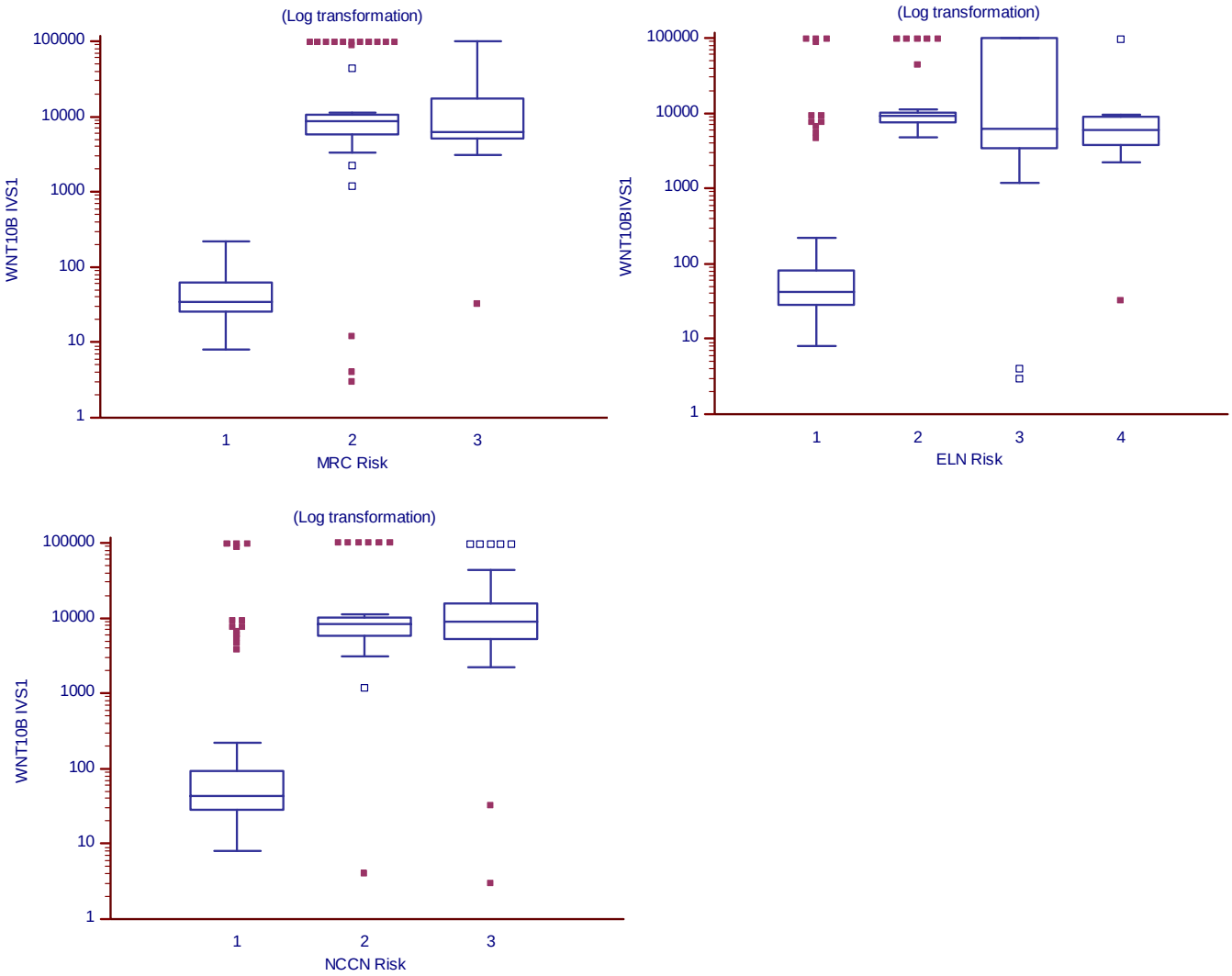

Given the significant difference in the expression of WNT10B^{IVS1} values in favorable-risk patients [namely, t(8;21), inv(16)/t(16;16), t(15;17)], we went to analyze patients subdivided by WHO classification.

3.3.4. Differences in distribution of WNT10B and WNT10BIVS1 per WHO classification

WNT10B transcript levels showed a statistical significative difference between the distinct WHO classes (*p* 0.0002; Kruskal-Wallis test). WNT10B mRNA was highly expressed in *de novo* AML (ie, AML with recurrent genetic abnormalities or AML not otherwise specified) and AML with myelodysplasia-related features, while we showed a significant lacking of mRNA expression in patients with therapy-related disease (*p* <0.002, Mann-Whitney U-test). No statistical significance in WNT10B transcript levels was found between patients with recurrent genetic abnormalities, myelodysplasia-related features or AML not otherwise specified (see **Figure 21**).

Figure 21 - Box-plot distribution of WNT10B transcript per WHO classes

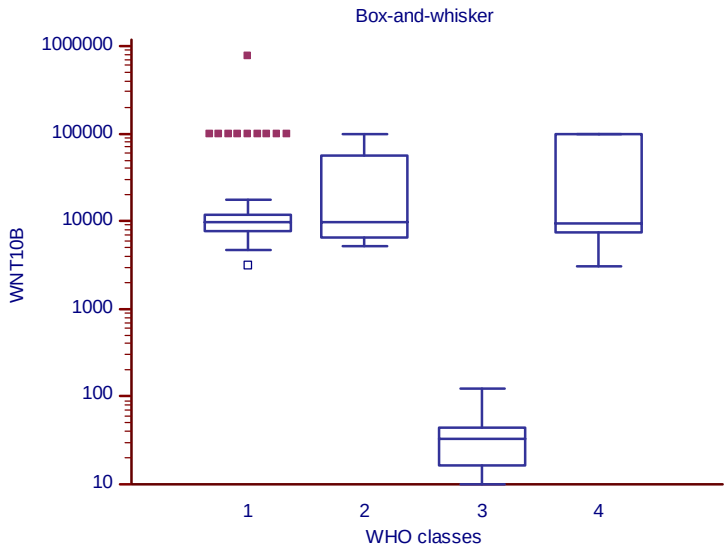

Legend for WHO classes: ***1.*** *AML with recurrent genetic abnormalities;* ***2.*** *AML with myelodysplasia-related features;* ***3.*** *therapy related AML;* ***4.*** *AML, not otherwise specified. Mann-Whitney U-test: 3 vs others: p < 0.002; 1 vs 2: p 0.9594; 1 vs 4: p 0.8801; 2 vs 4: p 0.9088.*

Statistical analysis showed a significative difference in $WNT10^{IVS1}$ distribuition (*p* <0.0001; Kruskal-Wallis test). Comparative U-test showed the presence of the $WNT10B^{IVS1}$ transcript in AML with myelodysplasia-related features and AML not otherwise specified groups, while we recorded absence of $WNT10B^{IVS1}$ mRNA in the therapy-related group (*p* <0.0005). Patients affected by AML with recurrent genetic abnormalities (see **Table 3** for details) showed a more heterogeneous distribution in $WNT10B^{IVS1}$ transcript levels, and they included both patients at high or absent mRNA expression. No statistical differences were found between patients with MDS-related features or AML not otherwise (see **Figure 22**).

Figure 22 - Box-plot distribution of WNT10B^{IVS1} transcript per WHO classes

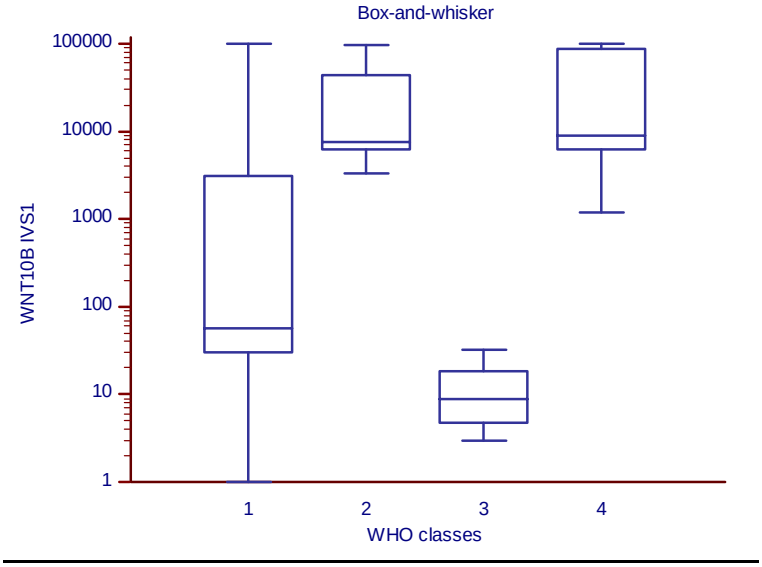

Legend for WHO classes: ***1.*** *AML with recurrent genetic abnormalities;* ***2.*** *AML with myelodysplasia-related features;* ***3.*** *therapy related AML;* ***4.*** *AML, not otherwise specified. Mann-Whitney U-test: 3 vs others: p <0.0005; 1 vs others: p <0.003; 2 vs 4: p 0.5475.*

Given this heterogeneous distribution in WNT10B^{IVS1} transcript values in patients with recurrent genetic abnormalities, and since the previous analysis based on genetic risk classes recognized a significant lacking of mRNA expression in patients classified as with favorable-risk prognosis, we went to hive off patients in the following genetic profiles:

1. core-binding factor AML (n = 40)
2. acute promyelocytic leukemia (n = 8)
3. AML with other recurrent cytogenetic abnormalities (n = 7)
4. normal karyotype AML with NPM1 or CEBPA mutation (n = 16)
5. AML with myelodysplasia-related features (n = 5)
6. therapy-related AML (n = 7)
7. normal karyotype AML (n = 32)
8. AML with cytogenetic number abnormalities (n = 4)
9. AML with cytogenetic structure abnormalities (n = 6)

Analysis confirmed a significative difference in WNT10B transcript levels (*p* 0.0008; Kruskal-Wallis test), and comparative Mann-Whitney U-test endorsed the presence of WNT10B mRNA in all groups of patients, with the exception of patients with therapy-related disease (*p* <0.01). No statistical significance in WNT10B levels was found between all the other groups (see **Figure 23**).

Figure 23 - Box-plot distribution of WNT10B transcript per splitted WHO classes

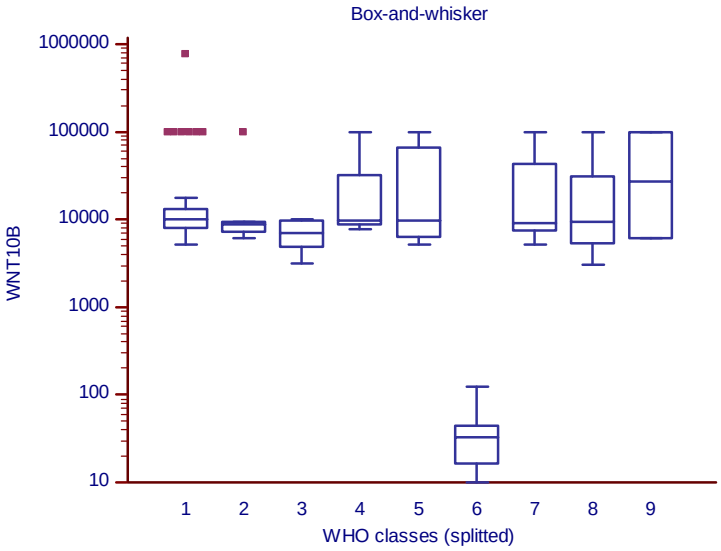

Legend for splitted WHO classes: ***1.*** *core-binding factor AML;* ***2.*** *acute promyelocytic leukemia;* ***3.*** *AML with other recurrent cytogenetic abnormalities;* ***4.*** *AML with NPM1 or CEBPA mutation;* ***5.*** *AML with myelodysplasia-related features;* ***6.*** *therapy-related AML;* ***7.*** *normal karyotype AML;* ***8.*** *AML with cytogenetic number abnormalities;* ***9.*** *AML with cytogenetic structure abnormalities. Mann-Whitney U-test: 6 vs others: p <0.01.*

WNT10B^{IVS1} transcript levels showed a statistical significative difference between the distinct genetic classes (p <0.0001; Kruskal-Wallis test). Comparative Mann-Whitney U-test showed that WNT10B^{IVS1} mRNA was non-detectable in core-binding factor AML, APL, and therapy-related diseases, while it was highly expressed in all the remaining groups of patients (p <0.01) (see **Figure 24**).

Figure 24 - Box-plot distribution of WNT10B^{IVS1} transcript per splitted WHO classes

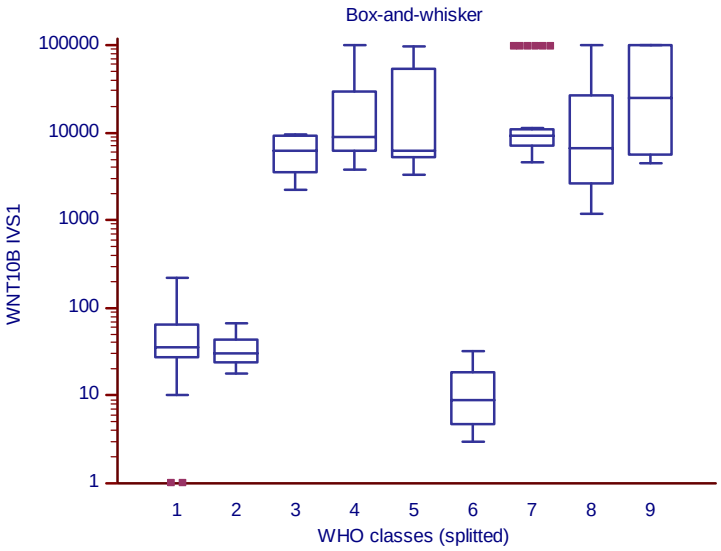

Legend for splitted WHO classes: ***1.*** *core-binding factor AML;* ***2.*** *acute promyelocytic leukemia;* ***3.*** *AML with other recurrent cytogenetic abnormalities;* ***4.*** *AML with NPM1 or CEBPA mutation;* ***5.*** *AML with myelodysplasia-related features;* ***6.*** *therapy-related AML;* ***7.*** *normal karyotype AML;* ***8.*** *AML with cytogenetic number abnormalities;* ***9.*** *AML with cytogenetic structure abnormalities. Mann-Whitney U-test: see text for details.*

These results were confirmed by grouping patients with normal karyotype AML (regardless of the presence of mutations in the NPM1 gene / CEBPA, n = 48) or structural or number cytogenetic abnormalities (n = 17) (see **Figure 25** and **Figure 26**).

Figure 25 - Box-plot distribution of WNT10B transcript by grouping patients

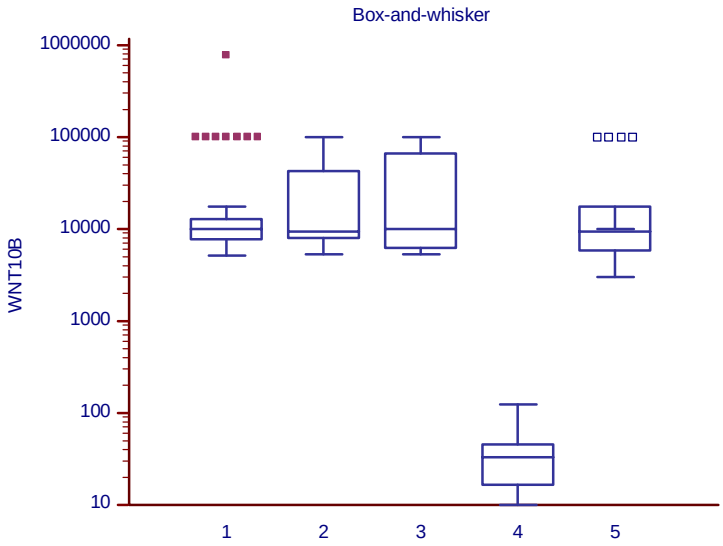

*Legend: **1.** core-binding factor AML or acute promyelocytic leukemia (n=48); **2.** normal karyotype AML (n=48); **3.** AML with myelodysplasia-related features (n=5); **4.** therapy-related AML (n=7); **5.** AML with cytogenetic abnormalities (n=17).*

Figure 26 - Box-plot distribution of WNT10B^{IVS1} transcript by grouping patients

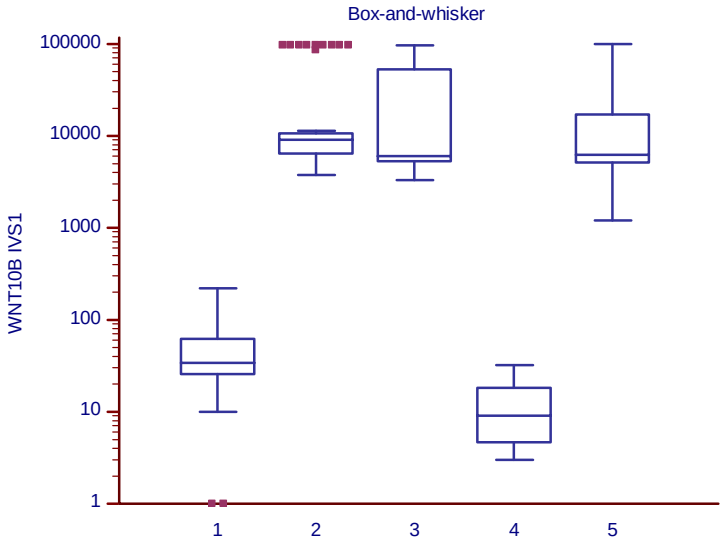

*Legend: **1.** core-binding factor AML or acute promyelocytic leukemia (n=48); **2.** normal karyotype AML (n=48); **3.** AML with myelodysplasia-related features (n=5); **4.** therapy-related AML (n=7); **5.** AML with cytogenetic abnormalities (n=17).*

3.3.5. WNT-based classification of AMLs

Combining these results, it is possible to recognize three distinct WNT10B / WNT10B^{IVS1} patterns:

- "double-positive": WNT10B + / WNT10B^{IVS1} +
- "single-positive": WNT10B + / WNT10B^{IVS1} -
- "double-negative": WNT10B - / WNT10B^{IVS1} -

Our analysis showed that all therapy-related AMLs fall in the first "double-negative" group, favorable-risk patients [namely, t(15;17), t(8;21), inv(16)/t(16;16)] are grouped in the "single-positive" group, whereas all the other AML-patients (AML with other recurrent genetic abnormalities, AML with MDS-related features, AML not otherwise specified) presented the WNT10B^{IVS1} allele variant and are part of the "double-positive" group (see **Table 15**).

Table 15 - WNT-based classification of AML-patients

Patient class	WNT arrangement	Termed
Therapy-related AMLs	WNT10B - / WNT10B^{IVS1} -	"double-negative"
Favorable-risk AMLs	WNT10B + / WNT10B^{IVS1} -	"single-positive"
All other AMLs	WNT10B + / WNT10B^{IVS1} +	"double-positive"

Statistical analysis confirmed a significative difference for both WNT10B and WNT10^{IVS1} transcript levels using this WNT-based classification (p <0.0001; Kruskal-Wallis test). Comparative Mann-Whitney U-test endorsed expression of WNT10B in patients with *de novo* AML, while confirmed a significant lacking of mRNA expression in therapy-related diseases (p <0.0001). Similarly, WNT10B^{IVS1} mRNA was highly expressed in AML patients, with the exception of favorable-risk or therapy-related (p <0.001) (**Figure 27**).

Figure 27 - Box-plot distribution of WNT10B and WNT10B^{IVS1} transcript per WNT-based classes

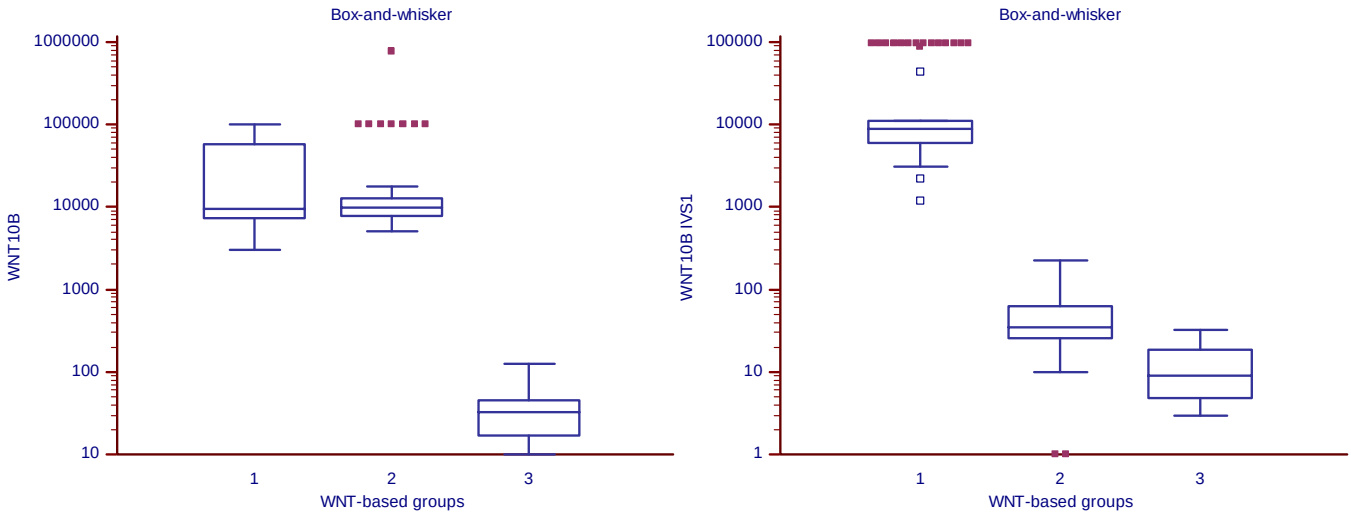

*Legend for WNT-based groups: **1.** other AMLs; **2.** core-binding factor AML; **3.** therapy related AML. Mann-Whitney U-test: see text for details.*

Scatter analysis confirmed the presence of these three distinct classes of patients based on WNT10B / WNT10B^{IVS1} arrangement (see **Figure 28**).

Figure 28 – Scatter diagram of WNT10B and WNT10B^{IVS1} transcript values

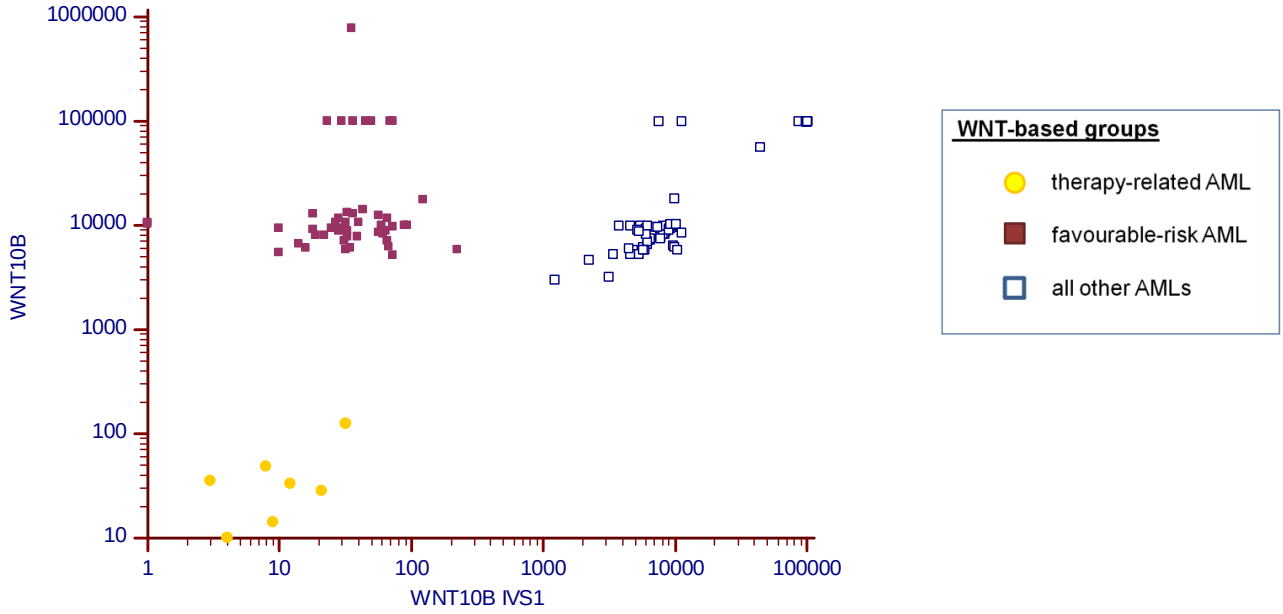

3.3.6. Receiver operating characteristic (ROC) curve analysis

We performed a receiver operating characteristic (ROC) curve analysis of WNT10B and WNT10B^{IVS1} levels towards those three groups (ie, therapy-related AML, CBF-AML, other AML) in search of possible cut-off values.

Canonical WNT10B analysis showed an optimal cut-point at 123 when test for therapy-related AMLs (AUC 1.0, sensitivity 100.0%, specificity 100.0%; *p* <0.0001), while no possible cut-off points were identified for favorable-risk (AUC 0.578, *p* 0.1432) or other AML-patients (AUC 0.533, *p* 0.5304) (see **Figure 29**).

Figure 29– ROC curve analysis for WNT10B transcript values

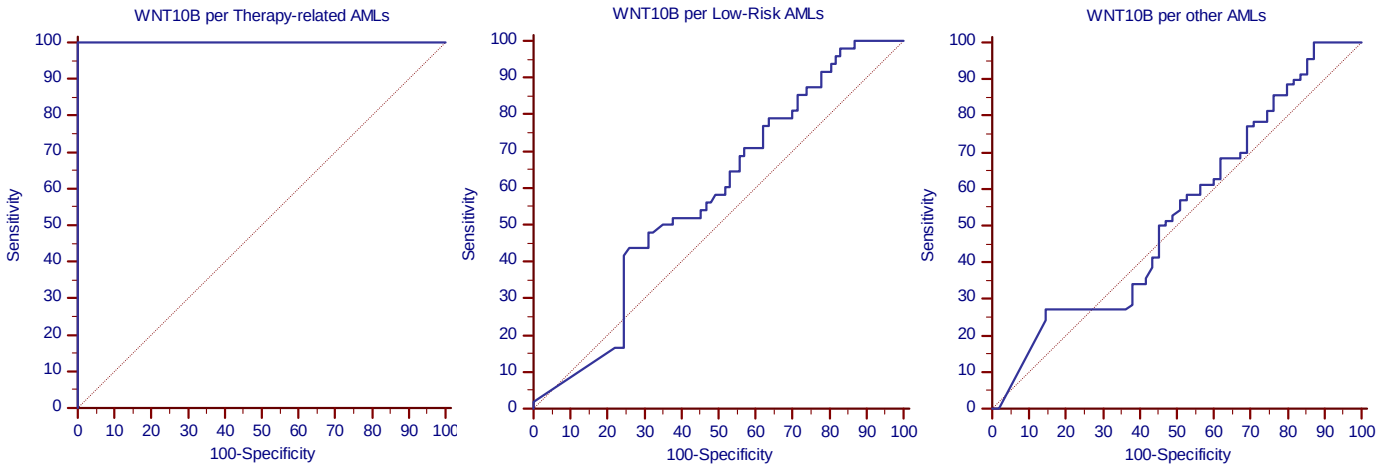

WNT10B^{IVS1} analysis showed an optimal cut-point at 221 when test for favourable-risk AMLs (AUC 0.918, sensitivity 100.0%, specificity 90.91%; *p* <0.0001), while a WNT10B^{IVS1} value lower then or egual to 32 is suggestive for therapy-related AMLs (AUC 0.96, sensitivity 100.0%, specificity 83.76; *p* 0.0001). Similarly, a WNT10B^{IVS1} value higher then 221 is indicative of non-CBF/APL or non-therapy-related AMLs (AUC 1.0, sensitivity 100.0%, specificity 100.0%; *p* 0.0001) (see **Figure 30**).

Figure 30 – ROC curve analysis for WNT10B^{IVS1} transcript values

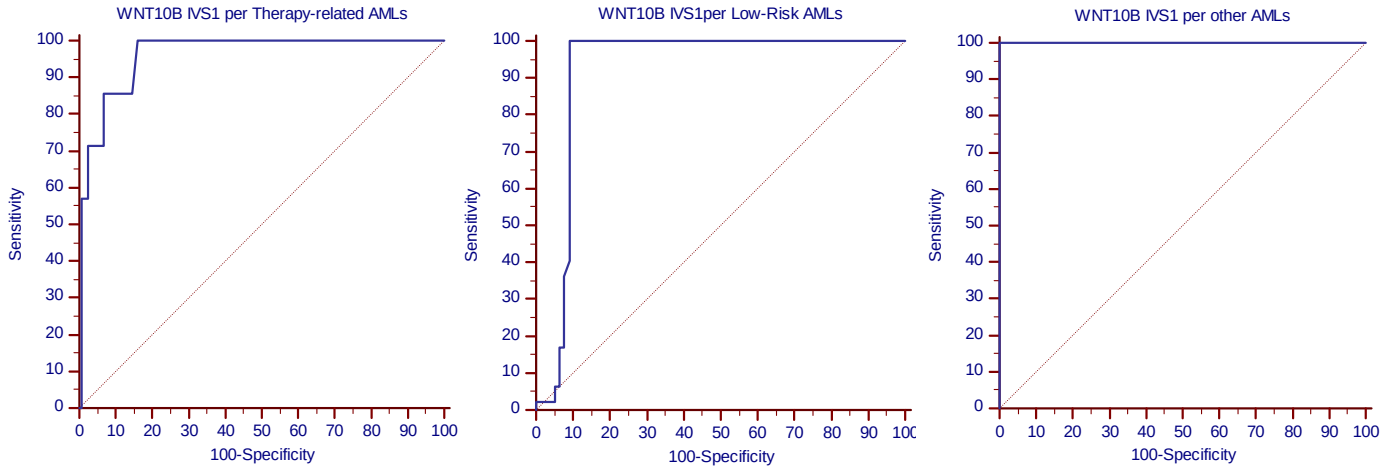

3.3.7. Analysis of molecular mutations influence on WNT levels

FLT3-ITD

Statistical analysis showed no significative difference for both WNT10B and WNT10^{IVS1} transcript levels according to FLT3-ITD mutational status (*p* 0.8818 and *p* 0.1271, respectively; Kruskal-Wallis test). These results were confirmed by comparative Mann-Whitney U-test (see **Figure 31**). The same results were obtained when considering only the "double-positive" population, whereas sample size was too small to perform the test for FLT3-ITD in favorable-risk ("single-positive") and therapy-related ("double-negative") groups.

Figure 31 – Box-plot distribution of WNT per FLT3-ITD

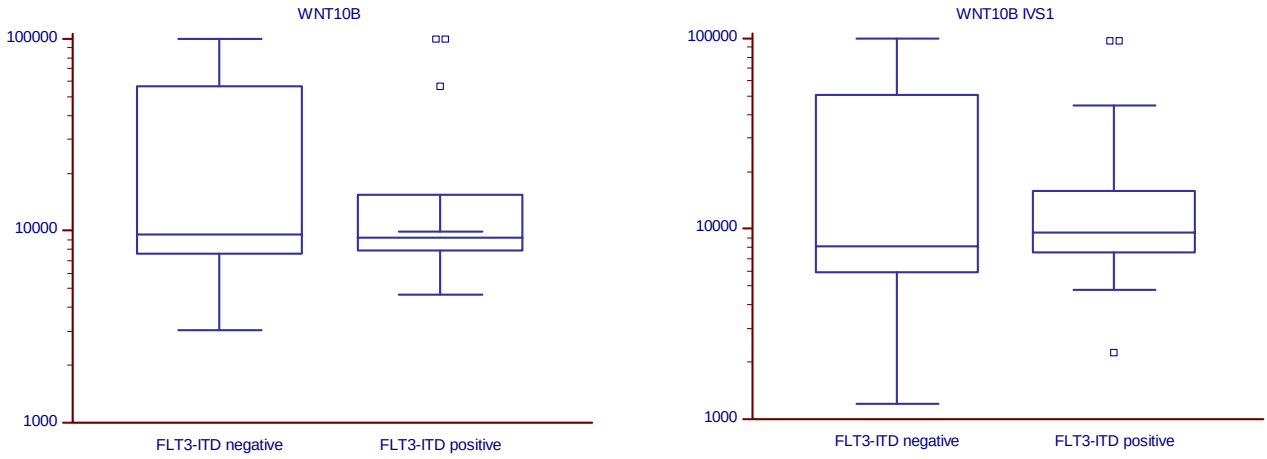

KIT in CBF-AML

Similarly, we observed no significative difference for both WNT10B and WNT10^{IVS1} transcript levels according to KIT mutational status in CBF-AML patients (*p* 0.4561 and *p* 0.4871, respectively; Kruskal-Wallis test). These results were confirmed by comparative Mann-Whitney U-test (see **Figure 32**).

Figure 32 – Box-plot distribution of WNT per KIT mutation in CBF-AML patients

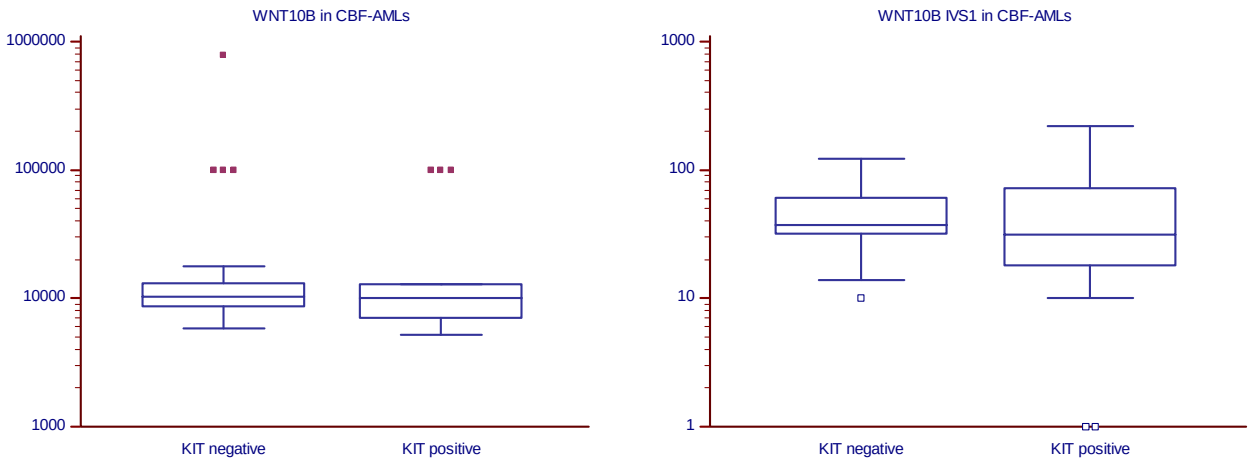

4. DISCUSSION

The deceivingly homogeneous, undifferentiated morphology of the leukemic blasts is now known to mask a heterogeneous collection of cells that recapitulate the hierarchy of precursor cells that characterize the normal process of blood-cell differentiation. According to recent evidences, the leukemia-initiating cell (LIC) properties occur in a self-renewing non-hematopoietic stem cell (HSC) progenitor cell population, preceded by the expansion of a pre-leukemic long-term hematopoietic stem cell (LT-HSC). The WNT/β-catenin pathway has been show to play a critical role in the regulation of cell proliferation, differentiation, and apoptosis of different malignant entities. Recently, Wnt/β-catenin pathway requirement for LIC development in AML has emerged in mouse model, but the molecular function responsible for the pre-leukemic LT-HSC expansion and the acquisition of self-renewal ability in acute myeloide leukemia (AML) remained poorly defined. Furthermore, recent studies revealed aberrant WNT signaling in AML cells that is independent from the occurrence of AML-associated fusion proteins or mutations in tyrosine kinase receptors. The previous results obtained by our research team using gene expression microarrays and pathway analysis, provided direct evidence that the WNT/β-catenin signaling is diffusely activated in the $AC133^{+}$ AML population, with a specific transcriptional signature involving over-expression of the WNT pathway agonists and down-modulation of the major antagonists. Analysis of freshly fractionated cells from AML patients showed that active WNT signaling was predominant in the population highly enriched for the AC133 marker. Notably, *WNT2B, WNT6, WNT10A*, and *WNT10B*, known to promote hematopoietic tissue regeneration, are the WNT mediators specifically upregulated in the $AC133^{+}$ AML cells. Taking these results into consideration, we focused on the characterization of a regenerative function associated to WNT pathway induction. The term "regeneration" has been used to define the physiological phenomena of reconstitution from damage due to injury or disease. Attention was placed on WNT10B, a well-known hematopoietic stem cell regenerative-associated molecule, which was the only one to be expressed by all AML patients. We applied the new *in situ* technique through the use of padlock probes and Rolling Circle Amplification (RCA) for detection and genotyping of individual mRNA molecules in cells and tissues. The mRNA *in situ* detection, performed on AML bone marrow sections, allowed to detect and visualize the WNT10B mRNA molecules at their exact location. We showed a dramatic increase of WNT10B expression and protein release within the microenvironment in the large majority of samples from AML patients recruited into the study. Hematopoietic regenerative-associated WNT ligand WNT10B was expressed at mRNA and protein levels on both leukemic blasts and stromal-like cells, as well as in interstitial spaces, suggesting its secretion and release in the bone marrow microenvironment and indicating a possible autocrine/paracrine mechanism. Conversely, the double immunostaining for WNT10B and dephosphorylated β-catenin (ABC) evidenced that the activation of WNT signaling was restricted only to a smaller subpopulation of cells. In order to better characterize the LICs, we performed a series of direct immunolabeling on AML bone marrow biopsies. The AC133 immunostaining revealed islands of highly positive $AC133^{bright}$ cells amid $AC133^{dim}$ or negative tumor blasts. These $AC133^{bright}$ represented only 8-10% of total marrow cells, and showed a small diameter of the nuclei with an increased nuclear/cytoplasmatic ratio. Activation of WNT signaling marked by expression of the dephosphorylated β-catenin was restricted to this $AC133^{bright}$ leukemic cell population. The reasons for these differences are unclear, but it is possible that β-catenin activation by WNTs requires the expression of specific Fzd receptors, conferring a responsive phenotype restricted to the rare $AC133^{bright}$ population of cells. These firsts results implicate that regeneration-associated WNT signaling affects responsive $AC133^{bright}$ cells whose renewal is promoted by WNT pathway activity.

Focusing our attention on the major locus associated to the regenerative function, we performed a 5'-Rapid Amplification of cDNA Ends (5'-RACE) analysis on WNT10B mRNA, evidencing the presence of a non-physiological transcript variant, termed WNT10B^{IVS1}. This alternative transcript is characterized by the absence of exon 1 and partial retention of 77 nucleotides of intervening sequence 1, and it does not seem to affect the production of the correct protein, since the start site of translation is localized on exon 2. In order to determine the mRNA levels of WNT10B and related WNT10B^{IVS1} transcript variant and to analyze the clinical relevance of WNT10B / WNT10B^{IVS1} expression, we carried out the gene expression analysis by Droplet Digital^{TM} PCR on mononucleated cells derived from 125 AML patients. The study population demonstrated to be a representative sample of leukemic patients described in literature, in term of clinical characteristics and outcomes. We demonstrated that canonical WNT10B was highly expressed in every risk group according to the three main scoring system, formerly the Medical Research Council (MRC), European LeukemiaNet (ELN), and National Comprehensive Cancer Network (NCCN), and we demonstrated high expressed WNT10B^{IVS1} transcript levels in intermediate or adverse-risk patients. Conversely, we recorded a significant lacking of WNT10B^{IVS1} mRNA expression in patients classified as with favorable prognosis, namely comprising patients with core-binding factor (CBF) AML [t(8;21) or inv(16)/t(16;16)] or acute promyelocytic leukemia (APL). Given the significant difference in the expression of WNT10B^{IVS1} values in favorable-risk patients, we analyzed patients subdivided by World Health Organization (WHO) classification. Actually, AML is classified using the WHO classification system based upon a combination of morphology, immunophenotype, genetics, and clinical features. There are four main groups of AML recognized in the 2008 WHO classification (AML with recurrent genetic abnormalities, AML with myelodysplasia-related features, therapy-related AML, AML not otherwise specified), and in the first class are included patients with favorable-risk disease (i.e., CBF-AML and APL). Appling analysis on WHO-based groups, we demonstrated that WNT10B mRNA was highly expressed in all *de novo* AML (ie, AML with recurrent genetic abnormalities and AML not otherwise specified) and AML with myelodysplasia-related features. Conversely, we showed a significant lacking of mRNA expression in patients with therapy-related disease. Non-physiological WNT10B^{IVS1} variant resulted homogenously expressed in AML with myelodysplasia-related features and AML not otherwise specified, while we recorded absence of WNT10B^{IVS1} mRNA in the therapy-related group. Interestingly, patients affected by AML with WHO-based recurrent genetic abnormalities showed a more heterogeneous distribution in WNT10B^{IVS1} transcript levels, including both patients at high or absent mRNA expression. Given this heterogeneous distribution of WNT10B^{IVS1} values, and since we recognized a significant lacking of WNT10B^{IVS1} mRNA expression in patients classified as with favorable-risk prognosis, we went to hive off patients in nine specific genetic profiles: CBF-AML, APL, AML with other recurrent cytogenetic abnormalities, AML with NPM1 or CEBPA mutation, AML with myelodysplasia-related features, therapy-related AML, normal karyotype AML, AML with cytogenetic number abnormalities, and AML with cytogenetic structure abnormalities. Analysis for canonical WNT10B confirmed elevated mRNA levels in all groups of AML patients, with the exception of patients with therapy-related disease. Conversely, WNT10B^{IVS1} mRNA was non-detectable in CBF-AML, APL, and therapy-related diseases, while it was highly expressed in all the remaining groups of patients. The same results were confirmed by grouping patients with *de novo* normal karyotype AML and structural or number cytogenetic abnormalities. Furthermore, we demonstrated the independence of WNT transcript levels from other concomitant molecular mutations, as if to indicate that

WNT represents an early molecular event, independent from the acquisition by the leukemic population of secondary additional events.

Combining these expression results, it was possible to recognize three distinct WNT10B / WNT10B^{IVS1} patterns, termed “double-positive” (WNT10B+ / WNT10B^{IVS1}+), “single-positive” (WNT10B+ / WNT10B^{IVS1}–), and “double-negative” (WNT10B– / WNT10B^{IVS1}–). Our analysis showed that all therapy-related AMLs were characterized by non-detectable levels of both WNT10B and WNT10B^{IVS1} mRNA (“double-negative”), while patients classified as with favorable-risk prognosis presented WNT10B mRNA at high levels and were negative for the variant WNT10B^{IVS1} transcript (“single-positive”). Notably, two patients presenting with CBF-AML inv(16)(p13q22) and one patient with normal karyotype AML with NPM1 mutation were clinically considered as to have a therapy-related AML because of a prior exposure to cytotoxic agents with an adequate latency period. Analysis for WNT10B / WNT10B^{IVS1} succeeded in recognize these therapy-related cases, confirming the lacking of both WNT transcript. Interestingly, all other patients with *de novo* or MDS-related AML expressed canonical WNT10B at high levels and are particularly characterized by the expression of the non-physiological WNT10B^{IVS1} allele variant.

In the last few years, it has become more widely appreciated that multiple genetic lesions, including not only microscopically detectable chromosomal rearrangements or numerical abnormalities but also point gene mutations, cooperate to establish the leukemic process and influence its morphologic and clinical characteristics. Although rearrangements of genes that encode transcription factors may lead to impaired maturation of one or more myeloid lineages, mutations of other genes (such as *FLT3*, *JAK2*, *RAS*, or *KIT)* that encode proteins involved in signal transduction pathways may be required for the proliferation and survival of the neoplastic clone. The discovery of the importance of gene mutations in leukemogenesis has also paved the way for the genetic characterization of many cases of cytogenetically normal AML. Although these leukemias with normal kayotype are actually categorized as a unique entity, it is important to realize that additional genetic abnormalities may coexist and explain their different biology and clinical behavior, including response to therapy and survival. One major challenge is how to incorporate genetic aberrations into a classification scheme of AML capable of defining homogeneous, biologically relevant, and mutually exclusive entities based not only on the prognostic value of a genetic abnormality, but on morphologic, clinical, phenotypic, and unique biologic properties.

The results presented here provided a compelling evidence that regeneration-associated WNT signaling exceeds the homeostatic range in the majority of human AML cases. These newly discovered genetic abnormalities WNT10B / WNT10B^{IVS1} seem to be associated with clinical, morphologic, and phenotypic features that allow identification of specific leukemic entity. Canonical WNT10B resulted expressed in all *de novo* AML patients here examined, representing the gene with the highest expression in leukemic patients among all the genes actually known. Furthermore, we found a non-physiological WNT10B^{IVS1} variant highly expressed in all non-favorable risk *de novo* AML, which may represent a possible marker for this setting of patients. Besides, WHO classification stated that in CBF-AML and APL the genetic abnormality is sufficient for the diagnosis of AML regardless of the blast percentage in peripheral blood or bone marrow. Here, we presented a distinct molecular signature capable of distinguish with extremely high accuracy these favorable-risk patients from all the other *de novo* AML patients, using a non-time consuming and inexpensive test.

Similarly, we demonstrated a specific molecular profile capable to recognize therapy-related disease, even in those setting in which cytogenetic or molecular analysis may be misleading.

These findings, if confirmed in a larger population of patients, may help in refine diagnostic or prognostic criteria for previously described neoplasms, and to introduce newly recognized disease entities possibly characterized by distinct causative pathogenic mechanisms.

References

1. Godin IE, Garcia-Porrero JA, Coutinho A, et al. Para-aortic splanchnopleura from early mouse embryos contains B1a cell progenitors. Nature 1993; 364:67.
2. Botnick LE, Hannon EC, Hellman S. Nature of the hemopoietic stem cell compartment and its proliferative potential. Blood Cells 1979; 5:195.
3. Orkin SH. Transcription factors and hematopoietic development. J Biol Chem 1995; 270:4955.
4. Tenen DG, Hromas R, Licht JD, Zhang DE. Transcription factors, normal myeloid development, and leukemia. Blood 1997; 90:489.
5. Rabbitts TH. Chromosomal translocations in human cancer. Nature 1994; 372:143.
6. Genovese G, Kähler AK, Handsaker RE, et al. Clonal hematopoiesis and blood-cancer risk inferred from blood DNA sequence. N Engl J Med 2014; 371:2477.
7. Jaiswal S, Fontanillas P, Flannick J, et al. Age-related clonal hematopoiesis associated with adverse outcomes. N Engl J Med 2014; 371:2488.
8. Xie M, Lu C, Wang J, et al. Age-related mutations associated with clonal hematopoietic expansion and malignancies. Nat Med 2014; 20:1472.
9. Fialkow PJ, Singer JW, Adamson JW, et al. Acute nonlymphocytic leukemia: expression in cells restricted to granulocytic and monocytic differentiation. N Engl J Med 1979; 301:1.
10. Fialkow PJ, Singer JW, Adamson JW, et al. Acute nonlymphocytic leukemia: heterogeneity of stem cell origin. Blood 1981; 57:1068.
11. Ferraris AM, Canepa L, Mareni C, et al. Reexpression of normal stem cells in erythroleukemia during remission. Blood 1983; 62:177.
12. Fearon ER, Burke PJ, Schiffer CA, et al. Differentiation of leukemia cells to polymorphonuclear leukocytes in patients with acute nonlymphocytic leukemia. N Engl J Med 1986; 315:15.
13. Keinänen M, Griffin JD, Bloomfield CD, et al. Clonal chromosomal abnormalities showing multiple-cell-lineage involvement in acute myeloid leukemia. N Engl J Med 1988; 318:1153.
14. van Lom K, Hagemeijer A, Smit EM, Löwenberg B. In situ hybridization on May-Grünwald Giemsa-stained bone marrow and blood smears of patients with hematologic disorders allows detection of cell-lineage-specific cytogenetic abnormalities. Blood 1993; 82:884.
15. Bonnet D, Dick JE. Human acute myeloid leukemia is organized as a hierarchy that originates from a primitive hematopoietic cell. Nat Med 1997; 3:730.
16. Turhan AG, Lemoine FM, Debert C, et al. Highly purified primitive hematopoietic stem cells are PML-RARA negative and generate nonclonal progenitors in acute promyelocytic leukemia. Blood 1995; 85:2154.
17. McCulloch EA. Stem cells in normal and leukemic hemopoiesis (Henry Stratton Lecture, 1982). Blood 1983; 62:1.
18. Bonnet D. Normal and leukaemic stem cells. Br J Haematol 2005; 130:469.
19. McCulloch EA. Stem cells in normal and leukemic hemopoiesis (Henry Stratton Lecture, 1982). Blood 1983; 62:1.
20. Bonnet D. Normal and leukaemic stem cells. Br J Haematol 2005; 130:469.
21. Civin CI, Strauss LC, Brovall C, et al. Antigenic analysis of hematopoiesis. III. A hematopoietic progenitor cell surface antigen defined by a monoclonal antibody raised against KG-1a cells. J Immunol 1984; 133:157.
22. Terstappen LW, Huang S, Safford M, et al. Sequential generations of hematopoietic colonies derived from single nonlineage-committed CD34+CD38- progenitor cells. Blood 1991; 77:1218.
23. Stubbs MC, Armstrong SA. Therapeutic implications of leukemia stem cell development. Clin Cancer Res 2007; 13:3439.
24. Huang S, Terstappen LW. Formation of haematopoietic microenvironment and haematopoietic stem cells from single human bone marrow stem cells. Nature 1992; 360:745.
25. Mehrotra B, George TI, Kavanau K, et al. Cytogenetically aberrant cells in the stem cell compartment (CD34+lin-) in acute myeloid leukemia. Blood 1995; 86:1139.

26. Haase D, Feuring-Buske M, Könemann S, et al. Evidence for malignant transformation in acute myeloid leukemia at the level of early hematopoietic stem cells by cytogenetic analysis of CD34+ subpopulations. Blood 1995; 86:2906.
27. Levis M, Murphy KM, Pham R, et al. Internal tandem duplications of the FLT3 gene are present in leukemia stem cells. Blood 2005; 106:673.
28. Nilsson L, Astrand-Grundström I, Arvidsson I, et al. Isolation and characterization of hematopoietic progenitor/stem cells in 5q-deleted myelodysplastic syndromes: evidence for involvement at the hematopoietic stem cell level. Blood 2000; 96:2012.
29. Miura I, Kobayashi Y, Takahashi N, et al. Involvement of natural killer cells in patients with myelodysplastic syndrome carrying monosomy 7 revealed by the application of fluorescence in situ hybridization to cells collected by means of fluorescence-activated cell sorting. Br J Haematol 2000; 110:876.
30. Lapidot T, Sirard C, Vormoor J, et al. A cell initiating human acute myeloid leukaemia after transplantation into SCID mice. Nature 1994; 367:645.
31. Jacobs A. Leukaemia Research Fund annual guest lecture 1990. Genetics lesions in preleukaemia. Leukemia 1991; 5:277.
32. Ley TJ, Mardis ER, Ding L, et al. DNA sequencing of a cytogenetically normal acute myeloid leukaemia genome. Nature 2008; 456:66.
33. Mardis ER, Ding L, Dooling DJ, et al. Recurring mutations found by sequencing an acute myeloid leukemia genome. N Engl J Med 2009; 361:1058.
34. Reilly JT. Pathogenesis of acute myeloid leukaemia and inv(16)(p13;q22): a paradigm for understanding leukaemogenesis? Br J Haematol 2005; 128:18.
35. Bachas C, Schuurhuis GJ, Hollink IH, et al. High-frequency type I/II mutational shifts between diagnosis and relapse are associated with outcome in pediatric AML: implications for personalized medicine. Blood 2010; 116:2752.
36. Fialkow PJ, Janssen JW, Bartram CR. Clonal remissions in acute nonlymphocytic leukemia: evidence for a multistep pathogenesis of the malignancy. Blood 1991; 77:1415.
37. Bartram CR, Ludwig WD, Hiddemann W, et al. Acute myeloid leukemia: analysis of ras gene mutations and clonality defined by polymorphic X-linked loci. Leukemia 1989; 3:247.
38. Busque L, Gilliland DG. Clonal evolution in acute myeloid leukemia. Blood 1993; 82:337.
39. Ding L, Ley TJ, Larson DE, et al. Clonal evolution in relapsed acute myeloid leukaemia revealed by whole-genome sequencing. Nature 2012; 481:506.
40. Cancer Genome Atlas Research Network. Genomic and epigenomic landscapes of adult de novo acute myeloid leukemia. N Engl J Med 2013; 368:2059.
41. Walter MJ, Shen D, Ding L, et al. Clonal architecture of secondary acute myeloid leukemia. N Engl J Med 2012; 366:1090.
42. Nucifora G, Larson RA, Rowley JD. Persistence of the 8;21 translocation in patients with acute myeloid leukemia type M2 in long-term remission. Blood 1993; 82:712.
43. Jurlander J, Caligiuri MA, Ruutu T, et al. Persistence of the AML1/ETO fusion transcript in patients treated with allogeneic bone marrow transplantation for t(8;21) leukemia. Blood 1996; 88:2183.
44. Pagana L, Pulsoni A, Tosti ME, et al. Clinical and biological features of acute myeloid leukaemia occurring as second malignancy: GIMEMA archive of adult acute leukaemia. Br J Haematol 2001; 112:109.
45. Levine EG, Bloomfield CD. Leukemias and myelodysplastic syndromes secondary to drug, radiation, and environmental exposure. Semin Oncol 1992; 19:47.
46. Seedhouse C, Russell N. Advances in the understanding of susceptibility to treatment-related acute myeloid leukaemia. Br J Haematol 2007; 137:513.
47. Guillem V, Tormo M. Influence of DNA damage and repair upon the risk of treatment related leukemia. Leuk Lymphoma 2008; 49:204.
48. Le Beau MM, Albain KS, Larson RA, et al. Clinical and cytogenetic correlations in 63 patients with therapy-related myelodysplastic syndromes and acute nonlymphocytic leukemia: further evidence for characteristic abnormalities of chromosomes no. 5 and 7. J Clin Oncol 1986; 4:325.
49. Thirman MJ, Gill HJ, Burnett RC, et al. Rearrangement of the MLL gene in acute lymphoblastic and acute myeloid leukemias with 11q23 chromosomal translocations. N Engl J Med 1993; 329:909.

50. Albain KS, Le Beau MM, Ullirsch R, Schumacher H. Implication of prior treatment with drug combinations including inhibitors of topoisomerase II in therapy-related monocytic leukemia with a 9;11 translocation. Genes Chromosomes Cancer 1990; 2:53.
51. Pedersen-Bjergaard J, Philip P. Two different classes of therapy-related and de-novo acute myeloid leukemia? Cancer Genet Cytogenet 1991; 55:119.
52. Super HJ, McCabe NR, Thirman MJ, et al. Rearrangements of the MLL gene in therapy-related acute myeloid leukemia in patients previously treated with agents targeting DNA-topoisomerase II. Blood 1993; 82:3705.
53. Little JB. Cellular, molecular, and carcinogenic effects of radiation. Hematol Oncol Clin North Am 1993; 7:337.
54. Ishimaru T, Otake M, Ischimaru M. Dose-response relationship of neutrons and gamma rays to leukemia incidence among atomic bomb survivors in Hiroshima and Nagasaki by type of leukemia, 1950--1971. Radiat Res 1979; 77:377.
55. Bizzozero OJ Jr, Johnson KG, Ciocco A. Radiation-related leukemia in Hiroshima and Nagasaki, 1946-1964. I. Distribution, incidence and appearance time. N Engl J Med 1966; 274:1095.
56. Yoshinaga S, Mabuchi K, Sigurdson AJ, et al. Cancer risks among radiologists and radiologic technologists: review of epidemiologic studies. Radiology 2004; 233:313.
57. Shuryak I, Sachs RK, Hlatky L, et al. Radiation-induced leukemia at doses relevant to radiation therapy: modeling mechanisms and estimating risks. J Natl Cancer Inst 2006; 98:1794.
58. Brandt L, Nilsson PG, Mitelman F. Occupational exposure to petroleum products in men with acute non-lymphocytic leukaemia. Br Med J 1978; 1:553.
59. Austin H, Delzell E, Cole P. Benzene and leukemia. A review of the literature and a risk assessment. Am J Epidemiol 1988; 127:419.
60. Schnatter AR, Glass DC, Tang G, et al. Myelodysplastic syndrome and benzene exposure among petroleum workers: an international pooled analysis. J Natl Cancer Inst 2012; 104:1724.
61. Rushton L, Schnatter AR, Tang G, Glass DC. Acute myeloid and chronic lymphoid leukaemias and exposure to low-level benzene among petroleum workers. Br J Cancer 2014; 110:783.
62. Irons RD, Gross SA, Le A, et al. Integrating WHO 2001-2008 criteria for the diagnosis of Myelodysplastic Syndrome (MDS): a case-case analysis of benzene exposure. Chem Biol Interact 2010; 184:30.
63. Smith MT, Wang Y, Kane E, et al. Low NAD(P)H:quinone oxidoreductase 1 activity is associated with increased risk of acute leukemia in adults. Blood 2001; 97:1422.
64. Larson RA, Wang Y, Banerjee M, et al. Prevalence of the inactivating 609C-->T polymorphism in the NAD(P)H:quinone oxidoreductase (NQO1) gene in patients with primary and therapy-related myeloid leukemia. Blood 1999; 94:803.
65. Rothman N, Smith MT, Hayes RB, et al. Benzene poisoning, a risk factor for hematological malignancy, is associated with the NQO1 609C-->T mutation and rapid fractional excretion of chlorzoxazone. Cancer Res 1997; 57:2839.
66. Poiesz BJ, Ruscetti FW, Gazdar AF, et al. Detection and isolation of type C retrovirus particles from fresh and cultured lymphocytes of a patient with cutaneous T-cell lymphoma. Proc Natl Acad Sci U S A 1980; 77:7415.
67. Gallo R, Ruscetti F, Collins S, et al. Human myeloid leukemia cells: Studies on oncornaviral related information and in vitro growth and differentiation. In: Hematopoietic Cell Differentiation, Golde D, Cline M, Metcalf D, et al. (Eds), Academic Press, Orlando 1979. Vol 10, p.335.
68. Grimwade D, Hills RK, Moorman AV, et al. Refinement of cytogenetic classification in acute myeloid leukemia: determination of prognostic significance of rare recurring chromosomal abnormalities among 5876 younger adult patients treated in the United Kingdom Medical Research Council trials. Blood 2010; 116:354.
69. Cancer Genome Atlas Research Network. Genomic and epigenomic landscapes of adult de novo acute myeloid leukemia. N Engl J Med 2013; 368:2059.
70. Bienz M, Ludwig M, Leibundgut EO, et al. Risk assessment in patients with acute myeloid leukemia and a normal karyotype. Clin Cancer Res 2005; 11:1416.
71. Marcucci G, Mrózek K, Bloomfield CD. Molecular heterogeneity and prognostic biomarkers in adults with acute myeloid leukemia and normal cytogenetics. Curr Opin Hematol 2005; 12:68.

72. Santamaría CM, Chillón MC, García-Sanz R, et al. Molecular stratification model for prognosis in cytogenetically normal acute myeloid leukemia. Blood 2009; 114:148.
73. Kottaridis PD, Gale RE, Frew ME, et al. The presence of a FLT3 internal tandem duplication in patients with acute myeloid leukemia (AML) adds important prognostic information to cytogenetic risk group and response to the first cycle of chemotherapy: analysis of 854 patients from the United Kingdom Medical Research Council AML 10 and 12 trials. Blood 2001; 98:1752.
74. Whitman SP, Archer KJ, Feng L, et al. Absence of the wild-type allele predicts poor prognosis in adult de novo acute myeloid leukemia with normal cytogenetics and the internal tandem duplication of FLT3: a cancer and leukemia group B study. Cancer Res 2001; 61:7233.
75. Schnittger S, Schoch C, Dugas M, et al. Analysis of FLT3 length mutations in 1003 patients with acute myeloid leukemia: correlation to cytogenetics, FAB subtype, and prognosis in the AMLCG study and usefulness as a marker for the detection of minimal residual disease. Blood 2002; 100:59.
76. Kottaridis PD, Gale RE, Linch DC. Flt3 mutations and leukaemia. Br J Haematol 2003; 122:523.
77. Yamamoto Y, Kiyoi H, Nakano Y, et al. Activating mutation of D835 within the activation loop of FLT3 in human hematologic malignancies. Blood 2001; 97:2434.
78. Fröhling S, Schlenk RF, Breitruck J, et al. Prognostic significance of activating FLT3 mutations in younger adults (16 to 60 years) with acute myeloid leukemia and normal cytogenetics: a study of the AML Study Group Ulm. Blood 2002; 100:4372.
79. Pollard JA, Alonzo TA, Gerbing RB, et al. FLT3 internal tandem duplication in CD34+/CD33- precursors predicts poor outcome in acute myeloid leukemia. Blood 2006; 108:2764.
80. Kayser S, Schlenk RF, Londono MC, et al. Insertion of FLT3 internal tandem duplication in the tyrosine kinase domain-1 is associated with resistance to chemotherapy and inferior outcome. Blood 2009; 114:2386.
81. Whitman SP, Maharry K, Radmacher MD, et al. FLT3 internal tandem duplication associates with adverse outcome and gene- and microRNA-expression signatures in patients 60 years of age or older with primary cytogenetically normal acute myeloid leukemia: a Cancer and Leukemia Group B study. Blood 2010; 116:3622.
82. Rockova V, Abbas S, Wouters BJ, et al. Risk stratification of intermediate-risk acute myeloid leukemia: integrative analysis of a multitude of gene mutation and gene expression markers. Blood 2011; 118:1069.
83. Patel JP, Gönen M, Figueroa ME, et al. Prognostic relevance of integrated genetic profiling in acute myeloid leukemia. N Engl J Med 2012; 366:1079.
84. Schlenk RF, Döhner K, Krauter J, et al. Mutations and treatment outcome in cytogenetically normal acute myeloid leukemia. N Engl J Med 2008; 358:1909.
85. Bacher U, Haferlach C, Kern W, et al. Prognostic relevance of FLT3-TKD mutations in AML: the combination matters--an analysis of 3082 patients. Blood 2008; 111:2527.
86. Falini B, Mecucci C, Tiacci E, et al. Cytoplasmic nucleophosmin in acute myelogenous leukemia with a normal karyotype. N Engl J Med 2005; 352:254.
87. Falini B, Nicoletti I, Martelli MF, Mecucci C. Acute myeloid leukemia carrying cytoplasmic/mutated nucleophosmin (NPMc+ AML): biologic and clinical features. Blood 2007; 109:874.
88. Hollink IH, Zwaan CM, Zimmermann M, et al. Favorable prognostic impact of NPM1 gene mutations in childhood acute myeloid leukemia, with emphasis on cytogenetically normal AML. Leukemia 2009; 23:262.
89. Schneider F, Hoster E, Unterhalt M, et al. NPM1 but not FLT3-ITD mutations predict early blast cell clearance and CR rate in patients with normal karyotype AML (NK-AML) or high-risk myelodysplastic syndrome (MDS). Blood 2009; 113:5250.
90. Becker H, Marcucci G, Maharry K, et al. Favorable prognostic impact of NPM1 mutations in older patients with cytogenetically normal de novo acute myeloid leukemia and associated gene- and microRNA-expression signatures: a Cancer and Leukemia Group B study. J Clin Oncol 2010; 28:596.
91. Falini B, Martelli MP, Bolli N, et al. Acute myeloid leukemia with mutated nucleophosmin (NPM1): is it a distinct entity? Blood 2011; 117:1109.
92. Nerlov C. C/EBPalpha mutations in acute myeloid leukaemias. Nat Rev Cancer 2004; 4:394.
93. Eyholzer M, Schmid S, Wilkens L, et al. The tumour-suppressive miR-29a/b1 cluster is regulated by CEBPA and blocked in human AML. Br J Cancer 2010; 103:275.

94. Marcucci G, Maharry K, Radmacher MD, et al. Prognostic significance of, and gene and microRNA expression signatures associated with, CEBPA mutations in cytogenetically normal acute myeloid leukemia with high-risk molecular features: a Cancer and Leukemia Group B Study. J Clin Oncol 2008; 26:5078.
95. Fröhling S, Schlenk RF, Stolze I, et al. CEBPA mutations in younger adults with acute myeloid leukemia and normal cytogenetics: prognostic relevance and analysis of cooperating mutations. J Clin Oncol 2004; 22:624.
96. Taskesen E, Bullinger L, Corbacioglu A, et al. Prognostic impact, concurrent genetic mutations, and gene expression features of AML with CEBPA mutations in a cohort of 1182 cytogenetically normal AML patients: further evidence for CEBPA double mutant AML as a distinctive disease entity. Blood 2011; 117:2469.
97. Renneville A, Boissel N, Gachard N, et al. The favorable impact of CEBPA mutations in patients with acute myeloid leukemia is only observed in the absence of associated cytogenetic abnormalities and FLT3 internal duplication. Blood 2009; 113:5090.
98. Wouters BJ, Löwenberg B, Erpelinck-Verschueren CA, et al. Double CEBPA mutations, but not single CEBPA mutations, define a subgroup of acute myeloid leukemia with a distinctive gene expression profile that is uniquely associated with a favorable outcome. Blood 2009; 113:3088.
99. Dufour A, Schneider F, Metzeler KH, et al. Acute myeloid leukemia with biallelic CEBPA gene mutations and normal karyotype represents a distinct genetic entity associated with a favorable clinical outcome. J Clin Oncol 2010; 28:570.
100. Green CL, Koo KK, Hills RK, et al. Prognostic significance of CEBPA mutations in a large cohort of younger adult patients with acute myeloid leukemia: impact of double CEBPA mutations and the interaction with FLT3 and NPM1 mutations. J Clin Oncol 2010; 28:2739.
101. Paschka P, Marcucci G, Ruppert AS, et al. Adverse prognostic significance of KIT mutations in adult acute myeloid leukemia with inv(16) and t(8;21): a Cancer and Leukemia Group B Study. J Clin Oncol 2006; 24:3904.
102. Lück SC, Russ AC, Du J, et al. KIT mutations confer a distinct gene expression signature in core binding factor leukaemia. Br J Haematol 2010; 148:925.
103. Cairoli R, Beghini A, Grillo G, et al. Prognostic impact of c-KIT mutations in core binding factor leukemias: an Italian retrospective study. Blood 2006;107:3463.
104. Cairoli R, Beghini A, Turrini M, et al. Old and new prognostic factors in acute myeloid leukemia with deranged core-binding factor beta. Am J Hematol 2013;88:594.
105. Bullinger L, Döhner K, Bair E, et al. Use of gene-expression profiling to identify prognostic subclasses in adult acute myeloid leukemia. N Engl J Med 2004; 350:1605.
106. Metzeler KH, Hummel M, Bloomfield CD, et al. An 86-probe-set gene-expression signature predicts survival in cytogenetically normal acute myeloid leukemia. Blood 2008; 112:4193.
107. Li Z, Herold T, He C, et al. Identification of a 24-gene prognostic signature that improves the European LeukemiaNet risk classification of acute myeloid leukemia: an international collaborative study. J Clin Oncol 2013; 31:1172.
108. Radmacher MD, Marcucci G, Ruppert AS, et al. Independent confirmation of a prognostic gene-expression signature in adult acute myeloid leukemia with a normal karyotype: a Cancer and Leukemia Group B study. Blood 2006; 108:1677.
109. Bullinger L, Rücker FG, Kurz S, et al. Gene-expression profiling identifies distinct subclasses of core binding factor acute myeloid leukemia. Blood 2007; 110:1291.
110. Haferlach T, Kohlmann A, Schnittger S, et al. Global approach to the diagnosis of leukemia using gene expression profiling. Blood 2005; 106:1189.
111. Mrózek K, Marcucci G, Paschka P, et al. Clinical relevance of mutations and gene-expression changes in adult acute myeloid leukemia with normal cytogenetics: are we ready for a prognostically prioritized molecular classification? Blood 2007; 109:431.
112. Greaves M. Cancer stem cells renew their impact. Nat Med 2011; 17:1046.
113. Bennett JM, Catovsky D, Daniel MT, et al. Proposed revised criteria for the classification of acute myeloid leukemia. A report of the French-American-British Cooperative Group. Ann Intern Med 1985; 103:620.
114. Koeffler HP. Syndromes of acute nonlymphocytic leukemia. Ann Intern Med 1987; 107:748.

115. Vardiman JW, Thiele J, Arber DA, et al. The 2008 revision of the World Health Organization (WHO) classification of myeloid neoplasms and acute leukemia: rationale and important changes. Blood 2009; 114:937.
116. Swerdlow SH, Campo E, Harris NL, et al. (Eds). World Health Organization Classification of Tumours of Haematopoietic and Lymphoid Tissues, IARC Press, Lyon 2008.
117. Granfeldt Østgård LS, Medeiros BC, Sengeløv H, et al. Epidemiology and Clinical Significance of Secondary and Therapy-Related Acute Myeloid Leukemia: A National Population-Based Cohort Study. J Clin Oncol 2015; 33:3641.
118. Morton LM, Dores GM, Tucker MA, et al. Evolving risk of therapy-related acute myeloid leukemia following cancer chemotherapy among adults in the United States, 1975-2008. Blood 2013; 121:2996.
119. Pedersen-Bjergaard J. Insights into leukemogenesis from therapy-related leukemia. N Engl J Med 2005; 352:1591.
120. Takeyama K, Seto M, Uike N, et al. Therapy-related leukemia and myelodysplastic syndrome: a large-scale Japanese study of clinical and cytogenetic features as well as prognostic factors. Int J Hematol 2000; 71:144.
121. Dores GM, Devesa SS, Curtis RE, et al. Acute leukemia incidence and patient survival among children and adults in the United States, 2001-2007. Blood 2012; 119:34.
122. Pedersen-Bjergaard J, Rowley JD. The balanced and the unbalanced chromosome aberrations of acute myeloid leukemia may develop in different ways and may contribute differently to malignant transformation. Blood 1994; 83:2780.
123. Rowley JD, Golomb HM, Vardiman JW. Nonrandom chromosome abnormalities in acute leukemia and dysmyelopoietic syndromes in patients with previously treated malignant disease. Blood 1981; 58:759.
124. Traweek ST, Slovak ML, Nademanee AP, et al. Clonal karyotypic hematopoietic cell abnormalities occurring after autologous bone marrow transplantation for Hodgkin's disease and non-Hodgkin's lymphoma. Blood 1994; 84:957.
125. Godley, LA, Larson, RA. Therapy-related myelodysplastic syndrome and myeloid leukemia. In: Myelodysplastic Syndrome: Pathology and Clinical Management, 2nd ed, Steensma, DP (Eds), Informa Healthcare, 2008.
126. Kantarjian HM, Keating MJ, Walters RS, et al. Therapy-related leukemia and myelodysplastic syndrome: clinical, cytogenetic, and prognostic features. J Clin Oncol 1986; 4:1748.
127. Le Beau MM, Albain KS, Larson RA, et al. Clinical and cytogenetic correlations in 63 patients with therapy-related myelodysplastic syndromes and acute nonlymphocytic leukemia: further evidence for characteristic abnormalities of chromosomes no. 5 and 7. J Clin Oncol 1986; 4:325.
128. Pedersen-Bjergaard J, Pedersen M, Roulston D, Philip P. Different genetic pathways in leukemogenesis for patients presenting with therapy-related myelodysplasia and therapy-related acute myeloid leukemia. Blood 1995; 86:3542.
129. Larson RA, Wang Y, Banerjee M, et al. Prevalence of the inactivating 609C-->T polymorphism in the NAD(P)H:quinone oxidoreductase (NQO1) gene in patients with primary and therapy-related myeloid leukemia. Blood 1999; 94:803.
130. Allan JM, Smith AG, Wheatley K, et al. Genetic variation in XPD predicts treatment outcome and risk of acute myeloid leukemia following chemotherapy. Blood 2004; 104:3872.
131. Smith AG, Worrillow LJ, Allan JM. A common genetic variant in XPD associates with risk of 5q- and 7q-deleted acute myeloid leukemia. Blood 2007; 109:1233.
132. Ahuja HG, Felix CA, Aplan PD. The t(11;20)(p15;q11) chromosomal translocation associated with therapy-related myelodysplastic syndrome results in an NUP98-TOP1 fusion. Blood 1999; 94:3258.
133. Arai Y, Hosoda F, Kobayashi H, et al. The inv(11)(p15q22) chromosome translocation of de novo and therapy-related myeloid malignancies results in fusion of the nucleoporin gene, NUP98, with the putative RNA helicase gene, DDX10. Blood 1997; 89:3936.
134. Leonard DG, Travis LB, Addya K, et al. p53 mutations in leukemia and myelodysplastic syndrome after ovarian cancer. Clin Cancer Res 2002; 8:973.
135. Pui CH, Relling MV. Topoisomerase II inhibitor-related acute myeloid leukaemia. Br J Haematol 2000; 109:13.

136. Pedersen-Bjergaard J, Philip P. Balanced translocations involving chromosome bands 11q23 and 21q22 are highly characteristic of myelodysplasia and leukemia following therapy with cytostatic agents targeting at DNA-topoisomerase II. Blood 1991; 78:1147.
137. Sobulo OM, Borrow J, Tomek R, et al. MLL is fused to CBP, a histone acetyltransferase, in therapy-related acute myeloid leukemia with a t(11;16)(q23;p13.3). Proc Natl Acad Sci U S A 1997; 94:8732.
138. Rowley JD, Reshmi S, Sobulo O, et al. All patients with the T(11;16)(q23;p13.3) that involves MLL and CBP have treatment-related hematologic disorders. Blood 1997; 90:535.
139. Shankar DB, Cheng JC, Sakamoto KM. Role of cyclic AMP response element binding protein in human leukemias. Cancer 2005; 104:1819.
140. Hoffmann L, Möller P, Pedersen-Bjergaard J, et al. Therapy-related acute promyelocytic leukemia with t(15;17) (q22;q12) following chemotherapy with drugs targeting DNA topoisomerase II. A report of two cases and a review of the literature. Ann Oncol 1995; 6:781.
141. Beaumont M, Sanz M, Carli PM, et al. Therapy-related acute promyelocytic leukemia. J Clin Oncol 2003; 21:2123.
142. Mistry AR, Felix CA, Whitmarsh RJ, et al. DNA topoisomerase II in therapy-related acute promyelocytic leukemia. N Engl J Med 2005; 352:1529.
143. Mays AN, Osheroff N, Xiao Y, et al. Evidence for direct involvement of epirubicin in the formation of chromosomal translocations in t(15;17) therapy-related acute promyelocytic leukemia. Blood 2010; 115:326.
144. Andersen MK, Christiansen DH, Jensen BA, et al. Therapy-related acute lymphoblastic leukaemia with MLL rearrangements following DNA topoisomerase II inhibitors, an increasing problem: report on two new cases and review of the literature since 1992. Br J Haematol 2001; 114:539.
145. Chen G, Zeng W, Miyazato A, et al. Distinctive gene expression profiles of CD34 cells from patients with myelodysplastic syndrome characterized by specific chromosomal abnormalities. Blood 2004; 104:4210.
146. Le Beau MM, Espinosa R 3rd, Neuman WL, et al. Cytogenetic and molecular delineation of the smallest commonly deleted region of chromosome 5 in malignant myeloid diseases. Proc Natl Acad Sci U S A 1993; 90:5484.
147. Zhao N, Stoffel A, Wang PW, et al. Molecular delineation of the smallest commonly deleted region of chromosome 5 in malignant myeloid diseases to 1-1.5 Mb and preparation of a PAC-based physical map. Proc Natl Acad Sci U S A 1997; 94:6948.
148. Horrigan SK, Arbieva ZH, Xie HY, et al. Delineation of a minimal interval and identification of 9 candidates for a tumor suppressor gene in malignant myeloid disorders on 5q31. Blood 2000; 95:2372.
149. Fairman J, Chumakov I, Chinault AC, et al. Physical mapping of the minimal region of loss in 5q- chromosome. Proc Natl Acad Sci U S A 1995; 92:7406.
150. Boultwood J, Fidler C, Lewis S, et al. Molecular mapping of uncharacteristically small 5q deletions in two patients with the 5q- syndrome: delineation of the critical region on 5q and identification of a 5q- breakpoint. Genomics 1994; 19:425.
151. Ebert BL. Deletion 5q in myelodysplastic syndrome: a paradigm for the study of hemizygous deletions in cancer. Leukemia 2009; 23:1252.
152. Ebert BL, Pretz J, Bosco J, et al. Identification of RPS14 as a 5q- syndrome gene by RNA interference screen. Nature 2008; 451:335.
153. Starczynowski DT, Kuchenbauer F, Argiropoulos B, et al. Identification of miR-145 and miR-146a as mediators of the 5q- syndrome phenotype. Nat Med 2010; 16:49.
154. Kumar M, Narla A, Nonami A, et al. Coordinate loss of a MicroRNA Mir 145 and a protein-coding gene RPS14 cooperate in the pathogeneiss of 5q- syndrome. Blood (ASH Annual Meeting Abstracts) 2009; 114:947.
155. Wang J, Fernald AA, Anastasi J, et al. Haploinsufficiency of Apc leads to ineffective hematopoiesis. Blood 2010; 115:3481.
156. Joslin JM, Fernald AA, Tennant TR, et al. Haploinsufficiency of EGR1, a candidate gene in the del(5q), leads to the development of myeloid disorders. Blood 2007; 110:719.
157. Liu TX, Becker MW, Jelinek J, et al. Chromosome 5q deletion and epigenetic suppression of the gene encoding alpha-catenin (CTNNA1) in myeloid cell transformation. Nat Med 2007; 13:78.

158. Shiseki M, Kitagawa Y, Wang YH, et al. Lack of nucleophosmin mutation in patients with myelodysplastic syndrome and acute myeloid leukemia with chromosome 5 abnormalities. Leuk Lymphoma 2007; 48:2141.
159. Le Beau MM, Espinosa R 3rd, Davis EM, et al. Cytogenetic and molecular delineation of a region of chromosome 7 commonly deleted in malignant myeloid diseases. Blood 1996; 88:1930.
160. Fischer K, Fröhling S, Scherer SW, et al. Molecular cytogenetic delineation of deletions and translocations involving chromosome band 7q22 in myeloid leukemias. Blood 1997; 89:2036.
161. McNerney ME, Brown CD, Wang X, et al. CUX1 is a haploinsufficient tumor suppressor gene on chromosome 7 frequently inactivated in acute myeloid leukemia. Blood 2013; 121:975.
162. Velloso ER, Michaux L, Ferrant A, et al. Deletions of the long arm of chromosome 7 in myeloid disorders: loss of band 7q32 implies worst prognosis. Br J Haematol 1996; 92:574.
163. Ernst T, Chase AJ, Score J, et al. Inactivating mutations of the histone methyltransferase gene EZH2 in myeloid disorders. Nat Genet 2010; 42:722.
164. Nikoloski G, Langemeijer SM, Kuiper RP, et al. Somatic mutations of the histone methyltransferase gene EZH2 in myelodysplastic syndromes. Nat Genet 2010; 42:665.
165. Ferrant A, Doyen C, Delannoy A, et al. Karyotype in acute myeloblastic leukemia: prognostic significance in a prospective study assessing bone marrow transplantation in first remission. Bone Marrow Transplant 1995; 15:685.
166. Keating MJ, Smith TL, Kantarjian H, et al. Cytogenetic pattern in acute myelogenous leukemia: a major reproducible determinant of outcome. Leukemia 1988; 2:403.
167. Bloomfield CD, Lawrence D, Byrd JC, et al. Frequency of prolonged remission duration after high-dose cytarabine intensification in acute myeloid leukemia varies by cytogenetic subtype. Cancer Res 1998; 58:4173.
168. Slovak ML, Kopecky KJ, Cassileth PA, et al. Karyotypic analysis predicts outcome of preremission and postremission therapy in adult acute myeloid leukemia: a Southwest Oncology Group/Eastern Cooperative Oncology Group Study. Blood 2000; 96:4075.
169. Byrd JC, Mrózek K, Dodge RK, et al. Pretreatment cytogenetic abnormalities are predictive of induction success, cumulative incidence of relapse, and overall survival in adult patients with de novo acute myeloid leukemia: results from Cancer and Leukemia Group B (CALGB 8461). Blood 2002; 100:4325.
170. Delaunay J, Vey N, Leblanc T, et al. Prognosis of inv(16)/t(16;16) acute myeloid leukemia (AML): a survey of 110 cases from the French AML Intergroup. Blood 2003; 102:462.
171. Schlenk RF, Benner A, Krauter J, et al. Individual patient data-based meta-analysis of patients aged 16 to 60 years with core binding factor acute myeloid leukemia: a survey of the German Acute Myeloid Leukemia Intergroup. J Clin Oncol 2004; 22:3741.
172. Grimwade D, Walker H, Oliver F, et al. The importance of diagnostic cytogenetics on outcome in AML: analysis of 1612 patients entered into the MRC AML10 trial. Blood. 1998; 92:2322.
173. Wheatley K, Burnett AK, Goldstone AH, et al. A simple, robust, validated and highly predictive index for the determination of risk-directed therapy in acute myeloid leukaemia derived from the MRC AML 10 trial. United Kingdom Medical Research Council's Adult and Childhood Leukaemia Working Parties. Br J Haematol 1999; 107:69.
174. Mrózek K, Marcucci G, Nicolet D, et al. Prognostic significance of the European LeukemiaNet standardized system for reporting cytogenetic and molecular alterations in adults with acute myeloid leukemia. J Clin Oncol 2012; 30:4515.
175. NCCN Clinical Practice Guidelines in Oncology. Acute Myeloid Leukemia: Version 2.2014. National Comprehensive Cancer Network.
176. Nusslein-Volhard C, Wieschaus E. Mutations affecting segment number and polarity in Drosophila. Nature 1980; 287:795.
177. Nusse R, Varmus HE. Many tumors induced by the mouse mammary tumor virus contain a provirus integrated in the same region of the host genome. Cell 1982; 31:99.
178. MacDonald BT, Tamai K, He X. Wnt/β-catenin signaling: components, mechanisms, and diseases. Dev Cell 2009; 17:9.
179. Cheyette BN , Waxman JS , Miller JR , at al. Dapper, a Dishevelled-associated antagonist of beta-catenin and JNK signaling, is required for notochord formation. Dev Cell 2002; 2:449.

180. Valenta T, Lukas J, Doubravska L, et al. HIC1 attenuates Wnt signaling by recruitment of TCF-4 and beta-catenin to the nuclear bodies. EMBO J. 2006; 25:2326.
181. Cao Y, Liu R, Jiang X, et al. Nuclear-cytoplasmic shuttling of menin regulates nuclear translocation of beta-catenin. Mol Cell Biol. 2009; 29:5477.
182. Clevers H. Wnt/beta-catenin signaling in development and disease. Cell 2006; 127:469.
183. Nelson WJ, Nusse R. Convergence of Wnt, beta-catenin, and cadherin pathways. Science 2004; 303:1483.
184. Mosimann C, Hausmann G, Basler K. Beta-catenin hits chromatin: regulation of Wnt target gene activation. Nat Rev Mol Cell Biol 2009; 10:276.
185. Staal FJ, Clevers HC. WNT signalling and haematopoiesis: a WNT-WNT situation. Nat Rev Immunol 2005; 5:21.
186. Rubinfeld B, Albert I, Porfiri E, Fiol C, Munemitsu S, Polakis P. Binding of GSK3beta to the APC-beta-catenin complex and regulation of complex assembly. Science 1996; 272:1023.
187. Munemitsu S, Albert I, Souza B, et a. Regulation of intracellular beta-catenin levels by the adenomatous polyposis coli (APC) tumor-suppressor protein. Proc Natl Acad Sci 1995; 92:3046.
188. Carron C, Pascal A, Djiane A, et al. Frizzled receptor dimerization is sufficient to activate the Wnt/beta-catenin pathway. J Cell Sci 2003; 116:2541.
189. Ozawa M, Baribault H, Kemler R. The cytoplasmic domain of the cell adhesion molecule uvomorulin associates with three independent proteins structurally related in different species. EMBO J 1989; 8:1711.
190. Wieschaus E, Nusslein-Volhard C, Kluding H. Krüppel, a gene whose activity is required early in the zygotic genome for normal embryonic segmentation. Dev Biol 1984; 104:172.
191. Behrens J, von Kries JP, Kühl M, et al. Functional interaction of beta-catenin with the transcription factor LEF-1. Nature. 1996 Aug 15;382(6592):638-42.
192. Huber O, Korn R, McLaughlin J, et al. Nuclear localization of beta-catenin by interaction with transcription factor LEF-1. Mech Dev 1996; 59:3.
193. Molenaar M, van de Wetering M, Oosterwegel M, et al. XTcf-3 transcription factor mediates beta-catenin-induced axis formation in Xenopus embryos. Cell 1996; 86:391.
194. Brunner E, Peter O, Schweizer L, et al. Pangolin encodes a Lef-1 homologue that acts downstream of Armadillo to transduce the Wingless signal in Drosophila. Nature 1997; 385:829.
195. van de Wetering M, Cavallo R, Dooijes Det al. Armadillo coactivates transcription driven by the product of the Drosophila segment polarity gene dTCF. Cell 1997; 88:789.
196. Xing Y, Takemaru K, Liu J, et al. Crystal structure of a full-length beta-catenin. Structure 200; 16:478.
197. Huber AH, Nelson WJ, Weis WI. Three-dimensional structure of the armadillo repeat region of beta-catenin. Cell 1997; 90:871.
198. Kimelman D, Xu W. Beta-catenin destruction complex: insights and questions from a structural perspective. Oncogene 2006; 25:7482.
199. Roberts DM, Pronobis MI, Poulton JS, et al. Deconstructing the beta-catenin destruction complex: mechanistic roles for the tumor suppressor APC in regulating Wnt signaling. Mol Biol Cell 2011; 22:1845.
200. Hur EM, Zhou FQ. GSK3 signalling in neural development. Nat Rev Neurosci 2010; 11:539.
201. Wu D, Pan W. GSK3: a multifaceted kinase in Wnt signaling. Trends Biochem Sci 2010; 35:161.
202. Su Y, Fu C, Ishikawa S, Stella A, et al. APC is essential for targeting phosphorylated beta-catenin to the SCFbeta-TrCP ubiquitin ligase. Mol Cell 2008; 32:65.
203. Fagotto F, Glück U, Gumbiner BM. Nuclear localization signal-independent and importin/karyopherin-independent nuclear import of beta-catenin. Curr Biol 1998; 8:181.
204. Shitashige M, Hirohashi S, Yamada T. Wnt signaling inside the nucleus. Cancer Sci 2008; 99:63.
205. Sharma A, Sen JM. Molecular basis for the tissue specificity of β-catenin oncogenesis. Oncogene 2013; 32:190.
206. Townsley FM, Cliffe A, Bienz M. Pygopus and Legless target Armadillo/beta-catenin to the nucleus to enable its transcriptional co-activator function. Nat Cell Biol 2004; 6:626.
207. Thompson B, Townsley F, Rosin-Arbesfeld R, et al. A new nuclear component of the Wnt signalling pathway. Nat Cell Biol 2002; 4:367.
208. Hoffmans R1, Städeli R, Basler K. Pygopus and legless provide essential transcriptional coactivator functions to armadillo/beta-catenin. Curr Biol 2005; 15:1207.

209. Lu Z, Hunter T. Wnt-independent beta-catenin transactivation in tumor development. Cell Cycle 2004; 3:571.
210. Simon M, Grandage VL, Linch DC, et al. Constitutive activation of the Wnt/beta-catenin signalling pathway in acute myeloid leukaemia. Oncogene 2005; 24:2410.
211. Reya T, Duncan AW, Ailles L, et al. A role for Wnt signalling in self-renewal of haematopoietic stem cells. Nature 2003; 423:409.
212. Congdon KL1, Voermans C, Ferguson EC. et al. Activation of Wnt signaling in hematopoietic regeneration. Stem Cells 2008; 26:1202.
213. Goessling W, North TE, Loewer S, et al. Genetic interaction of PGE2 and Wnt signaling regulates developmental specification of stem cells and regeneration. Cell 2009; 136:1136.
214. Malhotra S, Kincade PW. Wnt-related molecules and signaling pathway equilibrium in hematopoiesis. Cell Stem Cell 2009; 4:27.
215. Wang Y, Krivstov AV, Sinha AU, et al. The Wnt/beta-catenin pathway is required for the development of leukemia stem cells in AML. Science 2010; 327:1650.
216. Cozzio A, Passegué E, Ayton PM, et al. Similar MLL-associated leukemias arising from self-renewing stem cells and short-lived myeloid progenitors. Genes Dev 2003; 17:3029.
217. Somervaille TC, Matheny CJ, Spencer GJ, et al. Hierarchical maintenance of MLL myeloid leukemia stem cells employs a transcriptional program shared with embryonic rather than adult stem cells. Cell Stem Cell 2006; 4:129.
218. Kirstetter P, Schuster MB, Bereshchenko O, et al. Modeling of C/EBPα mutant acute myeloid leukemia reveals a common expression signature of committed myeloid leukemia-initiating cells. Cancer Cell 2008; 13:299.
219. Yin AH, Miraglia S, Zanjani ED, et al. AC133, a novel marker for human hematopoietic stem and progenitor cells. Blood 1997; 90:5002.
220. Brioschi M, Fischer J, Cairoli R, Rossetti S, Pezzetti L, Nichelatti M, Turrini M, Beghini A, et al. Down-regulation of microRNAs 222/221 in acute myelogenous leukemia with deranged core-binding factor subunits. Neoplasia 2010; 12:866.
221. Beghini A, Corlazzoli F, Del Giacco L, et al. Regeneration-associated WNT Signaling Is Activated in Long-term Reconstituting AC133^{bright} Acute Myeloid Leukemia Cells. Neoplasia 2012; 14:1236.
222. Katoh M, Katoh M. Cross-talk of WNT and FGF signaling pathways at GSK3β to regulate β-catenin and SNAIL signaling cascades. Cancer Biol Ther 2006; 5:1059.
223. Hamamoto R, Silva FP, Tsuge M, et al. Enhanced SMYD3 expression is essential for the growth of breast cancer cells. Cancer Sci 2006; 97:113.
224. Mao B, Niehrs C. Kremen2 modulates Dickkopf2 activity during Wnt/LRP6 signaling. Gene 2003; 302:179.
225. Sinner D, Kordich JJ, Spence JR, et al. Sox17 and Sox4 differentially regulate β-catenin/T-cell factor activity and proliferation of colon carcinoma cells.Moll Cell Biol 2007; 27:7802.
226. Olson LE, Tollkuhn J, Scafoglio C, et al. Homeodomain-mediated β-catenin-dependent switching events dictate cell-lineage determination. Cell 2006; 125:59.
227. Mieszczanek J, de la Roche M, Bienz M. A role of Pygopus as an anti-repressor in facilitating Wnt-dependent transcription. Proc Natl Acad Sci USA 2008; 105:19324.
228. Gu B, Sun P, Yuan Y, et al. Pygo2 expands mammary progenitor cells by facilitating histone H3 K4 methylation. J Cell Biol 2009; 185:811.
229. Gehrke I, Gandhirajan RK, Kreuzer KA. Targeting the WNT/β-catenin/TCF/LEF1 axis in solid and haematological cancers: multiplicity of therapeutic options. Eur J Cancer 2009 ;45:2759.
230. Angers S, Thorpe CJ, Biechele TL, et al. The KLHL12-Cullin-3 ubiquitin ligase negatively regulates the Wnt-β-catenin pathway by targeting Dishvelled for degradation. Nat Cell Biol 2006; 8:348.
231. Li Y, Lu W, King TDet al. Dkk1 stabilizes Wnt co-receptor LRP6: implication for Wnt ligand-induced LRP6 down-regulation. PloS One 2010; 5:e11014.
232. Wang K, Zhang Y, Li X, et al. Characterization of the Kremen-binding site on Dkk1 and elucidation of the role of Kremen in Dkk-mediated Wnt antagonism. Biol Chem 2008; 22:23371.
233. Morris EJ, Ji JY, Yang F, et al. E2F1 represses β-catenin transcription and is antagonized by both pRB and CDK8. Nature 2008; 25:552.

234. Gao X, Wen J, Zhang L, et al. Dapper1 is a nucleocytoplasmic shuttling protein that negatively modulates Wnt signaling in the nucleus. J Biol Chem 2008; 283:35679.
235. Sampson EM, Haque ZK, Ku MC, et al. Negative regulation of the Wnt-β-catenin pathway by the transcriptional repressor HBP1. EMBO J 2001; 20:4500.
236. Quéré R, Andradottir S, Brun AC, et al. High levels of the adhesion molecule CD44 on leukemic cells generate acute myeloid leukemia relapse after withdrawal of the initial transforming event. Leukemia 2011; 25: 515.
237. Congdon KL, Voermans C, Ferguson EC, et al. Activation of Wnt signaling in hematopoietic regeneration. Stem Cells 2008 ;26:1202.
238. Austin TW, Solar GP, Ziegler FC, et al. A role for the Wnt gene family in hematopoiesis: expansion of multilineage progenitor cells. Blood 1997; 89:3624.
239. Morra E, Barosi G, Bosi A, et al. Clinical management of primary non-acute promyelocytic leukemia acute myeloid leukemia: practice Guidelines by the Italian Society of Hematology, the Italian Society of Experimental Hematology and the Italian Group for Bone Marrow Transplantation. Haematologica 2009; 94:102.
240. Cheson BD, Bennett JM, Kopecky KJ, et al. Revised recommendations of the International Working Group for Diagnosis, Standardization of Response Criteria, Treatment Outcomes, and Reporting Standards for Therapeutic Trials in Acute Myeloid Leukemia. J Clin Oncol 2003; 21:4642.
241. Levsky JM, Singer RH. Fluorescence in situ hybridization: past, present and future. J Cell Sci 2003; 116:283.
242. Raj A, van den Bogaard P, Rifkin SA, et al. Imaging individual mRNA molecules using multiple singly labeled probes. Nat Methods 2008; 5:87.
243. Kaufmann BB, van Oudenaarden A. Stochastic gene expression: from single molecules to the proteome. Curr Opin Genet Dev 2007; 17:107.
244. Landegren U, Kaiser R, Sanders J, et al. A ligase-mediated gene detection technique. Science 1988; 241:1077.
245. Banér J, Isaksson A, Waldenström E, et al. Parallel gene analysis with allele-specific padlock probes and tag microarrays. Nucleic Acids Res 2003; 31:103.
246. Hardenbol P, Banér J, Jain M, et al. Multiplexed genotyping with sequence-tagged molecular inversion probes. Nat Biotechnol 2003; 21:673.
247. Hardenbol P, Yu F, Belmont J, et al. Highly multiplexed molecular inversion probe genotyping: over 10,000 targeted SNPs genotyped in a single tube assay. Genome Res 2005; 15:269.
248. Nilsson M, Malmgren H, Samiotaki M, el al. Padlock probes: circularizing oligonucleotides for localized DNA detection. Science 1994; 265:2085.
249. Lizardi PM, Huang X, Zhu Z, el al. Mutation detection and single-molecule counting using isothermal rolling-circle amplification. Nat Genet 1998; 19:225.
250. Banér J, Nilsson M, Mendel-Hartvig M, et al. Signal amplification of padlock probes by rolling circle replication. Nucleic Acids Res 1998; 26:5073.
251. Blab GA, Schmidt T, Nilsson M. Homogeneous detection of single rolling circle replication products. Anal Chem 2004; 76:49.
252. Sykes PJ, Neoh SH, Brisco MJ, et al. Quantitation of targets for PCR by use of limiting dilution. BioTechniques 1992; 13:444.
253. Vogelstein B, Kinzler KW. Digital PCR. Proc Nat Acd Sci 1999; 96:9236.
254. Hindson BJ, Ness KD, Masquelier DA, et al. High-throughput droplet digital PCR system for absolute quantitation of DNA copy number. Anal Chem 2011; 83:8604.